

Organic matter and iron along a transect from the deep forest to outer Oslofjord

*The relationship between organic matter and iron and their
optical properties in browning waters.*

Hanne Halkjelsvik Børseth



Thesis submitted for the degree of Master of Science in Marine
Biology and Limnology

60 credits

Department of Bioscience
Faculty of Mathematics and Natural Sciences
UNIVERSITY OF OSLO

December 2022

© Hanne Halkjelsvik Børseth

2022

Organic matter and iron along a transect from the deep forest to outer Oslofjord
The relationship between organic matter and iron and their optical properties in browning waters.

Author: Hanne Halkjelsvik Børseth

Department of Biosciences (IBV)
Faculty of Mathematics and Natural Sciences
UNIVERSITY OF OSLO (UiO)

<http://www.duo.uio.no/>

Print: Reprosentralen, Universitetet i Oslo

Abstract

An increased flux of organic matter (OM) and iron (Fe) from terrestrial sources into surface waters is observed in boreal areas. This increased concentration of chromophoric compounds affects the light attenuation in the water column, and thus the organisms living there. The aim of this study was to explore how Fe affects the optical properties of dissolved organic carbon (DOC), and to better understand the relationship of total organic carbon (TOC) and Fe following a salinity gradient.

Absorption measurements of solutions of freeze-dried DOC and FeCl₃ were used to investigate the effects of DOC and Fe on water colour. The interaction link between the substances was weak at all wavelengths, indicating an additive effect of DOC and Fe on water colour. Thus, no additional interaction effect is expected from the interaction between DOC and Fe.

To assess the relationship of TOC and Fe, samples were collected along a river transect from the inner Finnskogen area to the outer Oslofjord. The results demonstrate a tight correlation between TOC and Fe in along the river transect, yet with some scatter reflecting different properties among the tributaries. The relation between TOC and Fe was more relaxed in the marine transect, demonstrating different fates of the two compounds with increasing salinity. Since the association between TOC and Fe do impact optical properties in water, these insights have relevance for the light climate, primary production and visibility in aquatic systems.

Acknowledgments

There are many wonderful people who have been with me during this journey and helped me in the realization of this master thesis.

I would like to give a huge thank you to my supervisors Professor Dag O. Hessen and Professor Tom Andersen for their guidance during this thesis, and for always taking the time to help me with my endless questions. Your valuable knowledge has been extremely important to me in this process of writing a master thesis.

Others who kindly have used their time to help me and deserves a thank you: Jan David Heuschele for the help with and encouragement with the use of the lab robot. Magnus Kristoffersen for the help with the water metal analysis. William Martin Hagopian for the help with the analysis of water isotopes. Aleksandr Berezovski for waking up super early to drive Tonje and me to our fjord samplings, without your help on the boat none of these samples would be with us today. Sindre and the rest of the crew on Trygve Braarud, the time at sea would not have been as fun without you. Berit Kaasa for always helping me in the lab, and for the help with the TOC analysis of my samples. I am also truly thankful to Per Johan Færøvig who have helped me in lab and been with me in the field, driving many hours for me to collect my water samples. With good conversation and funny comments, the field trips would not have been as joyful without you in the car.

Tonje, I really appreciate our friendship and this master would not have been the same without you. During this last year we really have been through a lot. From being seasick together on the field cruises to living together at Svalbard, countless of fun hours in the office and dinner times together. I have truly found a lifelong friend in you. I am also very grateful for all my other good friends who always is there for me, keeping my mood up and take such good care of me, especially Mathilde, Sofia, and Eli. You guys are amazing <3. Also, a huge thanks to Eira (and Kasper) who have lived with me during this period, I love our little «Kollektiv» at Majorstuen.

Last, but not least, a huge thank you to my family, and especially my mom, always encouraging me to do my best, giving feedback and endless support, you truly are the best.

Abbreviations

2D - Two - dimensional

CDOM - Coloured/chromophoric dissolved organic matter

CO₂ - carbon dioxide

DIC - Dissolved inorganic carbon

DOC - Dissolved organic carbon

DOM - Dissolved organic matter

Fe - Iron

FR-Fe - Ferrozine reactive iron

IBV - Department of Biosciences

ICP-OES - Inductively coupled plasma optical emission spectrometry

NO - Nitric oxide

OCS - Optical cross section

OM - Organic matter

PAR - Photosynthetically active radiation

PIM - Particulate inorganic matter

PM - Particulate matter

POM - Particulate organic matter

PSU - Practical Salinity Unit

SOM - Soil organic matter

TC - Total carbon

TN - Total nitrogen

TOC - Total organic carbon

TPM -Total particulate matter

UiO - University of Oslo

Table of contents

Abstract	III
Acknowledgments	IV
Abbreviations	V
1 Introduction	1
1.1 Consequences of browning/increased light attenuation.....	1
1.2 Main drivers of increased DOM and Fe to surface waters.....	3
1.3 Objectives, hypothesis and aims	6
2 Materials and Methods	7
2.1 Field Sampling - From inner Finnskogen to outer Oslofjord	8
2.2 Lab experiments	11
2.2.1 Opentrons OT-2 lab robot.....	11
2.2.2 Two-dimensional photometric titration with-freeze dried DOC and FeCl ₃	11
2.3. Analysis of field samples	12
2.3.1 General.....	12
2.3.2 The ferrozine method – Fe(II) / Fe(III) Determination	12
2.3.3 Inductively coupled plasma – optical emission spectrometry (ICP-OES) – Water metal analysis	13
2.3.4 High-temperature catalytic oxidation – Analysis of total organic carbon and total nitrogen	14
2.3.5 UV-vis spectrophotometry – Absorbance of coloured dissolved organic matter (CDOM)	14
2.3.6 Filtration and determination of particulate matter in samples from the Glomma transect	15
2.3.7 Cavity ring-down spectroscopy – Analysis of water isotopes	15
2.4 Statistical analysis.....	16
3 Results	17
3.1 The effects of DOC and FeCl ₃ on water colour	17
3.2 The Glomma transect.....	21
3.2.1 Determination of iron	21
3.2.2 Determination of organic matter.....	23
3.2.3 Origin of the sample water	25
3.3 The Oslofjord transect	27
3.3.1 CTD-data and the change in water transparency from the innermost to the outermost sampling station.	27
3.3.2 Determination of iron	28
3.3.3 Determination of organic matter.....	29
3.4 Comparison of the Glomma and Oslofjord transect.....	32
4 Discussion	35
4.1 The effects of DOC and FeCl ₃ on water colour	35

4.2 The relationship between Fe and TOC - Changes along the transect	37
4.2.1 Iron from inner Finnskogen to outer Oslofjord	37
4.2.2 Organic matter from inner Finnskogen to outer Oslofjord	39
4.2.3 The Glomma transect	40
4.2.4 The Oslofjord transect	41
4.3 Potential ecosystem effects	42
4.4 Future prospects.....	43
5 Conclusions	44
References.....	45
Appendix	57

1 Introduction

A general trend in increased water colour has been observed in lakes and along the coasts the past decades (Arvola et al., 2010; de Wit et al., 2016; Hongve et al., 2004; Roulet & Moore, 2006). This browning or darkening of the water, the latter term commonly used for marine waters, has attracted major interests due to the potential adverse effects it may cause in the aquatic ecosystems (Urtizbera et al., 2013), and for its societal consequences where the production and quality of drinking water may be negatively affected (Matilainen et al., 2010). From an ecosystem point of view, the strong impact on optical properties, and thus productivity in response to browning, is a matter of concern (Thrane et al. 2014). Multiple factors contribute to the alteration of the optical properties of the water, e.g., increased concentration of both organic matter and iron from runoff to the water column (Kritzberg & Ekström, 2012).

The euphotic zone is where the aquatic primary producers have enough light to perform photosynthesis, and the lower limit of the euphotic zone is at depth of where 1% of the surface irradiance remains (Lee et al., 2007). Several factors may affect the euphotic zone, making the depth of it vary in different locations. Particles, such as OM and sediment, the abundance of primary producers and other coloured elements absorb and scatter light, thus affecting the light attenuation in water (Lee et al., 2013). The depth of the euphotic zone can be estimated by ocean-colour remote sensing (Hill & Zimmerman, 2010). The Secchi depth is also a well-known measurement of turbidity in water, and has been used to observe long term trends in water clarity (Dupont & Aksnes, 2013).

1.1 Consequences of browning/increased light attenuation

In aquatic ecosystems, available sunlight and its distribution in the water column constitute a key abiotic factor for survival, behaviour and activity of organisms inhabiting these environments (Mascarenhas & Keck, 2018). Visual predators use their eyesight to find prey, some fish and zooplankton are dependent on light as a cue for vertical migration (Lampert,

1989), and primary producers use the photosynthetically active radiation (PAR) as an energy source to perform photosynthesis. These processes may be adversely affected by the reduction of light in the water column caused by browning.

As more Fe and DOC enters the water, the light attenuation increases and less light penetrates the water column. Due to this reduction of the euphotic zone, a smaller amount of light is available for benthic algae, macrophytes and pelagic phytoplankton. This could lead to a general reduction in primary productivity as the reduction of available light limits the habitat for primary producers (Thrane et al., 2014). Furthermore, darker water will be more capable of absorbing solar energy, due to decreased albedo, which will increase the surface water temperature. This increase in surface water temperature intensifies the stratification in the water column, promoting changes in the habitat for the primary producers (Persson & Jones, 2008). Being at the base of the food web, primary producers determine the available energy for higher trophic levels, making them vulnerable to changes in the primary production rate (Grubisic et al., 2018). However, small increases of DOM in waters may be beneficial as DOM absorbs UV light, and thereby protects aquatic organisms against harmful radiation (Erickson III et al., 2015)

Runoff and riverine inputs are important sources of nutrients to aquatic ecosystems. The increased flux of Fe and DOM constitutes an important contribution to the nutrient supply in freshwater systems and coastal areas. In general, primary producers in lakes and coastal areas are more likely to be limited by light availability than nutrients (Jickells, 1998). It is well established that the limiting nutrient in freshwater systems is phosphorus and ocean productivity is limited by nitrogen (Rabalais, 2002), yet a co-limitation of these elements are common in all ecosystems (Harpole et al., 2011). Fe is an essential micronutrient, e.g., it is important in the synthesis of chlorophyll and functions as cofactor in the enzyme nitrogenase. In certain areas where Fe is the limiting factor for primary production, e.g., open marine waters, increased flux of Fe to the aquatic ecosystems can increase the aquatic productivity. DOM is an important energy source for heterotrophic bacteria, and enters the food web via the microbial loop (Tranvik, 1992). The increased availability of DOM may increase the abundance of bacteria in the waters (Hessen, 1985), and thus the food

availability for protist grazers. This may also have a positive impact on the availability of food for organisms further up the food web. On the other hand, a higher productivity of bacteria intensifies the competition of nutrients like phosphorus (P) which may suppress phytoplankton and increase the net heterotrophy for aquatic systems (Hessen et al., 2017).

1.2 Main drivers of increased DOM and Fe to surface waters

Coloured dissolved organic matter (CDOM) and Fe and are both known for their chromophoric properties, and their effect on reducing water transparency (Canfield Jr. et al., 1984; Maloney et al., 2005). The main source of DOM and Fe to the aquatic matrix is the catchment soils, and increased export of these substances to surface waters have been reported, resulting in increased browning (Kritzberg & Ekström, 2012). There are many drivers for increased concentration of DOC and Fe in water such as change in vegetation cover and reduction of sulphur deposition (Monteith et al., 2007). Climate driven effects, such as rising temperatures, increased watershed productivity and intensification of the hydrological cycle, are expected to affect the availability and transport of DOM and Fe from the terrestrial areas to surface waters, and thereafter coastal areas (de Wit et al., 2016; Finstad et al., 2016).

Soil organic matter (SOM) originates from decomposition of plant material, and a great part of SOM are humic substances (Schnitzer, 1983). The organic matter is characterized by different functional groups, such as phenols and carboxylic groups, which affect the solubility and mobility of OM. These structural properties may affect the quality of the OM, and thus the water colour (Ekström et al., 2011). The soil carbon pool is a good predictor for the concentration of DOC in stream water (Aitkenhead et al., 1999). Increased terrestrial primary production, such as forest growth, and lower decomposition rates contribute to the carbon pool in the soils, making more DOC available for transport. Both the catchment area the water travels through and the residence time in the soil play a major role in the export of DOC to surface waters and into the coastal areas. Thus, the soils constitute an important source of aquatic DOC (Larsen et al., 2011).

Iron is the fourth most abundant element in the crust of the Earth (Frey & Reed, 2012). The mobilization and availability of iron is strongly affected by redox conditions, pH and the availability of OM for complexation (Edmunds & Smedley, 1996). In general, lower pH increases the solubility of iron (Björnerås et al., 2019). Oxidised iron, Fe(III), is nearly insoluble in water, whilst reduced iron, Fe(II), is a lot more soluble (Falkowski et al., 1998). One find the concentration of Fe(II) to be higher than for Fe(III) for free ions in soil solution (Schwertmann, 1991). In seawater, the solubility of iron is enhanced by binding to other organic components (Rue & Bruland, 1995). In OM rich environments Fe is known to form relatively stable complexes with organic matter, Fe-OM, which then can be mobilized into solution (Škerlep et al., 2022; Sundman et al., 2014). Organic matter can stabilise both Fe(II) and Fe(III) in the aquatic environment. Even with the presence of dissolved oxygen, Fe(II) does not oxidate to Fe(III) when in complex with OM (Rue & Bruland, 1995). Whether Fe(II) will form complexes or oxidise to Fe(III) depend on the availability of OM and the pH in the environment (Rue & Bruland, 1995). Less common is the complex formation of iron with other elements, e.g. phosphorus (Rothe et al., 2016).

The export of DOC and Fe is influenced by alterations in hydrology and regulations of biogeochemical processes in the soils, land cover change, and especially afforestation and expansion of vegetation cover (Bowering et al., 2020). Spruce forest, in particular old forest (60-90 years old), have thick layers of organic matter and the pH in the soil layers are more acidic (Škerlep et al., 2022). It has been suggested that aging of spruce forest and forestry intensification contributes to increased mobilization of Fe from soils by increasing the concentrations of organic acids and thereby the acidity in the soil layer (Škerlep et al., 2022). A reduction of pH enhances the mobility of Fe, hence, the concentrations of Fe in surface waters will increase and contribute to further browning.

Recovery from acidification and declining atmospheric sulphur deposition are assumed to enhance the flux and mobility of DOM from soils (Kritzberg, 2017; Monteith et al., 2007). As pH decreases and the functional groups on OM become protonated, the mobility of OM is suppressed (Ekström et al., 2011). This indicates that DOM is more mobile at higher pH. The reduction of sulphur deposition is increasing the pH in the catchments, affecting the

solubility and export of DOM from soils, thus contributing to the brownification process (Ekström et al., 2011). Due to Fe(III) reduction, increased solubility, and increased mobility of Fe at low pH, the reduction in sulphur deposition is not a direct driver of increased Fe concentrations (Björnerås et al., 2019). However, an increase in pH might increase the Fe flux into soil solution due to the complex formation with OM (Neubauer et al., 2013).

Several factors contribute to the increased flux and mobilisation of Fe and OM. The consequences of darkening waters will strongly affect the aquatic ecosystems. Due to changing precipitation patterns and rising temperature, one expects an increased flux of DOM to surface waters (Finstad et al., 2016). As a consequence of climate change, increased temperatures affects several different mechanisms in boreal regions: prolonged growing season, faster decomposition rate of litter fall and increased production of DOC (Christ & David, 1996; Škerlep et al., 2020; Weyhenmeyer & Karlsson, 2009). In addition, increased watershed productivity contributes to changes in the DOC flux. Intensification of the hydrological cycle, due to climate change, will lead to more precipitation and thus increase the flux of OM and Fe into soil solution (de Wit et al., 2016). This change in hydrology leads to increased precipitation, thus more runoff from land which transports Fe and DOC into the aquatic environment. In dry periods OM accumulates in the soil matrix, and re-wetting of the soil accelerates the carbon flux to the water (Fenner & Freeman, 2011). In an ever-changing climate, these processes can become important for mobilisation of Fe and DOC.

The Glomma watershed and its relation to Skagerrak gives a natural laboratory to investigate the relationship between the catchment processes and the transport of OM and Fe from the inner Finnskogen area to the outer Oslofjord. The Glomma catchment is the largest in Norway with an area of [41 967 km²](#). Surrounded by forest, agriculture, and cities, there are many potential sources for both iron and organic matter to enter the surface water stream, and subsequently the coastal areas. Glomma's largest tributary, Vormå, brings fresh water from Norway's largest lake Mjøsa, and is not as heavily affected by forest as Glomma. The Oslofjord spans over an area of 120 km from Bonnebukta to Skagerrak and receives runoff from approximately [70 000 km²](#) of land.

Negative impacts from e.g. trawling and eutrophication is already affecting the ecosystem in the Oslofjord (Moland et al., 2021). Increased light attenuation in the water column due to increased flux of terrestrial OM and Fe, is a contributing factor to the worsening state of the fjord, and further, adverse effects for the aquatic organisms (Moland et al., 2021).

1.3 Objectives, hypothesis and aims

This thesis consists of two parts: a laboratory experiment where the main objective was to better understand the optical properties of Fe and DOC in water, and a field study where the main objective was to explore the relationship between Fe and TOC through a transect from the deep forest to outer Oslofjord.

Firstly, we hypothesised that iron will strongly affect the chromophoric properties of DOC. The specific aim was therefore to explore whether the effect of Fe on the chromophoric properties of DOC is additive or interactive when measuring absorbance.

Secondly, we hypothesised that the relationship between Fe and TOC will be more relaxed with increasing salinity, whilst they are strongly correlated in freshwater. Thus, the specific aim was to explore the fate of Fe and TOC from inner Finnskogen to outer Oslofjord.

2 Materials and Methods

Three samplings from the outer Oslofjord and one riverine sampling from the Glomma transect were conducted. All samples were analysed by the ferrozine method, high-temperature catalytic oxidation and UV-vis spectrophotometry. The freshwater samples were also analysed by cavity ring-down spectroscopy, inductively coupled plasma – optical emission spectrometry (ICP-OES) and the determination of particulate matter (PM). A simple visualisation of the methods used in this thesis is shown in Figure 1.

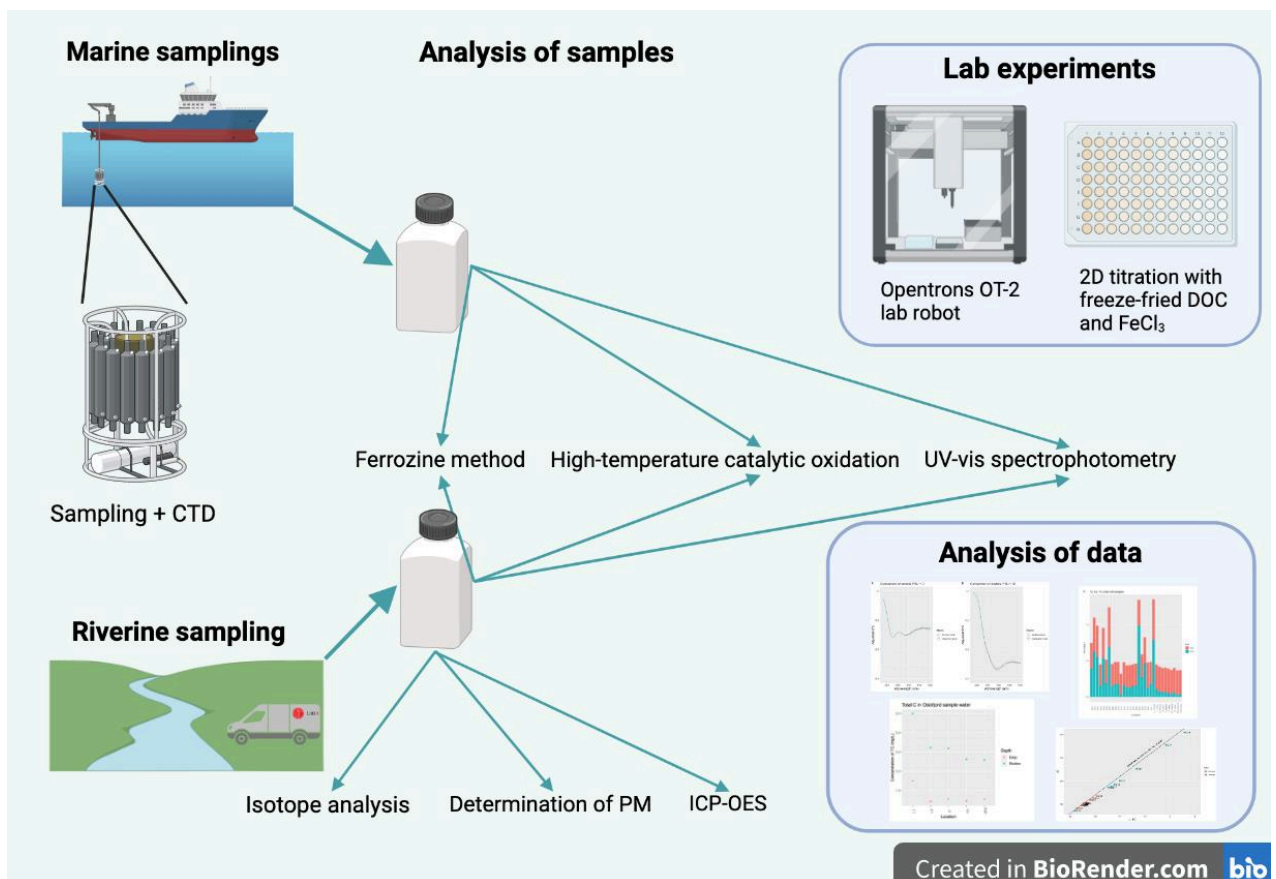


Figure 1. Simple visualisation of methods used in this thesis. Illustration created in BioRender.com.

2.1 Field Sampling - From inner Finnskogen to outer Oslofjord

The samplings in the outer Oslofjord were conducted 12th of May, 2nd of June and 29th of June 2022 with the research vessel Trygve Braarud. The same transect, with five sampling sites, was used for all three of the field samplings (Figure 2). This transect, which covers standard monitoring stations in the outer Oslofjord, was chosen to compare brackish areas with more coastal water. The sampling sites from most to least brackish: L1 (Glomma, Fredrikstad), L5 (Kjøkkøy), I1 (Ramsø), Ø1 (Leira, O1 in figures), OF2 (Missingene). Originally there were six sampling sites, but the outermost site at Torbjørskjær, OF-1, was renounced due to bad weather conditions. For a closer look at the sampling sites please look at [Outer Oslofjord](#) and the coordinates in Table 1 in Appendix.

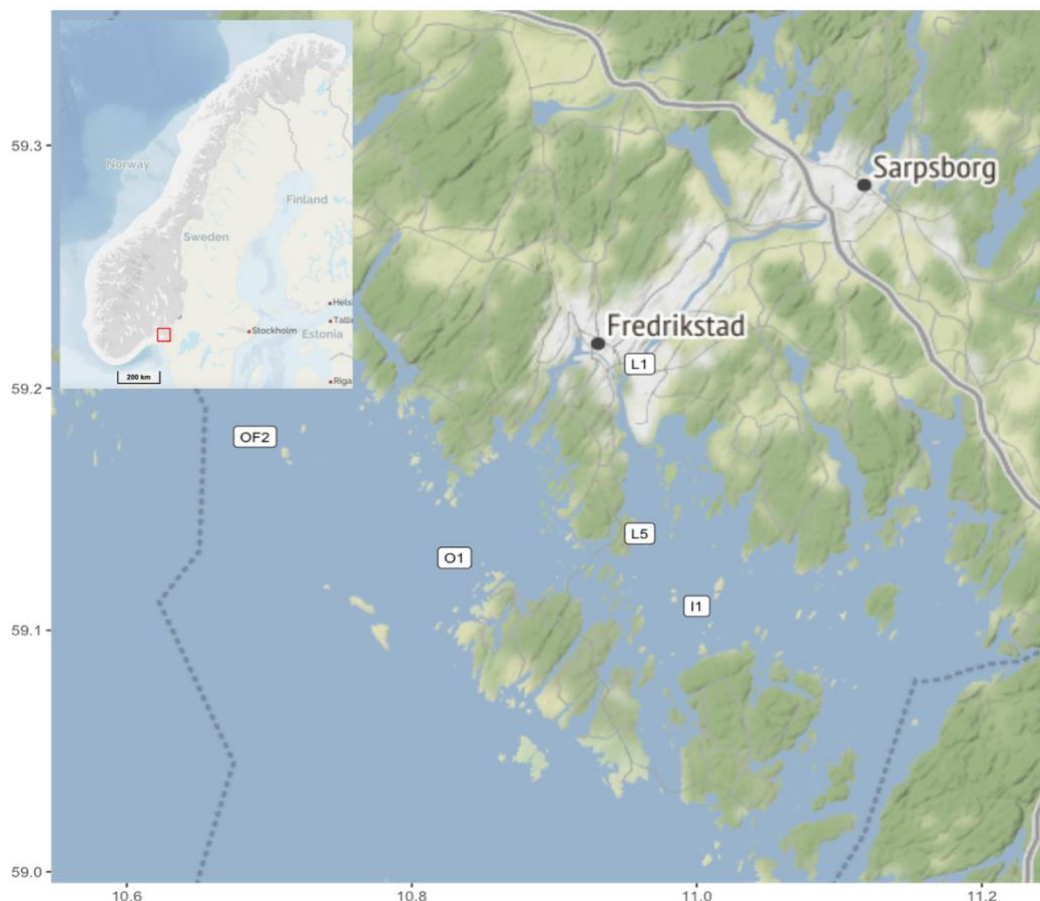


Figure 2. Sampling sites outer Oslofjord. Map of Norway from © Norgeskart.no. Map of Outer Oslofjord created in R [Stamen maps](#) with ggmap (Kahle & Wickham, 2013).

The sampling was done by a rosette sampler with 5L Niskin bottles which collected water at 40 m, 4 m, and 3 m depths. At site L1, in the Glomma River under the Fredrikstad bridge, the deepest sample was collected from 16 m. The surface water, samples from 3 m and 4 m, was mixed in a 10 L canister before transferred to a 1 L plastic bottle. The deep-water samples were transferred directly to a 1 L bottle. To measure water transparency the Secchi depth was measured on the sunny side of the vessel. The Secchi disk was forgotten on the first cruise. A CTD-profile was done at each site. The CTD instrument measures conductivity, temperature, and depth, with additional sensors for oxygen, light and fluorescence measurements. All the sample bottles were stored in a dark climate room with a temperature of 2-4°C.

The riverine sampling was conducted May 23rd, 2022, after the snowmelt ended. After careful planning of the route, the sampling started in a side stream of the Flisa River in the Finnskogen area, near the Swedish border, and followed a 275 km long transect of 20 more sampling sites to the river mouth of Glomma in Fredrikstad (Figure 3). For a closer look at the maps see Figure 24 and 25, and table with coordinates and description in Table 2 in Appendix. For a closer look at the sampling sites, please look at the [Glomma Transect](#). The rationale for selecting these sites is that this eastern area close to the Swedish border typically have high concentrations of DOC (Andersen et al., 2020; Larsen et al., 2011), with a gradual dilution from the main river and its alpine tributaries. The surface samples were collected both from tributaries of Glomma, to investigate which other catchments contribute to the main river flow, and directly from the Glomma River with a telescopic pole (3 m). The telescopic pole was rinsed between every sample. The water samples were directly transferred from the water collector on the telescopic pole to 1 L plastic bottles. The plastic bottles were stored in a dark climate room with a temperature of 2-4°C.



Figure 3. Map of Norway from © Norgeskart.no. Red box on the small map of Norway marks the Glomma transect. Map overview of the sites of the Glomma transect, created in R [Stamen maps](#) with *ggmap* (Kahle & Wickham, 2013).



Figure 4. Pictures from sample site 2, 8, 17 and 19, showing different impact of chromophoric compounds.

2.2 Lab experiments

When trying to understand how Fe affects DOC and their optical properties in water, a two-dimensional (2D) photometric titration was performed by the Opentrons OT-2 lab robot before absorbance was measured with a Synergy™ MX microplate reader.

2.2.1 Opentrons OT-2 lab robot

To reduce the impact of human error some time was spent learning how to use the [Opentrons](#) OT-2 lab robot, how the different commands work, and thus, make a script for the 2D titration with Fe and DOC and for the determination of Fe(II) / Fe(III) (subsection 2.3.2). The script was made in Spyder (version 5.1.5), written in Python (version 3.9.7). In the beginning this was done with water, coffee, and candy water to make simple transfers and thereafter gradients. With an [Ultimaker](#) 2+ 3D printer a new Eppendorf tube rack was 3D printed; this was needed in the Fe(II)/Fe(III) determination part of the analysis.

2.2.2 Two-dimensional photometric titration with-freeze dried DOC and FeCl₃

A 2D photometric titration was performed in a flat bottom 96-well plate to explore how Fe affects DOC, and their optical properties in water. To create the gradient between the parameters, FeCl₃ and freeze-dried DOC from the small catchment Hellerudmyra, from the NOM-project (Gjessing et al., 1999) was used. FeCl₃ stock solution (1.2 µg / µL) and DOC stock solution (0.22 µg / µL) were distributed in correct volumes by the Opentrons OT-2 lab robot to get specific concentrations of the reagents in the wells.

To look at the difference in absorption in fresh and saline water, two different 96-wells plates were made; one with practical salinity unit (PSU) = 0 and one with PSU = 33, which matches the salinity in fresh river water and the coastal water. Milli-Q water was used for PSU = 0, and artificial seawater was made with Milli-Q water and NaCl for PSU = 33. The absorbance was measured from 280 to 700 nm in each well with a Synergy™ MX microplate reader. The concentration gradient of Fe and DOC was the same for both salinities.

2.3. Analysis of field samples

2.3.1 General

The analysis of Fe was composed of two parts: the ferrozine method was used to determine the ratio of the concentrations of Fe(II) and Fe(III) in the samples, and ICP-OES determined the concentration of total dissolved iron, as well as other elements. Analysis of organic matter was divided into three parts: high-temperature catalytic oxidation to determine the concentration of TOC, determination of PM from filters to differentiate between organic and inorganic particles, and measurements of absorbance of dissolved organic matter. Cavity ring-down spectroscopy was used for analysis of stable water isotopes. Only samples from the Glomma transect were analysed by ICP-OES, cavity ring-down spectroscopy and the determination of PM.

The plastic bottles were manually shaken every time they were taken out of the cold storage room to stir up the suspension of particles before analysis. After each field sampling the pH was measured with a Radiometer Copenhagen PHM92 lab pH meter. For the Glomma samples conductivity was also measured with a Radiometer Copenhagen CDM 80 Conductivity Meter. The measurements of pH and conductivity were not further used in this thesis.

2.3.2 The ferrozine method – Fe(II) / Fe(III) Determination

To analyse the concentration of ferrozine reactive iron (FR-Fe) and distinguish between the two iron species, Fe(II) and Fe(III), the ferrozine method was performed according to the SOP for the method (SOP in Appendix). The ferrozine method primarily measures ionic iron, but can also react with Fe in complex (Viollier et al., 2000). Ferrozine reacts with Fe(II) and forms a magenta-coloured complex which can be measured spectrophotometrically at 562 nm (Stookey, 1970). One gets the total FR-Fe in the sample when the reducing agent hydroxylamine hydrochloride reduces Fe(III) to Fe(II) (Viollier et al., 2000).

Fresh reagents used in the Fe(II)/Fe(III) determination were prepared the day before the field day according to the SOP (SOP in Appendix). The OpenTrons OT-2 lab robot was programmed to perform the pipetting. All the reagents, pipet tips, flat bottom 96 wells plates and Eppendorf tubes racks were placed in the lab robot. The tube racks were filled with 2 mL Eppendorf tubes, one rack with 1 mL sample water in each tube and one rack with empty tubes for the making of the standards. For each time it says “mix thoroughly” in the protocol, a total of 3 times, the snap cap tubes were taken out and mixed by hand with the help of a Mini Vortex Mixer. After the robot had added the reagents, the finished 96 well plates were directly inserted into a Synergy™ MX microplate reader, and the absorbance was measured at 562 nm.

The Fe concentrations in the samples were calculated using the slope and intercept of the standard curve. The standard curves were made from the absorption of the ferrozine-ferrous iron complex in the wells with known concentration of Fe. The analysis was based on four replicates per sample.

2.3.3 Inductively coupled plasma – optical emission spectrometry (ICP-OES) – Water metal analysis

ICP-OES was used to detect low concentrations of elements in the Glomma samples. Filtered water, the filtrate from subsection 2.3.6, was used to remove particles that could clog the instrument. For 1% acid preservation 150 µL suprapur HNO₃ was added to each 15 mL sterile centrifuge tube filled with filtered sample water. Two replicates per site were made from all the samples from the Glomma transect, including 4 reference tubes filtered with Milli-Q water. The tubes were then sent to Magnus Kristoffersen for water metal analysis at the Department of Chemistry at UiO. No samples from the outer Oslofjord were analysed by this method.

To determine the metal concentrations in the samples the Jobin Yvon Horiba – ULTIMA 2 instrument transformed the sample water into aerosols which then were ionized and/or excited by the plasma at high temperatures (10 000K). The instrument detect the radiation

from the ionized/excited atoms and sort them by wavelength (Ghosh et al., 2013). The concentrations of Ca, Fe, Mg, Mn, and Na were determined by this method.

2.3.4 High-temperature catalytic oxidation – Analysis of total organic carbon and total nitrogen

The analysis system, comprised by Shimadzu ASI-V Autosampler and Shimadzu TOC-V_{CPH} Total organic carbon analyser, was used to measure total carbon (TC), total organic carbon (TOC), and total nitrogen (TN) in all the water samples, both from the three cruises in the outer Oslofjord and from the Glomma transect. The samples were analysed by the 680°C combustion catalytic oxidation method. For the carbon analysis carbon dioxide (CO₂) was generated by oxidation and detected using an infrared gas analyser. A similar principle applied to the detection of nitrogen where nitric oxide (NO) was measured by chemiluminescence by the N-detector after catalytic combustion at high temperature (Badr et al., 2003). The measurement of nitrogen was not further used in this thesis.

Approximately 24 mL of sample water was poured directly into the glass vials, placed on the tray carousel which was then placed into the ASI-V Autosampler. The first three and last three vials were filled with Milli-Q water to wash the instrument between the different analyses. All the glass vials were washed and combusted for 2h at 500 degrees beforehand to remove all organic matter from previous analysis.

2.3.5 UV-vis spectrophotometry – Absorbance of coloured dissolved organic matter (CDOM)

DOM absorbs light in the ultraviolet and visible part of the spectrum, UV-vis spectrophotometry was used to determine the CDOM absorbance at different wavelengths in the water samples. Filtered water was used to analyse the absorbance of CDOM. The water from the Oslofjord was filtered through 25 mm GF/C filters, and the filtered freshwater from the Glomma transect was the filtrate from subsection 2.3.6. Filtered water is used to remove e.g., phytoplankton pigments.

The SHIMADZU UV-2550 spectrophotometer sends light in the wavelength interval 250-750 nm through 50 mm quartz cuvettes, one reference filled with Milli-Q water, and one filled with filtered sample water, and measures the absorption in the sample cuvette with respect to the reference cuvette. The computer program used was UVProbe Ver. 2.21.

2.3.6 Filtration and determination of particulate matter in samples from the Glomma transect

The samples from the Glomma transect were filtered through a 47 mm GFF-filter. The filters used are hygroscopic as they absorb moisture from the air, hence, all the filters were dried at 60°C for 24h and weighed before the filtering of the samples. The filters were weighed with a Mettler Toledo MX5 Microbalance.

First, the filter was washed with 100 mL Milli-Q water, then, 500 mL of sample water was filtered with the vacuum pump set up. The filtrate was poured into a 0.5 L plastic bottle, and the used filter was placed into a container after the filtration. Four filters were filtered with only milli Q water to see what leaches out of the filter and whether it affects the results, especially for the ICP-OES analysis. Five filters were only weighed to have as reference filters to see what was lost in the oven. After the filtering the filters were placed in a freezer and the filtrate were placed in the climate room with the original samples.

To determine the difference between organic and inorganic particulate matter, the filters were firstly placed on a tray and placed in a Termaks drying cabinet at 60 °C for 24h before they were weighed again. The weight added to the filters after the filtration and drying is the total particulate matter (TPM). To burn off the particulate organic matter (POM) and find the particulate inorganic matter (PIM = TPM – POM) the filters were then placed in a Heraeus oven at 600°C for 2 hours before the last weighing.

2.3.7 Cavity ring-down spectroscopy – Analysis of water isotopes

The isotopic composition could indicate the origin of the sample water from the Glomma transect, if it consists of more rain or soil water. Higher $\delta^{18}\text{O}$ values, less ^{16}O , indicate that

the samples are more affected by soil water than the samples with more negative $\delta^{18}\text{O}$ values (Hsieh et al., 1998). To identify the water sources from the Glomma transect (precipitation, soil water etc), a water analysis was done in a Picarro L2140-I Cavity Ring-Down Spectroscopy instrument. This instrument uses a near-infrared absorption spectrum to determine the concentration of different element species, and thus the different water isotopomers (Berden et al., 2000). To prepare the samples 2*950 μL of filtered water from the Glomma transect (filtrate from subsection 2.3.6) was added to isotope vials and sent to analysis at the IBV stable isotope laboratory ([CLIPT](#)). Filtered sample water was used to avoid accumulation of particles in the inlet vaporizer.

2.4 Statistical analysis

All statistical analyses were performed using R version 4.2.1, and the package ggplot2 was used to make figures (Wickham, 2016). The maps were made using R Stamen maps with ggmap (Kahle & Wickham, 2013). Linear models (multiple regression) were made using the lm()-function in base R, e.g., to look at the relationship between absorbance of Fe and DOC. The predict()-function was used to make predictions from linear models and calculate their standard errors and confidence intervals.

CDOM (m^{-1}) is calculated from absorbance by the equation $\text{CDOM} = 100 * ((\text{abs})/h) * \log(10)$, where h is the cuvette path length in cm. The absorption/optical cross section(OCS) is dependent on the molecule diameter and gives information about a substance capability to absorb/scatter light (Evanoff & Chumanov, 2004). One gets the OCS of DOM and Fe from the slopes for the linear models of CDOM as a function of DOC and Fe concentrations ($\text{CDOM} \sim \text{Fe} + \text{DOC}$), such that OCS becomes the change in CDOM per mg Fe or DOC for each wavelength.

3 Results

3.1 The effects of DOC and FeCl₃ on water colour

The results from the 2D titration experiment with freeze dried DOC and FeCl₃ were used to investigate the chromophoric properties of DOC and Fe in fresh and saline water, and their effect on each other. The results were based on the absorption spectra from two flat bottom 96 well plates, one with PSU = 0 and one with PSU = 33.

To explore the differences in absorption in fresh and saline water, subsets were made to look at the absorption of DOM without the effects of Fe and vice versa. Fe has the highest absorbance in saline water (Figure 5), whilst DOC has the highest absorption in fresh water (Figure 6). One assumes constant background absorbance of the plate, and to correct for this a mean was calculated from all the blank wells. This mean was then subtracted from the absorbance values.

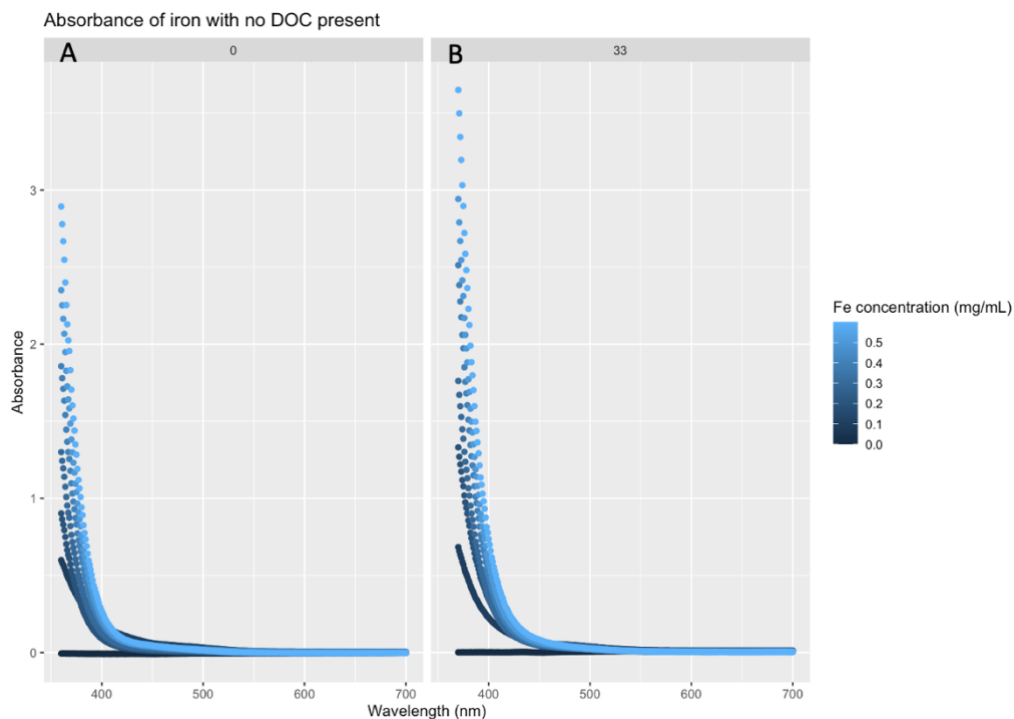


Figure 5. Absorption spectra of Fe with no DOC present. Comparison of water with PSU = 0 (A) and PSU = 33 (B).

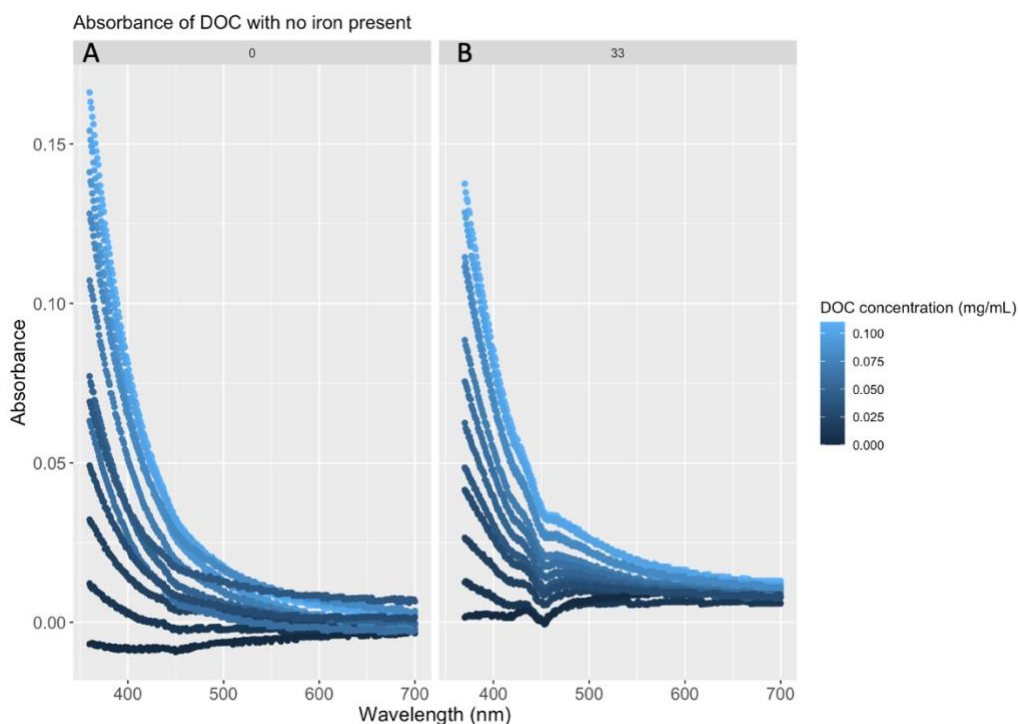


Figure 6. Absorption spectra of DOC with no iron present. Comparison of water with PSU = 0 (A) and PSU = 33 (B).

A subset of the data was made including the wavelengths 380-600 nm, as the absorbance of Fe and DOC is very low above 600 nm. To investigate how Fe will affect the optical properties of DOC, and if the effects of Fe and DOC were additive or interactive, a loop function was made for both the additive model ($\text{Im}(\text{CDOM}) \sim \text{Fe} + \text{DOC}$) and the interaction model ($\text{Im}(\text{CDOM}) \sim \text{Fe} * \text{DOC}$) which collected the adjusted R^2 from the model summaries for each wavelength. This was done for both salinities. Figure 7 gives an overview of the adjusted R^2 for all the models of the different wavelengths and shows the comparison of the additive and interaction models for PSU = 0 and PSU = 33. The line charts are similar for both salinities as the models fit the best at low wavelengths, both for PSU = 0 and PSU = 33. In freshwater (PSU = 0) the models stabilize at adjusted $R^2 = 0.75$ after a dip around 425 nm (Figure 7 A), i.e., 75% of the variance the response variable can be explained by the predictor variable. For the saline water, PSU = 33, the models stabilize around adjusted $R^2 = 0.50$, after a dip around 490 nm (Figure 7 B). The adjusted R^2 has higher values for PSU = 0, this means that the model fits the freshwater data better. The interaction model was slightly better at

higher wavelengths, but the adjusted R^2 for both the additive and interaction models are similar.

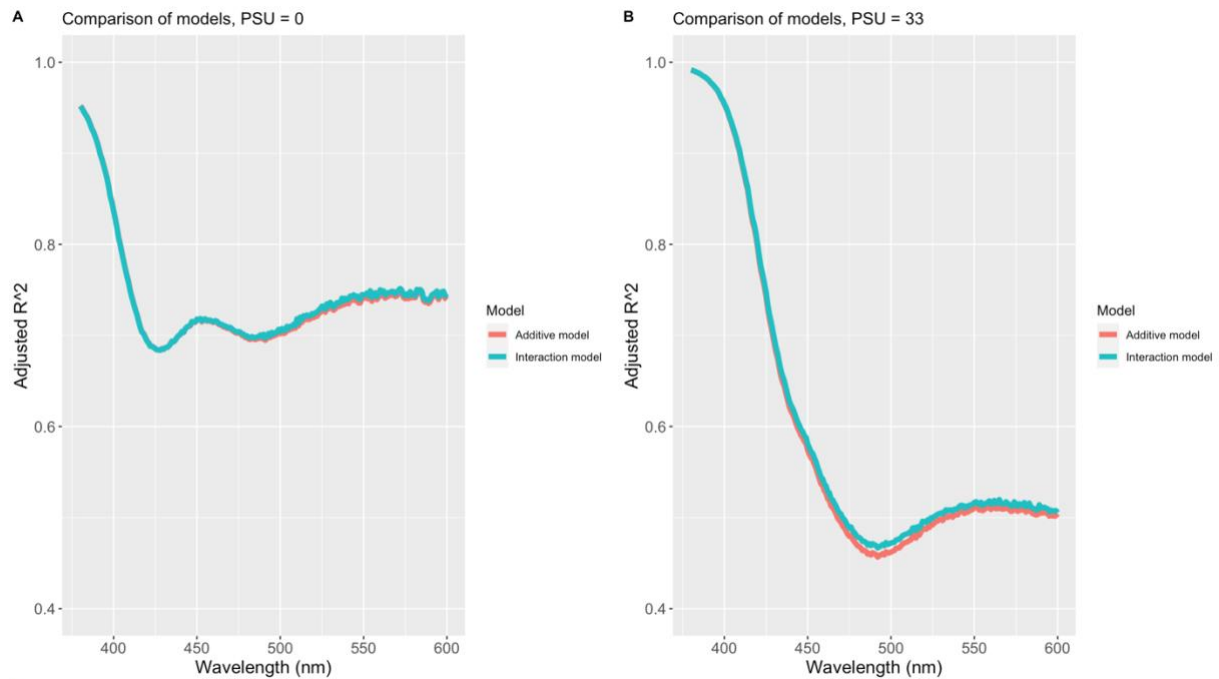


Figure 7. Comparison of the additive ($lm(CDOM \sim Fe + DOC)$) and interaction model ($lm(CDOM \sim Fe * DOC)$) for adjusted R^2 for PSU = 0 (A) and PSU = 33 (B).

The OCS for the different wavelengths is the slope from the linear models, CDOM is the response variable and DOC and Fe are the predictor variables, where one look at the change in CDOM per mg DOC or Fe. The OCS in response to DOC for the different wavelengths for both salinities are displayed in Figure 8 A and B. The figures suggest higher effect of DOM at low wavelengths. The confidence intervals are quite similar for all the wavelengths, but for the OCS of DOC in saline water the confidence intervals are wider than those in fresh water. The relationship is close to log-linear for both salinities.

The OCS in response to Fe for the different wavelengths for both salinities are displayed in Figure 8 C and D. The OCS for the Fe curves consists of two segments with a log-slope change around 425 nm. Fe affects the absorbance more towards low wavelengths, where the confidence belts are narrower. For Figure 8 D, the confidence limits at high wavelengths become negative and can therefore not be shown on a log scale.

The background absorbance (m^{-1}) in the plate with PSU = 0 and PSU = 33 differs (Figure 8 E and F). For PSU = 0 the intercept confidence intervals enclose 0 at all wavelengths (Figure 8 E), this is not the case for PSU = 33 (Figure 8 F). This indicates that there is some background absorbance for the wells with PSU = 33, and that this background is more or less constant across all wavelengths.

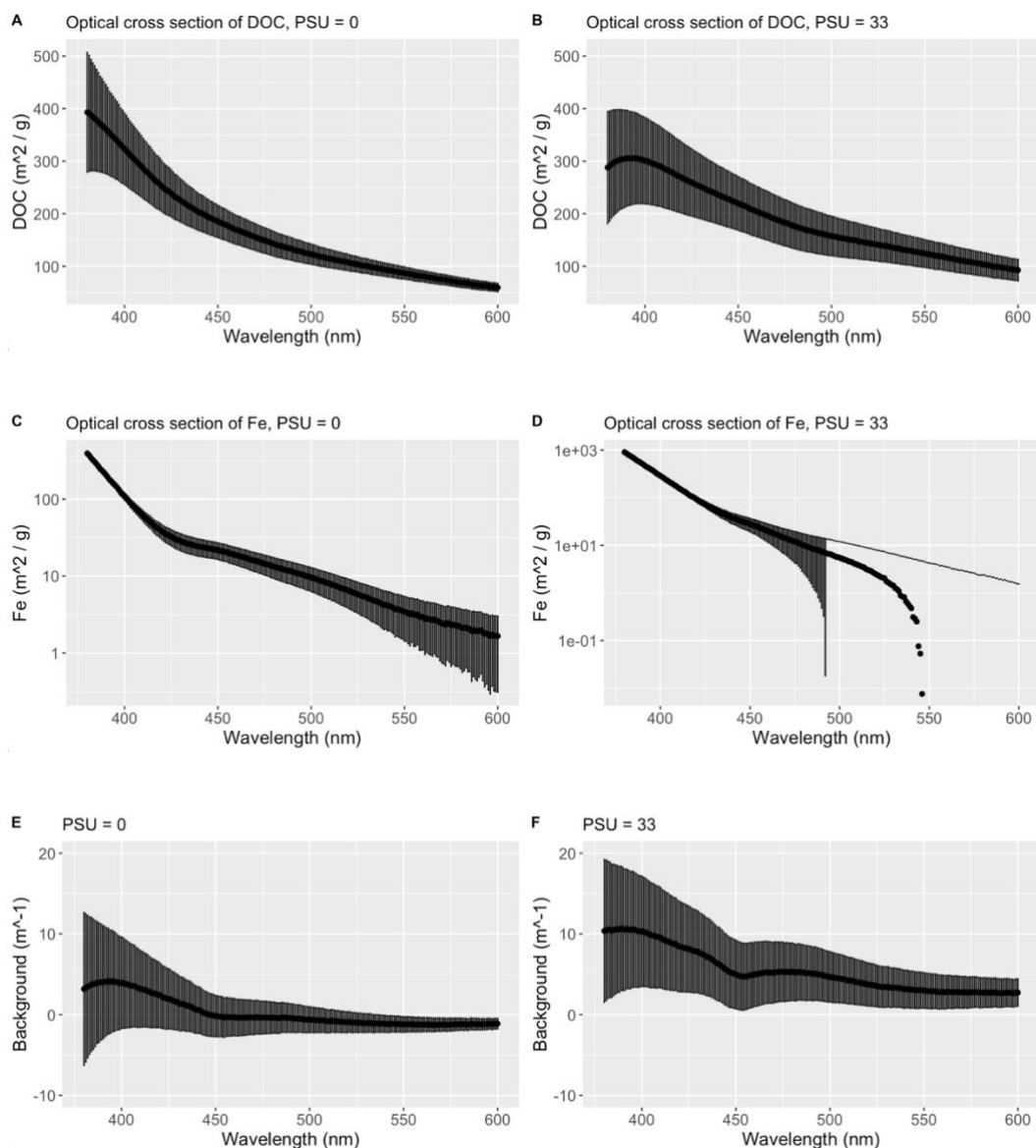


Figure 8. Overview of the optical properties of Fe/DOC from the 2D titration experiment at different wavelengths. A and B: Optical cross section of DOC for PSU = 0 and PSU = 33, C and D: Optical cross section of Fe on log scale for PSU = 0 and PSU = 33, E and F: Background absorbance (m^{-1}).

3.2 The Glomma transect

3.2.1 Determination of iron

The concentration and distribution of the iron species from the Glomma transect determined by the ferrozine method are presented in Figure 9. Most samples from the tributaries had a higher concentration of Fe(III) than Fe(II), whereas the Glomma River had higher concentrations of Fe(II) than Fe(III) (Figure 9 A). Along the transect, the concentrations of Fe are quite similar in the main river (Glomma), whilst the tributaries represent the more extreme observations. All values for total FR-Fe are below 0.1 mg/L, except G06 and G18, for the Glomma River (Figure 9 B). For the tributaries, the total FR-Fe concentrations ranged between 0.064 mg/L (G11, Vormsa) and 0.27 mg/L (G17) (Figure 9 B).

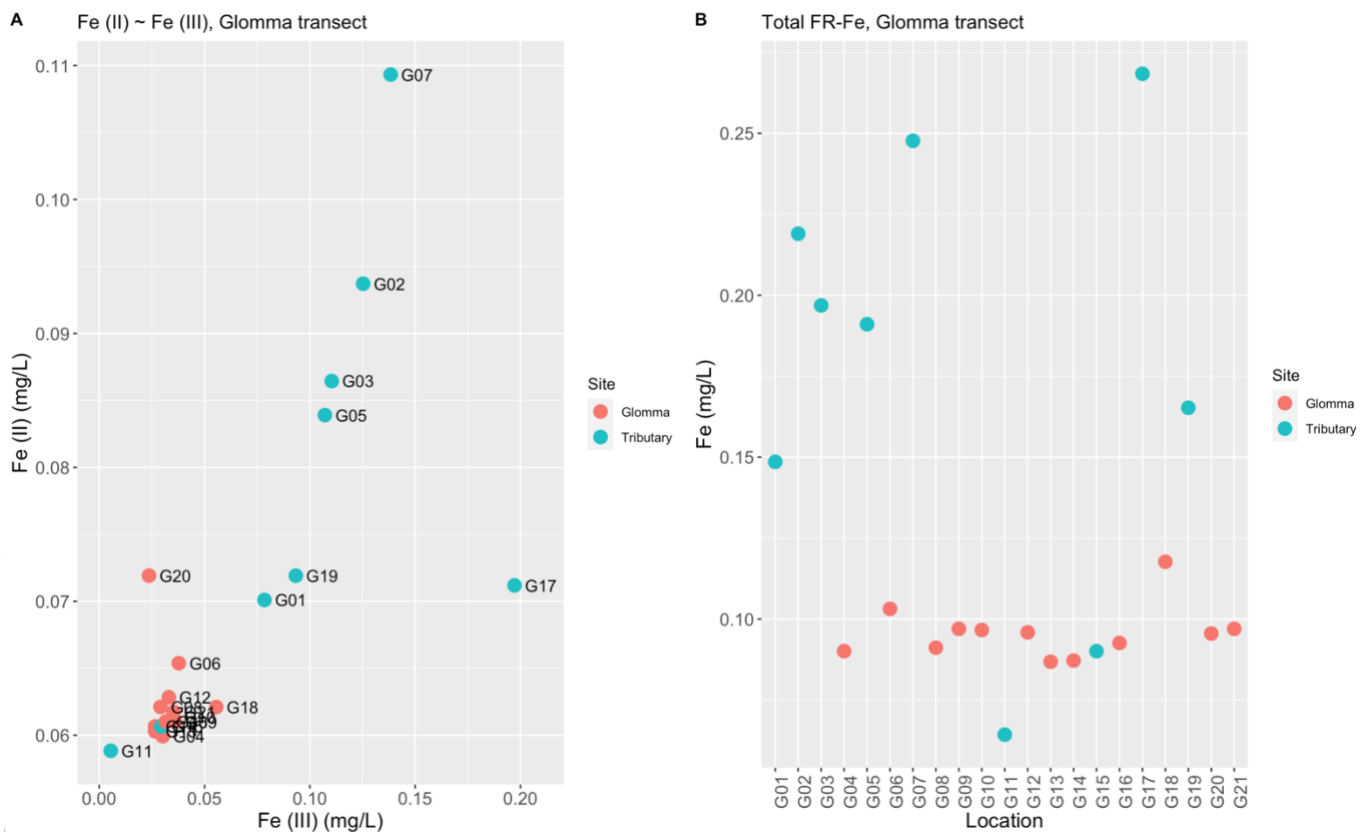


Figure 9. Iron in the Glomma transect determined by the ferrozine method: A) Determination of the concentrations of the iron species Fe(II) / Fe(III). B) Total FR-Fe concentration at each sampling site.

The two methods of measuring the concentration of Fe, the ferrozine method and ICP-OES, could lead to different results as the ferrozine method measured FR-Fe and ICP-OES measured total dissolved Fe (Figure 10). The slope for the relationship between FR- Fe and total dissolved Fe = 0.45. The adjusted R squared for the model for the Fe concentrations determined by the ferrozine method and by ICP-OES is 0.85. With respect to total dissolved Fe, the tributaries displayed a high variation, ranging from 0.099 mg/L to 0.47 mg/L, the Glomma samples are more similar.

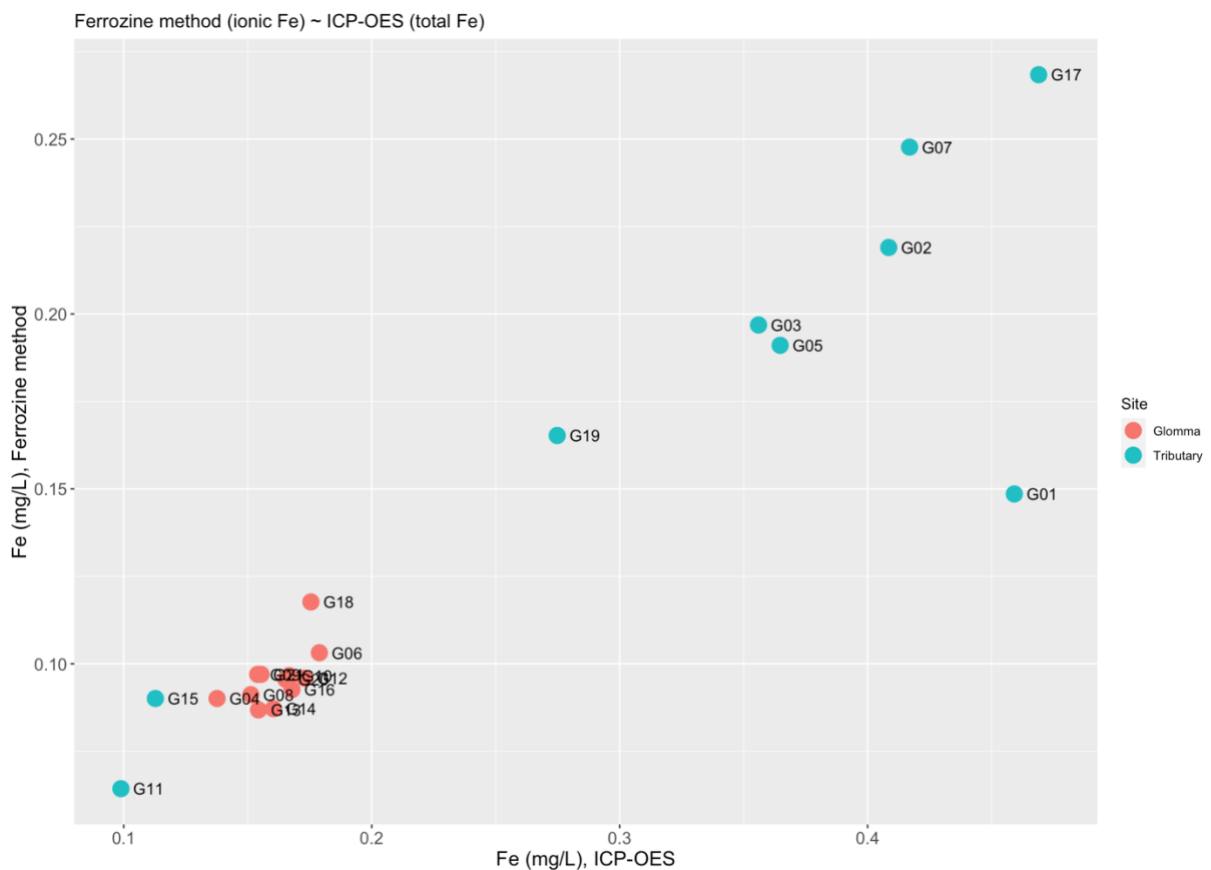


Figure 10. Fe (mg/L) from the ferrozine method as a function of Fe (mg/L) from ICP-OES.

The outermost site, G21 Fredrikstad, was strongly affected by the seawater input (Figure 32 Appendix). There was no clear correlation between Fe and the other elements determined by ICP-OES (Figure 33 Appendix).

3.2.2 Determination of organic matter

CDOM at 440 nm and the TOC concentration for all the Glomma samples are quite similar (Figure 11). The samples from the tributaries differs from the main river flow. The samples from Glomma have a concentration of TOC between 3.1 mg/L and 4.3 mg/L, and for the tributaries the concentration ranged from 2.0 to 9.3 mg/L. For the CDOM absorbance at 440 nm the Glomma samples was between 9.9 m^{-1} and 17 m^{-1} , and the tributaries ranged between 3.9 m^{-1} and 64 m^{-1} . All the tributaries, except G11, had higher CDOM absorbance and TOC concentration than the Glomma River, G15 had a similar concentration of TOC and absorbance of CDOM compared to the main river. The slope for the relationship between CDOM and TOC = 6.3, this corresponds to an optical cross section for TOC at 440 nm.

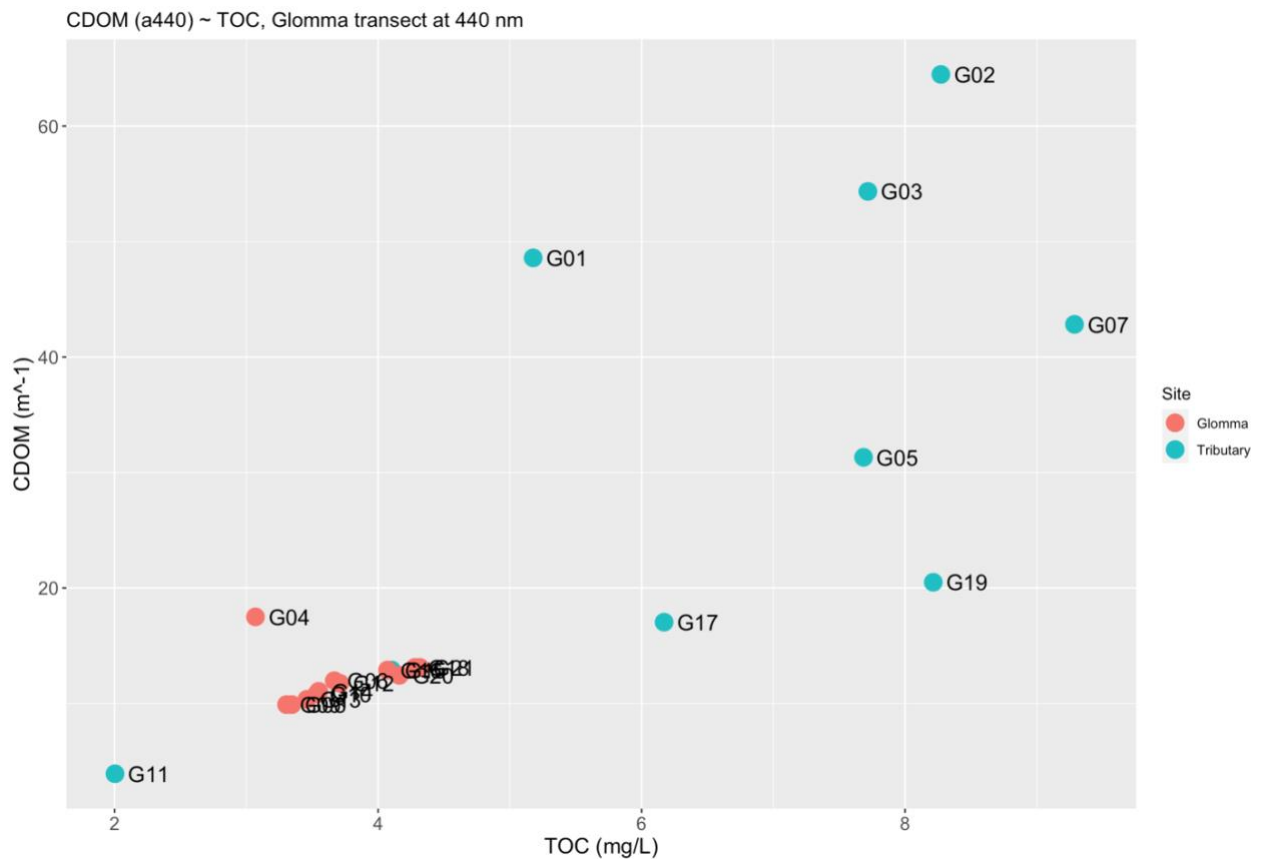


Figure 11. CDOM (m^{-1}) as a function of TOC (mg/L) for the Glomma transect.

The relationship between TOC and FR-Fe for the Glomma transect is shown in Figure 12. The adjusted $R^2 = 0.77$, indicating strong correlation between TOC and Fe. The slope = 0.025, and gives the average ratio between FR-Fe and TOC.

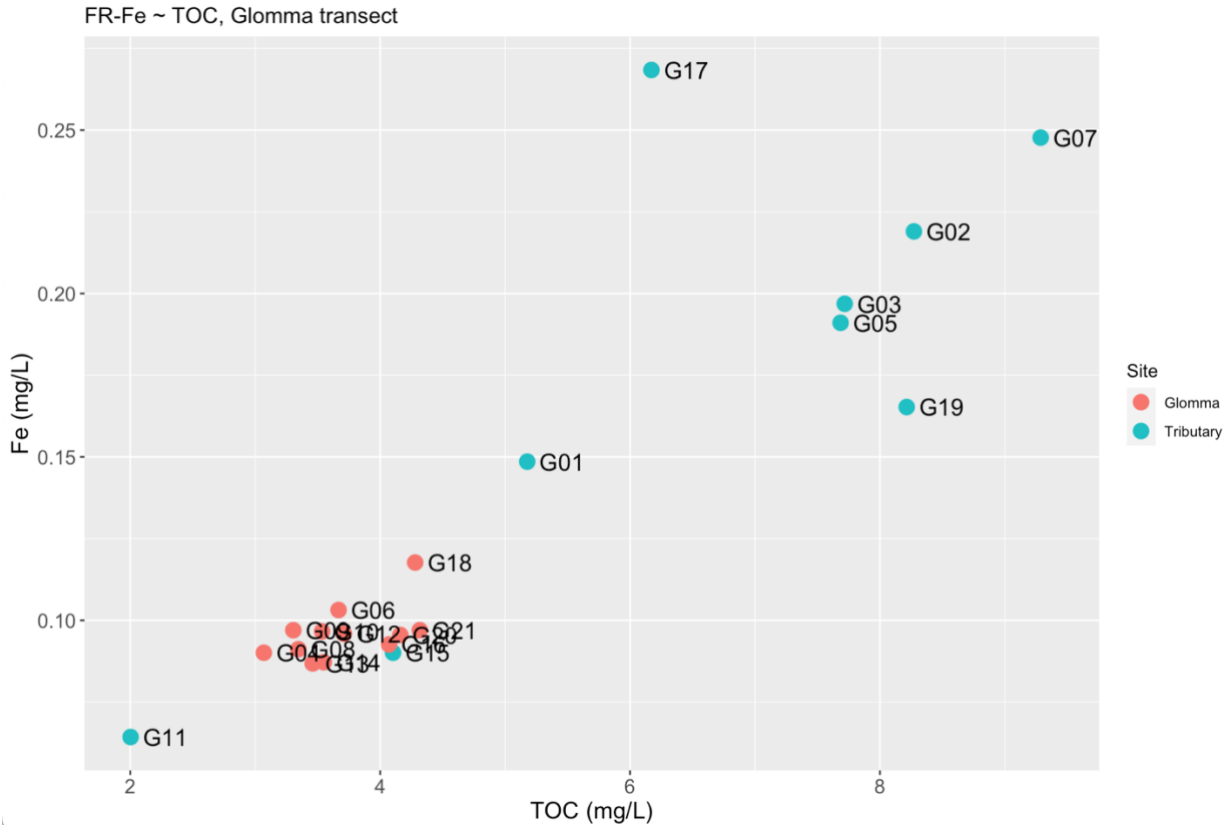


Figure 12. Total FR-Fe (mg/L) as a function of TOC (mg/L) for the Glomma transect.

The visual presentation of the distribution of total particulate matter (TPM), divided into sections of particulate inorganic matter (PIM) and particulate organic matter (POM), for the Glomma water samples is presented in Figure 13. For distribution of the data, see boxplots, Figure 36, in Appendix. G7, G17 and G19, all samples from tributaries, stands out as they hold more TPM than the all the other samples. G19 has the highest concentration with TPM = 8.36 mg/L. Of all the samples, the Vormaa tributary has the lowest concentration of particulate matter with a TPM = 0.72 mg/L. When looking at the relationship between POM and TOC the linear model, $POM \sim TOC$, gives a slope = 0.18, this indicates the proportion of POM per unit TOC.

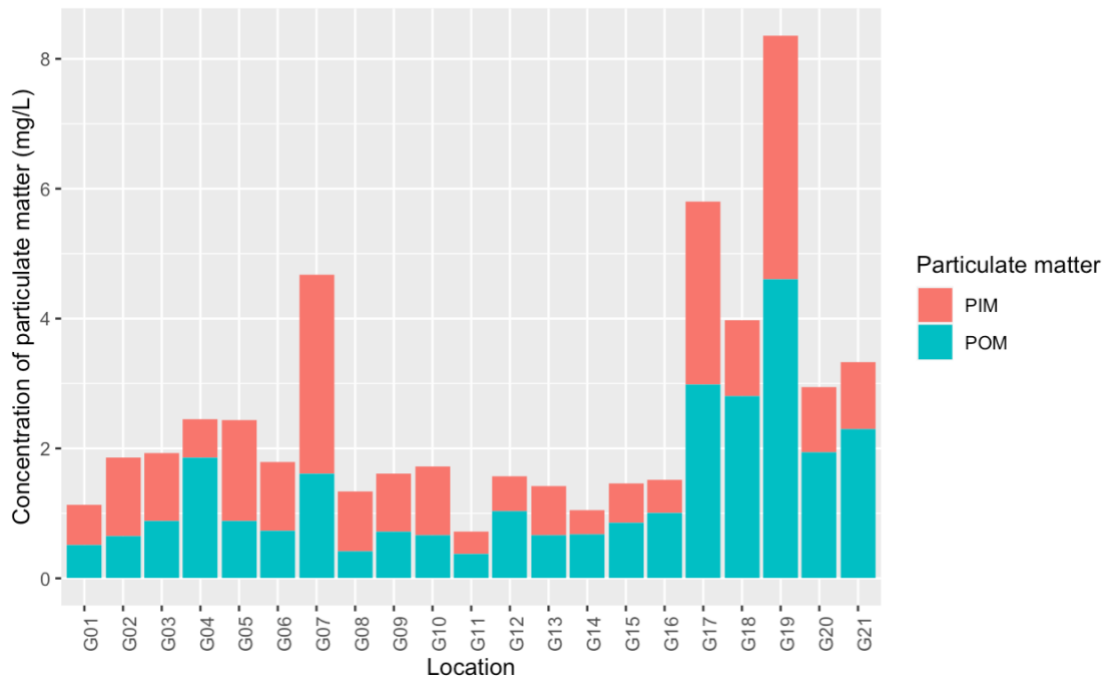


Figure 13. Distribution of PIM (mg/L) and POM (mg/L) for the samples in the Glomma transect.

3.2.3 Origin of the sample water

When trying to identify the origin of the water from the Glomma transect, the samples were analysed for the isotope ratio of oxygen, ^{18}O and ^{16}O , and deuterium/hydrogen, ^2H and ^1H . The isotopic composition of the samples was close to the global meteoric water line (GMWL) (Figure 14). The negative values of $\delta^{18}\text{O}$ indicates that there is dominance of isotopically lighter water (^{16}O) at the different sampling sites. The tributaries stand out with less negative values. Lighter isotope ratio, more ^{16}O , dominates in the Glomma River and in the tributaries G11 and G15. The relationship between TOC and $\delta^{18}\text{O}$ shows that the main river has less variability, both for the concentration of TOC and the isotopic ratio (Figure 15). G11, Vormå, is significantly different from the other tributaries.

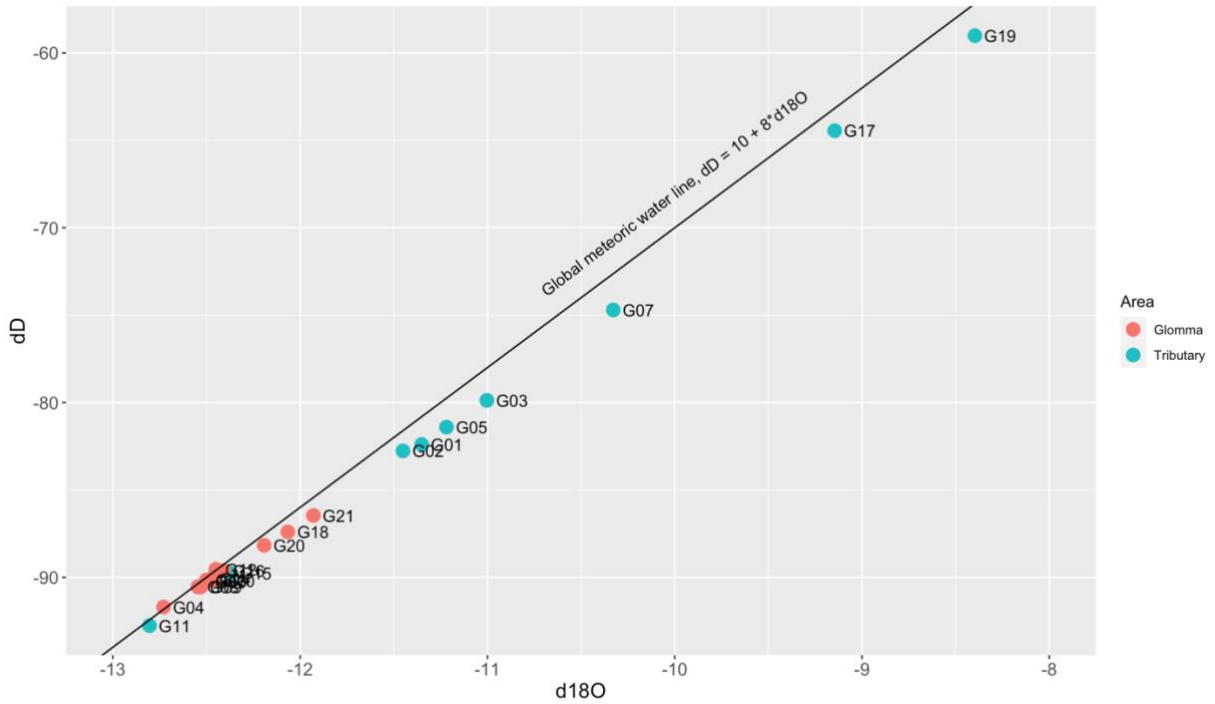


Figure 14. Global meteoric water line applied to the measurements of δD and $\delta^{18}O$. The global meteoric waterline (GMWL) was calculated by the formula: $\delta D = 10 + 8 * \delta^{18}O$ (Craig, 1961).

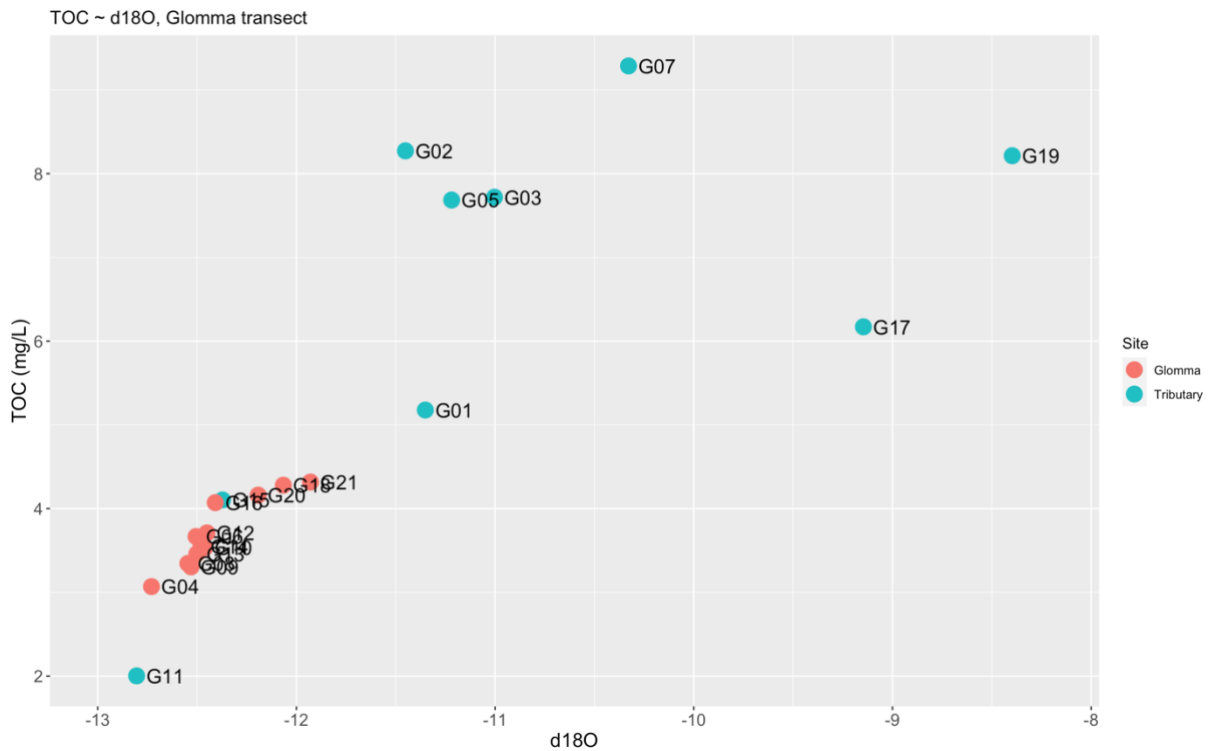


Figure 15. TOC (mg/L) as a function of $\delta^{18}O$ for samples from the Glomma transect.

3.3 The Oslofjord transect

3.3.1 CTD-data and the change in water transparency from the innermost to the outermost sampling station.

CTD profiles were made from all the stations from each cruise. All the CTD-profiles were quite similar. Figure 26 in Appendix is an example from cruise 3 station OF2 where the salinity of the surface water sample was close to 25 PSU, and the deep-water sample at 40 m was close to 32 PSU. The water temperature varied from 18°C to 11°C. The Brunt-Väisälä frequency squared (N^2) maximum, the largest density change per unit depth, indicates the location of the pycnocline. In this case, cruise 3 station OF2, it is located at 8 meters deep.

A comparison of the temperature, salinity, depth of pycnocline and Secchi depth at the different stations from the three cruises in the Oslofjord transect is displayed in Figure 16. For the “Deep” observations the deepest observation from the CTD was chosen to represent samples, close to 16 m for L1, the Glomma sample, and close to 40 m for the other sites. For the “Shallow” observations, data close to 3.5 m depth was chosen to represent the surface water. For each cruise, the shallow surface water had higher temperatures than the deep water at all the locations, but the shallow surface water follows no clear trend between stations (Figure 16 A). The salinity of the deep water was quite similar for all the sample sites, and the surface water followed a clear gradient from lowest to highest PSU from the innermost to the outermost station for all cruises (Figure 16 B). The water was the freshest at site L1 and most saline at site OF2. The pycnocline varied from the first to the last two cruises, but not for the innermost site L1 (Figure 16 C). The Secchi depth at the different stations from cruise 2 and 3 also followed a clear trend where the water transparency increases from the innermost station at Glomma, L1, to the outermost station at Missingene, OF2 (Figure 16 D).

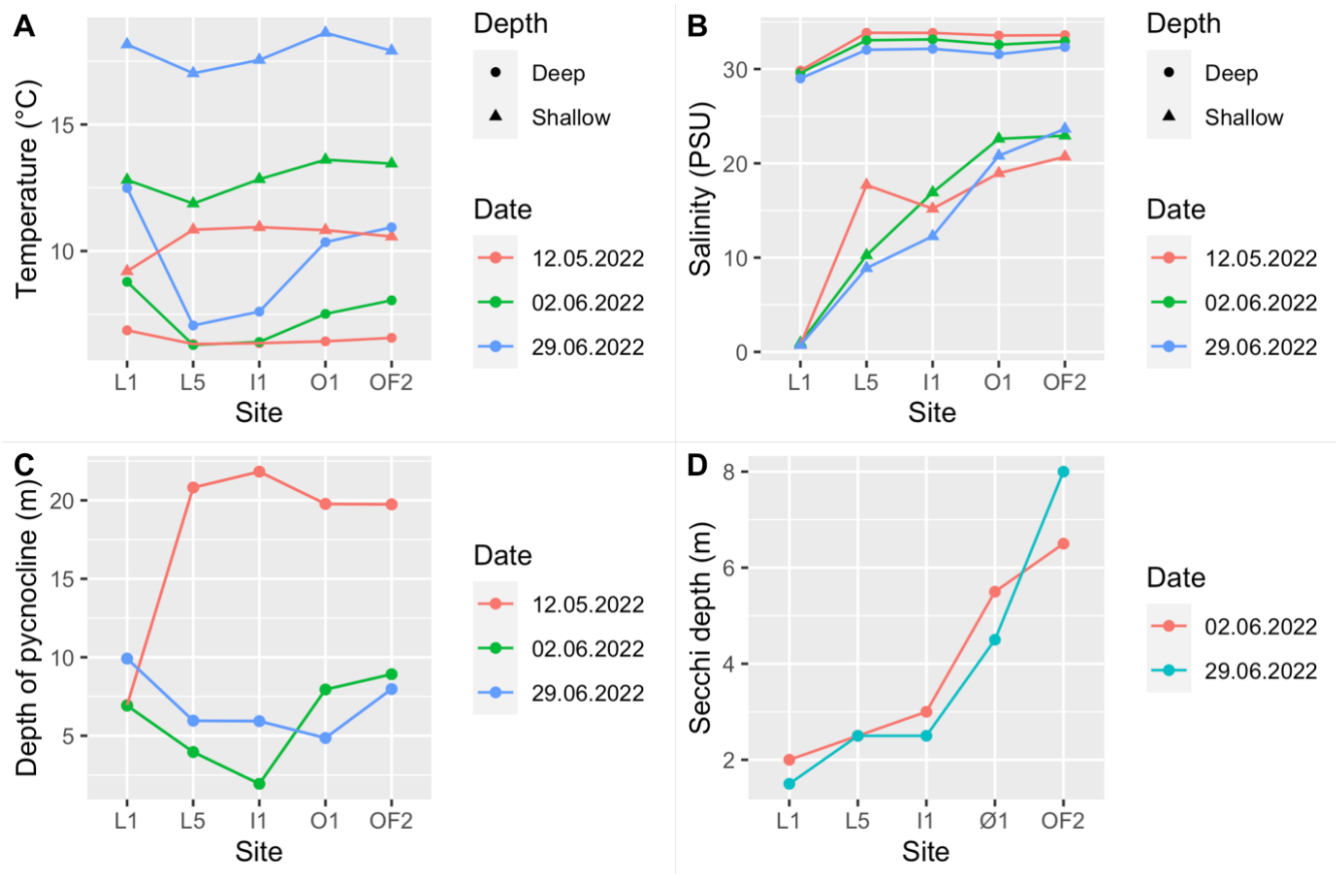


Figure 16. Comparison of parameters describing the different sites in the Oslofjord transect; A = Temperature (°C), B = Salinity (PSU), C = Depth of pycnocline (m), D = Secchi depth (m).

3.3.2 Determination of iron

To investigate the fate of Fe from the river mouth of Glomma to more coastal areas, the concentration of FR-Fe and the determination of the Fe species at the different sites from the Oslofjord transect was determined by the ferrozine method (Figure 17). As the values for the shallow L1 sample (Glomma under the Fredrikstad bridge) was significantly higher than for the rest of the values (total FR-Fe = 0.27 mg/L), this sample is not displayed in Figure 17, but in the Appendix (Figure 30). The differentiation of the iron species is shown in Figure 17 A. Fe(II) is the dominating iron species for all the samples, except for the surface water sample at L1. Figure 17 B compares total iron at the different depths at the different sites in the Oslofjord. The iron concentrations in the Oslofjord transect decreases as the water becomes more oceanic. The shallow Glomma sample, L1, had the highest concentration of

FR-Fe (0.27 mg/L), the rest of the samples had concentrations between 0.073 mg/L and 0.089 mg/L.

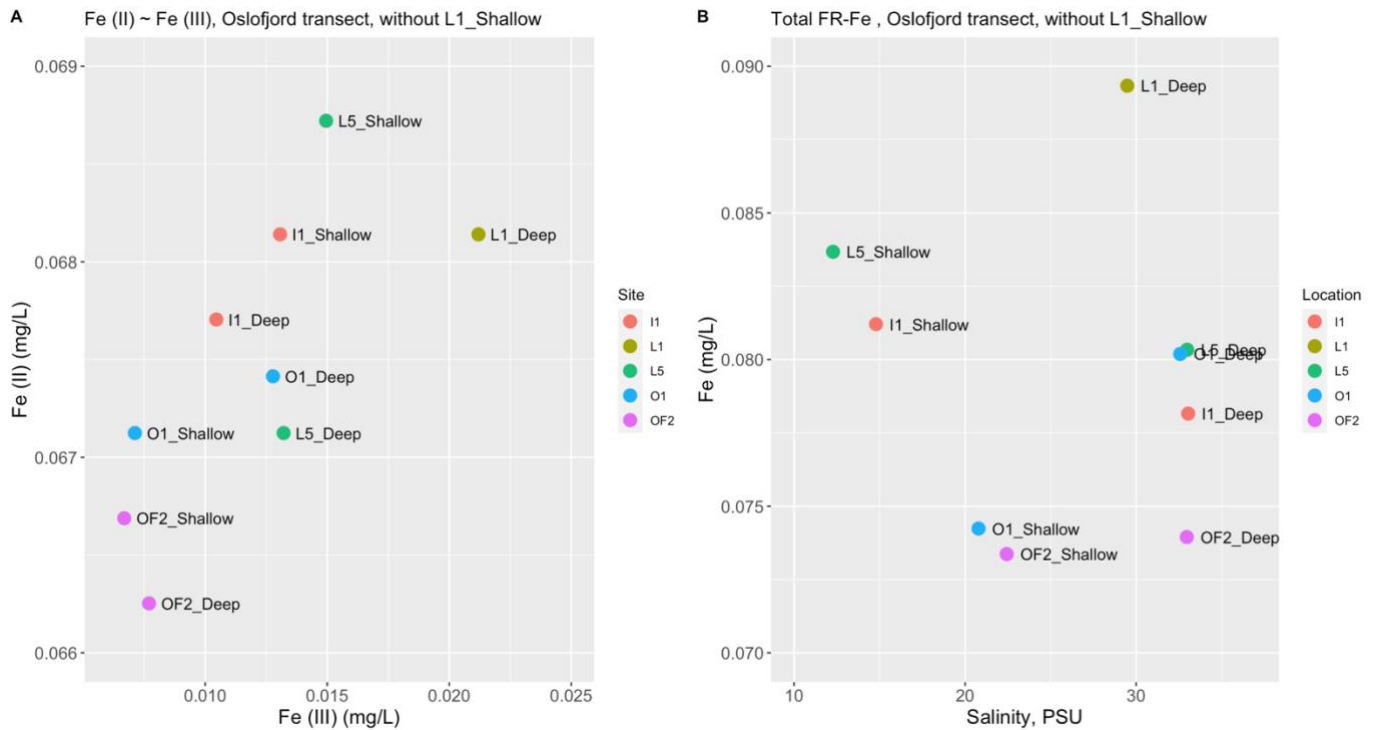


Figure 17. Iron in the Oslofjord transect determined by the ferrozine method: A) Determination of the concentrations of the iron species Fe(II) / Fe(III). B) Relationship between the concentration of total FR-Fe and salinity at each sampling site.

3.3.3 Determination of organic matter

TOC in the surface water followed a gradient where the concentration of TOC was highest at the innermost station (TOC = 3.5 mg/L), and lower at the outermost station (TOC = 2.3 mg/L), whilst the deep-water samples had a more stable concentration throughout the transect ranging between 1.2 and 1.7 mg/L (Figure 18). All the shallow water samples contain a higher concentration of TOC than the deep-water samples.

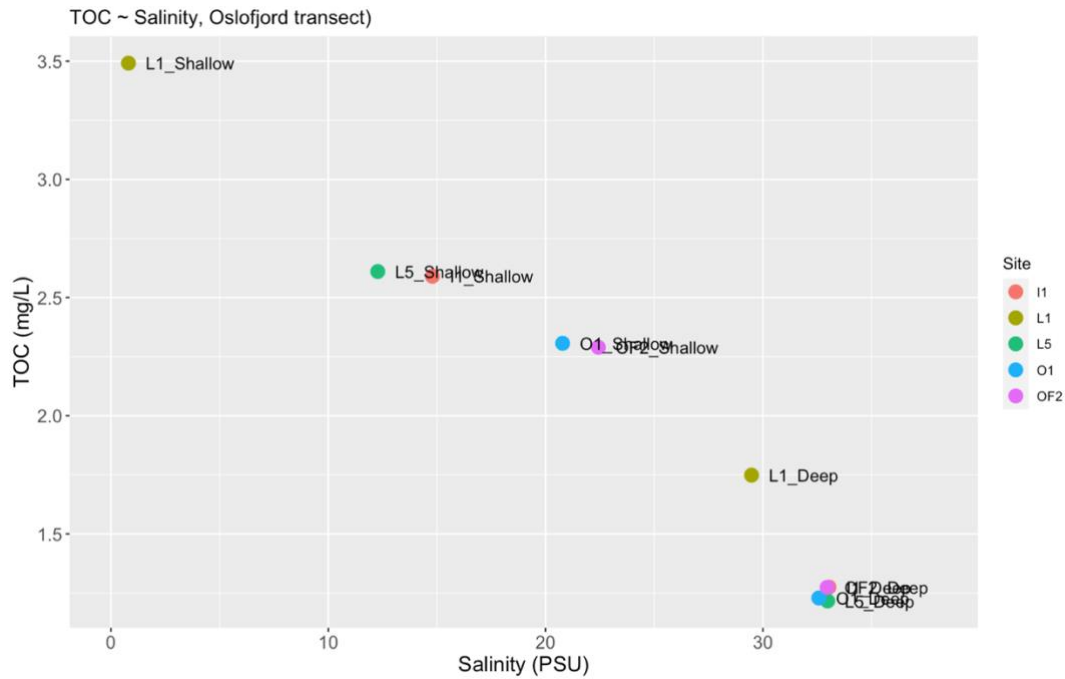


Figure 18. TOC (mg/L) as a function of salinity (PSU) for the Oslofjord transect.

All the deep-water samples have lower concentrations of TOC and lower absorbance of CDOM at 440 nm than the shallow water samples (Figure 19). The deep-water samples had $CDOM < 5 \text{ m}^{-1}$, and the shallow samples ranged between 4 m^{-1} and 13 m^{-1} . The OCS for TOC at 440 nm corresponds to the slope for this relationship = 3.8.

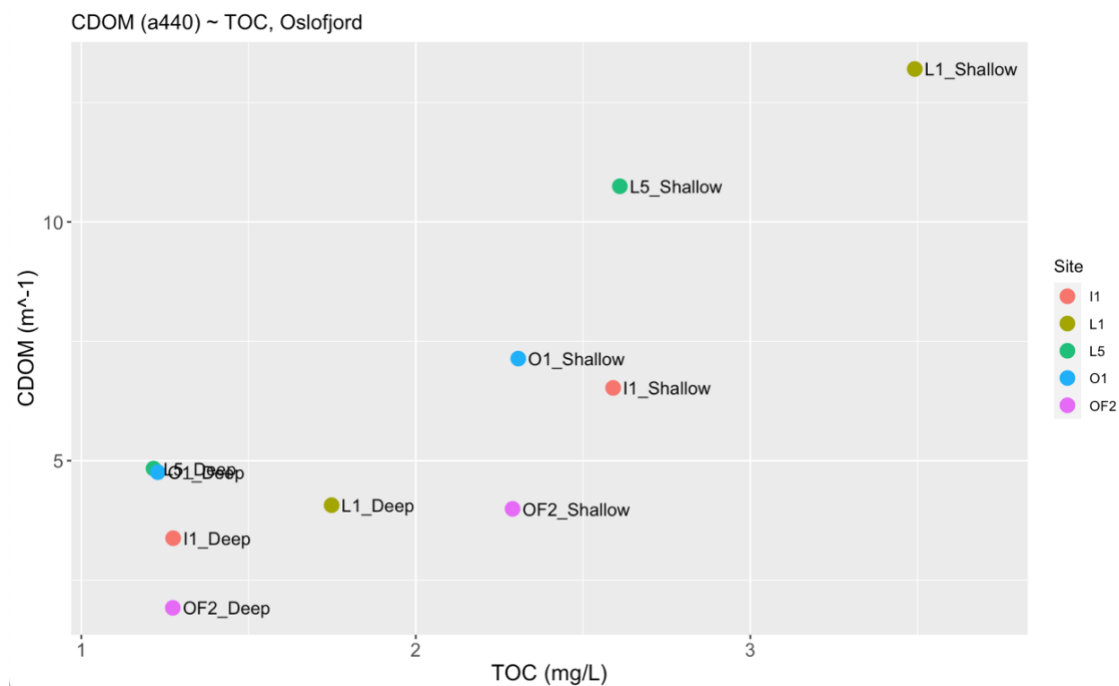


Figure 19. CDOM (m^{-1}) as a function of TOC (mg/L) for the Oslofjord transect.

The relationship between FR-Fe and TOC for the Oslofjord transect is displayed in Figure 20, Figure 31 in Appendix is including L1_Shallow. The slope for the Oslofjord transect 0.00045 without the extreme outlier L1_shallow, and 0.52 with L1_Shallow. The adjusted $R^2 = 0.38$ (-0.14 without the extreme outlier L1_shallow).

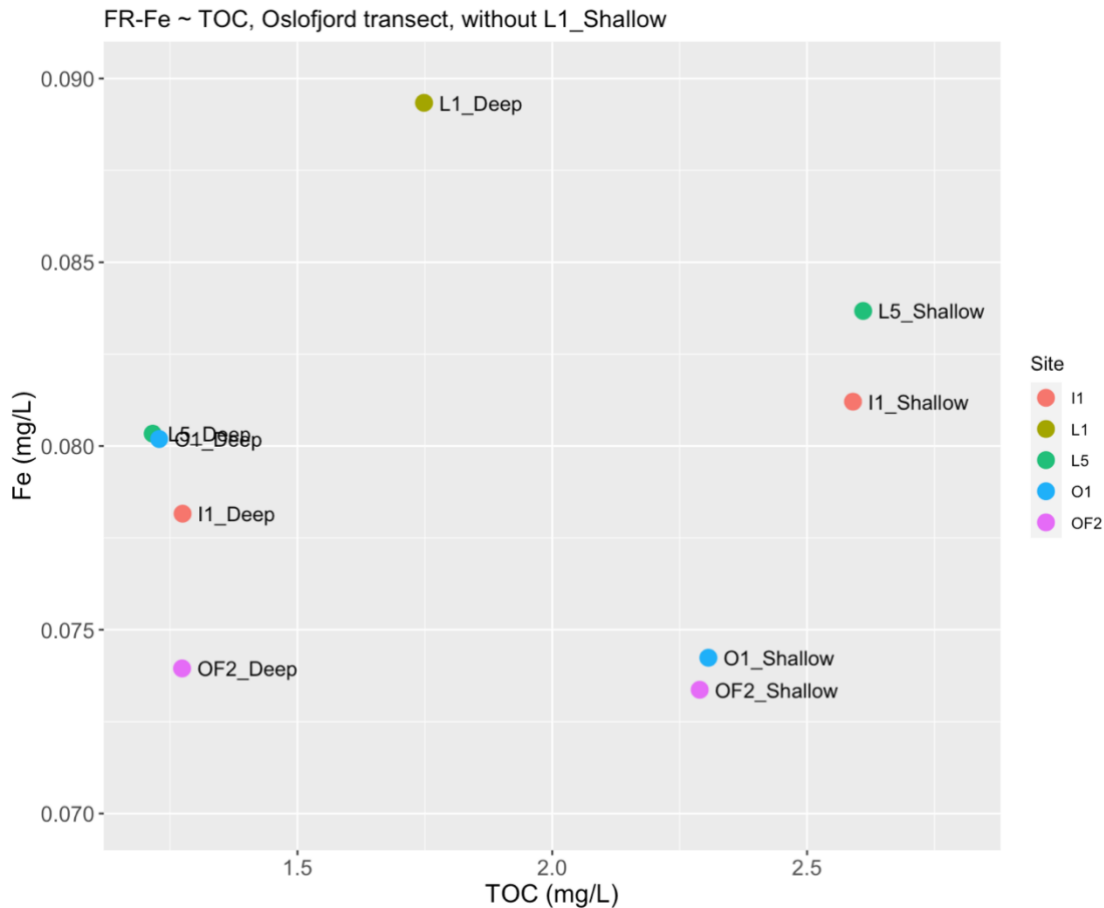


Figure 20. FR-Fe (mg/L) as a function of TOC (mg/L) for the Oslofjord transect, without L1_Shallow.

Freshwater and marine endmembers of CDOM, TOC and Fe were predicted from the data from the Oslofjord transect (Figure 21). The values were predicted from linear models with salinity as predictor variable for PSU = 0 and PSU = 33. All the predicted endmembers were higher in fresh water. For CDOM, the predicted endmembers were between 10 m^{-1} and 15 m^{-1} for the fresh water (PSU = 0), and between 1.7 m^{-1} and 4.8 m^{-1} for saline water (PSU = 33). For TOC, the predicted endmembers were between 3.3 mg/L and 3.9 mg/L in fresh water, and 1.2 mg/L and 1.5 mg/L in saline water. The predicted values for Fe ranged

between 0.11 mg/L and 0.27 mg/L for fresh water and 0.016 mg/L and 0.11 mg/L for saline water.

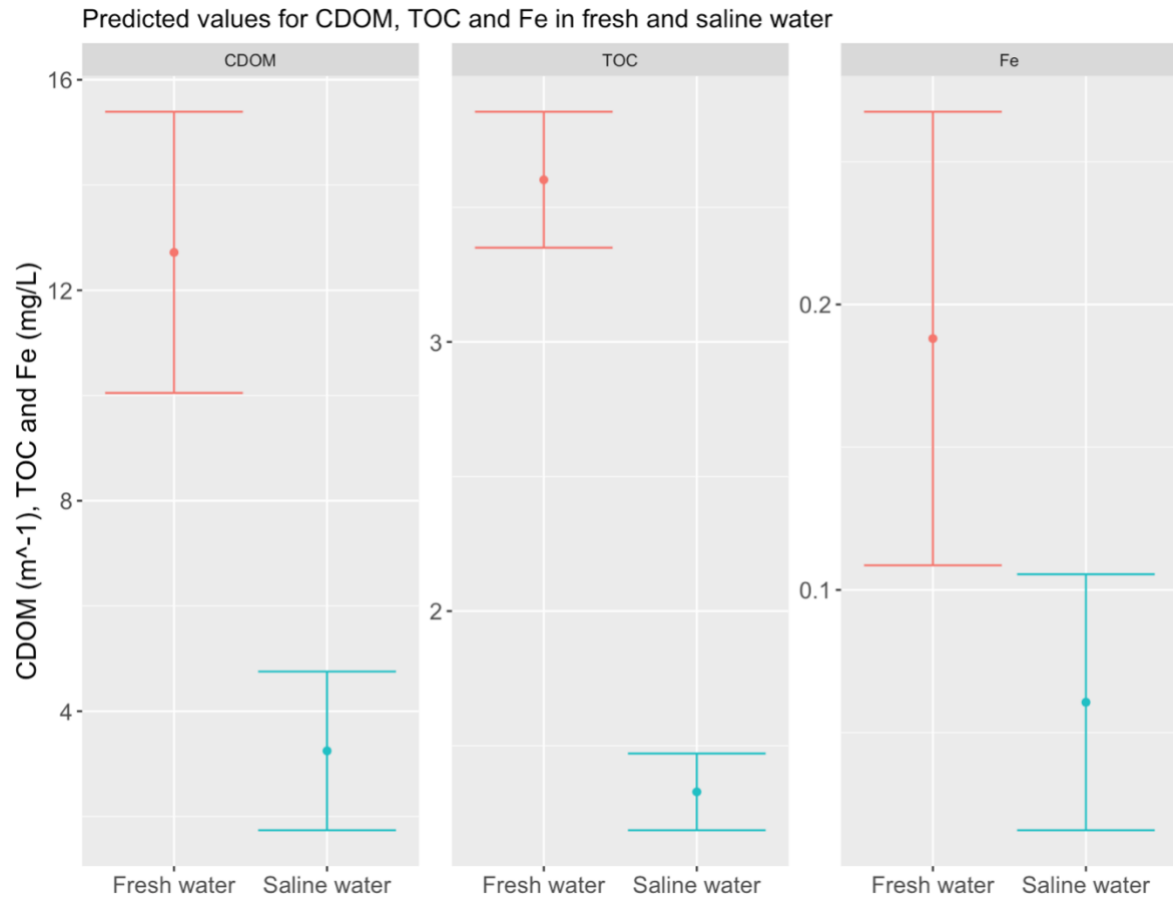


Figure 21. Predicted freshwater and marine endmembers for CDOM (m^{-1}), TOC (mg/L) and Fe (mg/L).

3.4 Comparison of the Glomma and Oslofjord transect

The FR-Fe and TOC concentrations from the samples from both the Glomma and Oslofjord transect are displayed in Figure 22. The samples from the tributaries are more scattered and have higher concentrations of both TOC and FR-Fe than the other samples. The Glomma samples are more similar in Fe and TOC concentrations, and the data points are therefore closer together. The samples from the Oslofjord transect is also closer to each other with lower concentrations of both Fe and TOC, except the shallow L1 sample. For both the

transects, the adjusted $R^2 = 0.57$, and the slope of the relationship between Fe and TOC = 0.021. This indicates the amount of Fe per TOC (in mg/L) present in the samples.

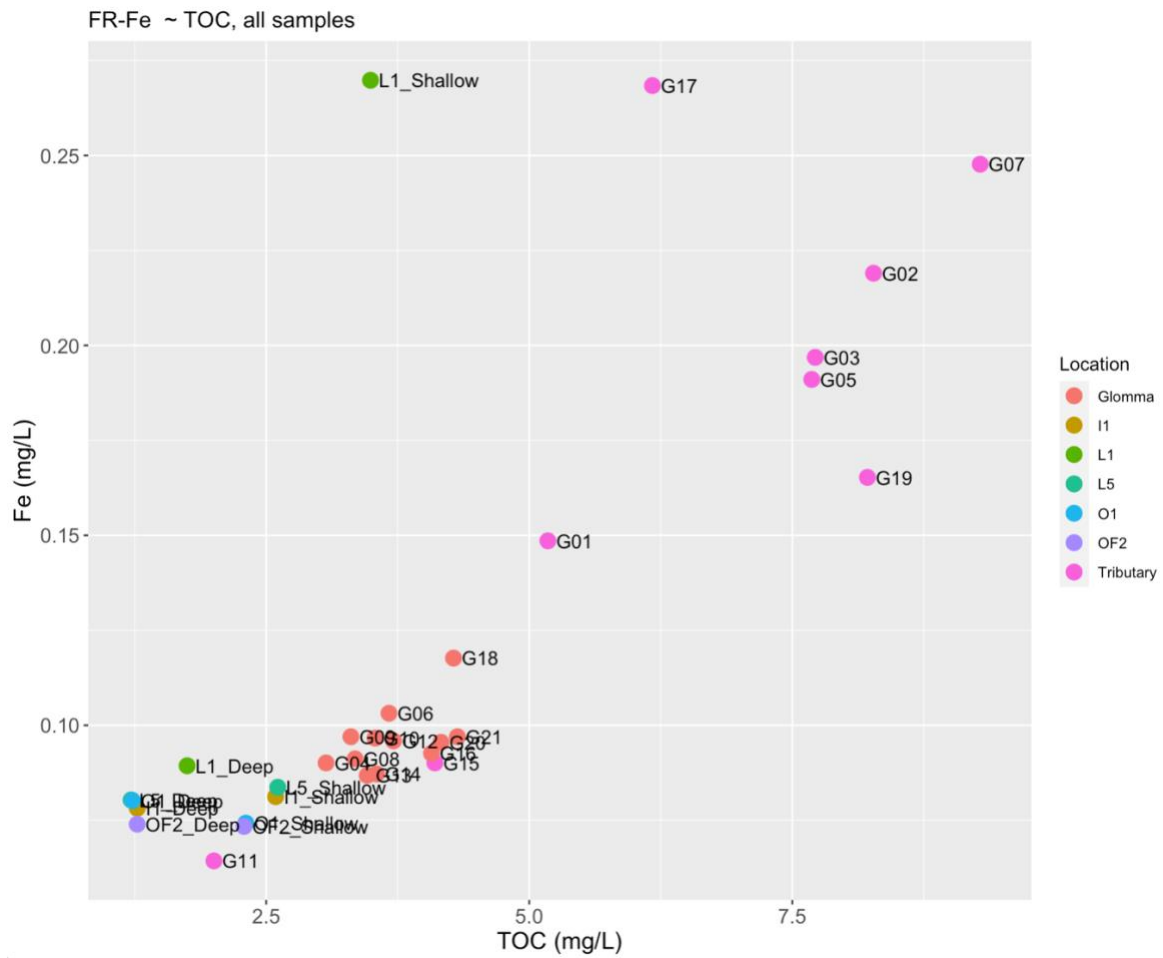


Figure 22. Total FR- Fe (mg/L) as a function of TOC (mg/L) for all samples.

The trend is the same for the plot of the relationship between CDOM and TOC where the tributary samples have the highest concentrations and are the most scattered, and the Oslofjord samples have lower values of CDOM and TOC than the samples from the Glomma transect (Figure 23).

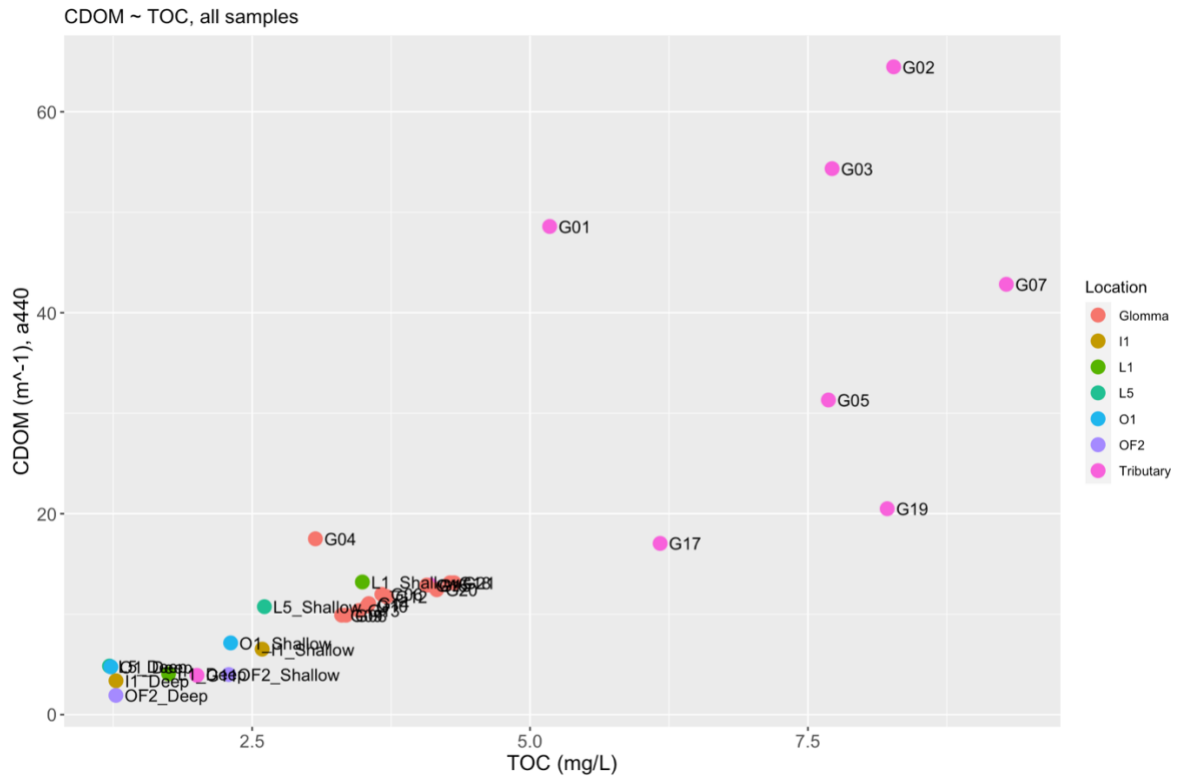


Figure 23. CDOM (m⁻¹) as a function of TOC (mg/L) for all samples.

4 Discussion

4.1 The effects of DOC and FeCl₃ on water colour

From the introduction we hypothesised that iron strongly would affect the chromophoric properties of DOC. The results from the 2D titration experiment with freeze dried DOC and FeCl₃ shows that the interaction link in the models is weak. The interaction model was slightly better than the additive model at higher wavelengths, but the interaction link is still insignificant. This indicates that Fe will not affect the optical properties of DOC, at least not on the time scale of this experiment. Thus, the effects of DOC and Fe on absorbance appear to be additive.

The comparison of the additive and interaction model, with the adjusted R² values, for the different salinities shows that all the models are better at low wavelengths (Figure 7). This could be due to the low absorbance of Fe and DOC at high wavelengths. At higher wavelengths, the absorption is slightly affected by the interaction between DOC and Fe. But, since the interaction link is very weak, we assume an additive effect for the relationship between Fe and DOC for all wavelengths. As both DOC and Fe absorb light, an addition of Fe will increase the water colour (Kritzberg & Ekström, 2012; Maloney et al., 2005). An additive effect of Fe and DOC on absorbance is also suggested by Weyhenmeyer et al. (2014).

As the effects of Fe and DOC on absorbance appear to be additive, the effect of a given concentration of DOC is the same regardless of the concentration of Fe, and vice versa. The effects of both DOC and Fe are greatest at low wavelengths. Since the slopes differs from each other, Figure 8 A-D, the absorption of the substances can be the same at one wavelength and differ in other parts of the spectrum. Thus, the effects on water colour could differ at different wavelengths.

There is some background absorbance for PSU = 33 as the intercepts does not enclose zero, Figure 8 F. This background absorbance could appear due to the addition of NaCl to the water, as increased concentrations of the salt increase the absorption of light (Li et al.,

2015). This could indicate that there already is more absorption/scatter of light in saltwater environments.

DOC and Fe primarily absorb light at low wavelengths (Figure 5 and 6). From the optical cross sections, one sees that the effect of DOC and Fe is higher in the blue-violet part of the visible spectrum, and that the effect is less significant at higher wavelengths, yet the wide confidence intervals of the OCS of DOC also point to the higher variability in the lower end of the spectrum.

The absorption spectra of Fe, Figure 5, shows that Fe have higher absorbance at PSU = 33 than at PSU = 0. For DOC, this trend is opposite, Figure 6, clearly demonstrating the modifying impacts of salinity, either directly by changing the chromophoric properties in response to surface charges and 3D structure of the humic compounds, the interactions between DOC and Fe, or eventually also changing the Fe speciation. For both substances, the absorption of light increases with increasing concentration. It was difficult to locate any literature addressing this effect of Fe/DOC and salinity alone, but in estuarine systems, the Fe-OM complex is demonstrated to have high stability along a salinity gradient, as other forms of Fe, e.g., Fe (oxy)hydroxides, are more prone to aggregate and settle into the sediments (Herzog et al., 2017, 2020).

The experiments done in this thesis and the results are not directedly transferrable to natural systems as we do not know the effects of DOC and Fe at lower concentrations and the complexation of the substances. There are some sources of error that could have affected the results in the 2D titration experiment. The freeze-dried DOC already contains some Fe, and other elements (Gjessing et al., 1999), so we do not know the optical properties of DOC alone. The concentrations used in the experiment was 100 times higher than natural concentrations. Thus, the testing was done with extreme concentrations of Fe and DOC, which are not environmentally relevant. But, with high concentrations one get more accurate measurements of absorption, and even with these high concentration we did not observe a significant interactive effect. Weyhenmeyer et al. (2014), suggests that Fe will cause additional browning of waters when in complex with DOC. The Fe-DOC complexation

is ubiquitous, due to the strong co-variation between Fe and DOC in the aquatic system (Figure 12) (Weyhenmeyer et al., 2014), but from the experiments and analysis of the field samples, nothing is known about the complexation of Fe and DOC.

4.2 The relationship between Fe and TOC - Changes along the transect

The relationship between TOC and Fe is stronger in the Glomma transect than in the Oslofjord transect. Thus, as hypothesised in the introduction, the tight correlation between TOC and Fe are more relaxed in the coastal area, reflecting an impact of salinity on TOC or Fe - or both. In general, the concentrations of both TOC and Fe are the highest in the Glomma transect, especially in the tributaries, which are more directly affected by the terrestrial input. The concentrations of TOC and total Fe follow the same trends (Figure 22). The adjusted R^2 for the relationship between TOC and Fe in the Glomma transect and the Oslofjord transect shows a decrease in correlation of the parameters, this indicates that the substances have different fates in the different areas. The origin of both OM and Fe in the aquatic environment are mainly terrestrial (Aitkenhead et al., 1999; Kritzberg & Ekström, 2012), and the concentrations of these substances get diluted on its way from terrestrial areas to the open ocean. It is suggested that similar drivers, e.g., afforestation, are making more DOC and Fe available for export to the aquatic systems (Bowering et al., 2020; Škerlep et al., 2020), yielding a close association between these compounds in freshwater. The outermost sites in the Oslofjord transect, with less freshwater input, gives the lowest concentrations of DOC and Fe.

4.2.1 Iron from inner Finnskogen to outer Oslofjord

The concentrations of Fe in the main river flow of Glomma display low variability, whilst the concentrations in the tributaries are more scattered (Figure 9 and 10). From the scatter plot matrix, Figure 33 in Appendix, it is evident that there is no clear correlation between Fe and the other elements analysed with ICP-OES. This suggests that different mechanisms

determines the flux of the different elements into the aquatic environment, while similar mechanisms controls the concentration of Fe and DOC (Kritzberg & Ekström, 2012).

The concentration of Fe along the marine transect in the Oslofjord declines from the innermost to the outermost station as the coastal water is less affected by freshwater input, Figure 17 B. There are higher concentrations of Fe in the shallow marine water samples which are most affected by the freshwater runoff. This relationship shifts for the two outermost stations. Iron is an important micronutrient, and as the river input decreases, the water masses become more depleted of essential nutrients. In open ocean areas with small freshwater input, Fe could be a limiting nutrient for primary production. Addition of Fe in such areas could increase the primary production, and bind more CO₂ from the atmosphere (Aumont & Bopp, 2006), but this is not as relevant for coastal areas.

The results from the analysis of the two iron species, Fe(II)/Fe(III), shows that the concentration of Fe(II) is dominating in the large water streams, Glomma and Vorma, and in the Oslofjord transect. In most of the tributaries, however, the concentration of Fe(III) has a larger portion of the total FR-Fe concentrations. Higher concentrations of Fe(II) is expected in coastal areas (Zhuang et al., 1995), this is also confirmed from the ferrozine method. The higher proportion of Fe(II) in the water masses may be explained by the fact that Fe(II) is more soluble as free ions (Falkowski et al., 1998), and that Fe(II) can exist under oxidizing conditions in complex with humic substances (Suzuki et al., 1992). Fe(II) is also known to be formed from photochemical reduction of organic Fe(III) complexes (Rose & Waite, 2003). This suggests more reducing conditions in the main river than in the tributaries, or that Fe(II) is complexed with OM.

For the shallow L1 sample, Glomma under the Fredrikstad Bridge, the iron concentration is significantly higher than for the other samples from Glomma and the other sampling sites in the Oslofjord transect. Based on the other samples one would not expect this high concentration of total FR-Fe. This could indicate an error in the method, or that there is some industry which releases Fe into the river around the area where the samples were collected. In general, the concentrations of Fe in the Oslofjord were low, Figure 17, and

accurate measurements of low concentrations may be difficult to detect in the microplate reader.

Despite being analysed with two very different methods, the results from ICP-OES and the ferrozine method are comparable. When comparing the Fe concentrations from the Glomma transect, based on the different methods, one sees that the samples follow the same trend, Figure 10. The concentrations of total dissolved Fe from ICP-OES are about twice as high as the concentrations of FR-Fe. The slope for the relationship between FR-Fe and Fe determined from ICP-OES, Figure 10, indicates that approximately 45% of total dissolved Fe is in ionic form. The other 55% of Fe could be bound to organic complexes, making Fe(II) unavailable for the ferrozine complex. The iron concentrations determined by the ferrozine method are lower than the concentrations determined by ICP-OES. As the ICP-OES is a very sensitive instrument, a suggestion would be to trust the concentrations determined by this method the most. There are several sources of error for the ferrozine method, e.g., that the ferrozine have not bound to all the Fe(II) in the sample tube, or that the reduction agent has failed to reduce Fe(III) to Fe(II) (Luther et al., 1996). Thus, there are multiple factors that could affect the determination of Fe(II) / Fe(III) and total FR-Fe. The sample water used in ICP-OES was filtered, removing large, aggregated particles, possibly containing Fe.

4.2.2 Organic matter from inner Finnskogen to outer Oslofjord

The samples from the main river flow of Glomma have similar concentrations of TOC, whilst the tributaries have more extreme concentrations (Figure 11). This is also the case for the analysis of CDOM and PM. The tributaries are probably strongly affected by the surrounding areas and the forest soils which contributes to elevated concentrations of PM, and thus TOC and CDOM. The innermost sites in the Glomma transect, in the Finnskogen area, have a higher proportion of CDOM per TOC than the sites further down the transect, this suggest that these areas are more affected by CDOM from the forest soils. One could also see the differences in water colour at the different sites directly during the sampling (Figure 4).

The relationship between POM and TOC indicates that 91% of TOC is dissolved. From the analysis it was determined that 18% of TOC is POM, and as the carbon content in POM is approximately 50% (Noji et al., 1993), the results from the determination of particulate organic matter correlates with the findings of that and 90-95% of TOC is dissolved (de Wit et al., 2007).

The concentration of TOC and absorption of CDOM decreased from the innermost to the outermost station in the Oslofjord transect as the freshwater input declined. For the determination of TOC, there is a clear trend where the concentration of TOC is higher in the shallow water samples than in the deep-water samples, and the measured concentrations of TOC decline from the innermost to the outermost sample site. The trend is the same for the absorption of CDOM where all the deep-water samples have more similar absorption at 440 nm. The surface water samples have higher CDOM absorbance, following the same trend as the measurements of TOC, with higher absorbance at the innermost site. This clearly shows the contribution of freshwater to the concentration of TOC and absorption of CDOM in the coastal area, and that the dilution effect/ removal of TOC is significant.

4.2.3 The Glomma transect

From all the analysis, the main water flow of Glomma has a similar composition of both Fe and TOC, whilst the concentrations in the tributaries have more extreme observations and is very different from each other. Glomma is a relatively large river and it is reasonable that the water composition is about the same throughout the river channel. This indicates that the surrounding areas affect the small water streams more than for Glomma where the concentrations of the substances are more diluted in the large water masses.

Negative values of $\delta^{18}\text{O}$ indicates that there is dominance of isotopically lighter oxygen isotope (^{16}O) for all the samples, which is normal in evaporative systems (Gat, 1996). $\delta^{18}\text{O}$ values for rain water are more negative than $\delta^{18}\text{O}$ for soil water as ^{16}O evaporates (Hsieh et al., 1998). More negative values, a greater portion of the lighter isotope ^{16}O , indicates that the sites with the lowest $\delta^{18}\text{O}$ values are more affected by rainwater than soil water. The

results from the cavity ring-down spectroscopy indicates that most of the tributaries consists of a bit more soil water than the main river flow of Glomma as they stand out with less negative values of $\delta^{18}\text{O}$. The isotope data follow a linear trend, most of them differs slightly from the global meteoric water line (GMWL), Figure 14. The isotopic composition of the tributaries is more scattered and differs from the main river flow. This indicates that there is a build-up of the heavy isotopes at these sites, or that they are more affected by soil water. The concentrations of Fe and DOC also appear to be high at the same sites as the tributaries are more affected by soil water. Subsequently, the flux of substances from the soil to the aquatic environment is higher at these sites, thus indicating that the sites with higher $\delta^{18}\text{O}$ will have higher concentrations of Fe/DOM (Figure 12 and 15). The concentration of Fe and DOC, and thus water colour, has a certain connection to the origin of the water, and the impact of the inflow from tributaries gets diluted in the large river as lower levels of DOC and Fe were observed here.

G11, Vormå, and G15, Øyern, are more comparable to the Glomma River than the other tributaries in the transect. The samples from the tributary Vormå, G11, stands out with lower concentrations of both TOC and Fe, and have the highest ^{18}O depletion. Vormå flows from Norway's largest lake, Mjøsa, and was the largest tributary sampled from. The residence time in Mjøsa is long, approximately 5 years, and numerous factors, both biotic and abiotic, determine the available TOC and Fe for export (Dillon & Molot, 2005). DOM may accumulate with Fe and other particles, thus removing both Fe and DOC from the water column by settling into the bottom sediments in Mjøsa (Einola et al., 2011). Photomineralization in lakes may also remove DOC from the water column by the production of CO_2 (Alleson et al., 2021).

4.2.4 The Oslofjord transect

The water transparency in the Oslofjord transect follows a gradient from the innermost to the outermost station (Figure 16 D). This also correlates with the concentrations of Fe and TOC at the different sites. The surface samples represent water over the pycnocline, and the deep samples are sampled under the pycnocline. The salinity gradient of the surface water,

Figure 16 B, indicates which samples are most and least affected by the freshwater stream. The stations with less freshwater input, and thus lower concentrations of Fe and TOC, have less water colour. The concentrations of Fe and TOC in the Oslofjord are highest at the innermost sites. The predicted endmembers also suggest higher concentrations of TOC, Fe and CDOM absorbance in freshwater. Increased input of riverine discharge increases the potentially bioavailable Fe in the outer Oslofjord system (Kritzberg et al., 2014). For phytoplankton, the uptake of both free ions of Fe and organically bound Fe are important sources of the micronutrient (Shaked & Lis, 2012). Estuarine mixing removes Fe from the water column, and with increasing salinity, a gradual loss of iron from suspension is expected (Kritzberg et al., 2014; Sholkovitz, 1976). During estuarine mixing, Fe, both in complex and dissolved Fe, are lost to the sediment (Herzog et al., 2020). Aggregation of particles, flocculation of Fe-OM complexes, may remove both substances from the water column (Sholkovitz et al., 1978).

The Secchi disk measurements indicates a clear trend in water transparency following a gradient from the innermost to the outermost station in the Oslofjord transect. The deepest Secchi depth is at the most oceanic site, OF2, where the freshwater impact was the lowest, Figure 16 B and D. At site L1, in the Glomma River, the Secchi depth was the most shallow. The riverine discharge brings along DOC and Fe making the water less transparent (Kritzberg & Ekström, 2012).

4.3 Potential ecosystem effects

In an already pressured situation in the Oslofjord (Moland et al., 2021), the additive effect of DOC and Fe on water colour is a problem concerning aquatic life (Frigstad et al., 2020; Lampert, 1989; Mascarenhas & Keck, 2018). The ecosystem in the fjord is negatively affected by a number of factors, such as overfishing, trawling, eutrophication and hypoxia (Moland et al., 2021). The increased flux of DOC and Fe to the aquatic environment will increase the concentration of both compounds, and thus the light attenuation in the water column, making life more difficult for phytoplankton and visual predators (Frigstad et al., 2020; Kritzberg & Ekström, 2012; Lampert, 1989; Mascarenhas & Keck, 2018; Thrane et al., 2014)

A shift in the mesopelagic regime can be expected in darkening waters due to the negative effects of the reduced visibility for visual predators (Aksnes et al., 2009). Organisms with different foraging strategies, e.g. tactile predators such as jellyfish, may increase their success rate as they do not depend on their eyesight for prey foraging (Dupont & Aksnes, 2013). This could lead to a shift in the predator-prey interactions in waters with higher light attenuation (Dupont & Aksnes, 2013), possibly altering the aquatic food webs and the composition of species living there.

4.4 Future prospects

It is important to understand the mechanisms of browning waters due to the adverse effects it may cause in the aquatic environment. It is essential to link the changes in optical data with underwater light and the adverse effects on primary production and other organisms in the water column. This is especially relevant for the Oslofjord, as the ecosystem already is experiencing negative pressure from other stressors (Moland et al., 2021).

For future experiments, it could be interesting to investigate the optical properties of DOC and Fe with an extended range of different concentrations, e.g., more natural concentrations, and at different salinities. For more accurate measurements of natural concentrations, it could be an idea to perform the experiment in a cuvette with longer path length, instead of in a well plate, as the sensitivity of the spectrophotometer could limit the measurement of Fe/TOC at low concentrations. Testing the effects of pH, temperature and the effects of other metals could also be an interesting aspect.

5 Conclusions

The 2D photometric titration experiment revealed that Fe and DOC both affect the optical properties of water, and that the effects of the compounds are additive rather than interactive. The effect on absorbance of both DOC and Fe is higher at low wavelengths, but with a weak interaction link between the compounds, no additional interaction effect is expected. Thus, regardless of the concentration of Fe, the optical effect of a certain concentration of DOC in water is the same.

The results from the riverine and marine transects confirmed that the concentrations of TOC and Fe both influence water transparency, and that the relationship between the two compounds was more relaxed with increasing salinity. The strong correlation between TOC and Fe in the Glomma transect is unsurprising given their common origin in terrestrial soils, and the coupling between them vanishes, to some extent, in marine waters.

Climate change, afforestation and recovery from acidification increase the transport and availability of TOC and Fe into the aquatic system. A proper understanding of the intertwined effects of TOC and Fe in aquatic systems is important for several reasons, but notably due to their effects on light attenuation and thus primary production, underwater visibility, and ecosystem processes.

References

- Aitkenhead, J. A., Hope, D., & Billett, M. F. (1999). The relationship between dissolved organic carbon in stream water and soil organic carbon pools at different spatial scales. *Hydrological Processes*, *13*(8), 1289–1302. [https://doi.org/10.1002/\(SICI\)1099-1085\(19990615\)13:8<1289::AID-HYP766>3.0.CO;2-M](https://doi.org/10.1002/(SICI)1099-1085(19990615)13:8<1289::AID-HYP766>3.0.CO;2-M)
- Aksnes, D., Dupont, N., Staby, A., Fiksen, Ø., Kaartvedt, S., & Aure, J. (2009). Coastal water darkening and implications for mesopelagic regime shifts in Norwegian fjords. *Marine Ecology Progress Series*, *387*, 39–49. <https://doi.org/10.3354/meps08120>
- Allesson, L., Koehler, B., Thrane, J.-E., Andersen, T., & Hessen, D. O. (2021). The role of photomineralization for CO₂ emissions in boreal lakes along a gradient of dissolved organic matter. *Limnology and Oceanography*, *66*(1), 158–170. <https://doi.org/10.1002/lno.11594>
- Andersen, T., Hessen, D. O., Håll, J. P., Khomich, M., Kyle, M., Lindholm, M., Rasconi, S., Skjelbred, B., Thrane, J.-E., & Walseng, B. (2020). Congruence, but no cascade—Pelagic biodiversity across three trophic levels in Nordic lakes. *Ecology and Evolution*, *10*(15), 8153–8165. <https://doi.org/10.1002/ece3.6514>
- Arvola, L., Rask, M., Ruuhijärvi, J., Tulonen, T., Vuorenmaa, J., Ruoho-Airola, T., & Tulonen, J. (2010). Long-term patterns in pH and colour in small acidic boreal lakes of varying hydrological and landscape settings. *Biogeochemistry*, *101*(1), 269–279. <https://doi.org/10.1007/s10533-010-9473-y>
- Aumont, O., & Bopp, L. (2006). Globalizing results from ocean in situ iron fertilization studies. *Global Biogeochemical Cycles*, *20*(2). <https://doi.org/10.1029/2005GB002591>

- Badr, E.-S. A., Achterberg, E. P., Tappin, A. D., Hill, S. J., & Braungardt, C. B. (2003). Determination of dissolved organic nitrogen in natural waters using high-temperature catalytic oxidation. *TrAC Trends in Analytical Chemistry*, 22(11), 819–827. [https://doi.org/10.1016/S0165-9936\(03\)01202-0](https://doi.org/10.1016/S0165-9936(03)01202-0)
- Berden, G., Peeters, R., & Meijer, G. (2000). Cavity ring-down spectroscopy: Experimental schemes and applications. *International Reviews in Physical Chemistry*, 19(4), 565–607. <https://doi.org/10.1080/014423500750040627>
- Björnerås, C., Škerlep, M., Floudas, D., Persson, P., & Kritzberg, E. S. (2019). High sulfate concentration enhances iron mobilization from organic soil to water. *Biogeochemistry*, 144(3), 245–259. <https://doi.org/10.1007/s10533-019-00581-6>
- Bochdansky, A. B., Dunbar, R. B., Hansell, D. A., & Herndl, G. J. (2019). Estimating Carbon Flux From Optically Recording Total Particle Volume at Depths Below the Primary Pycnocline. *Frontiers in Marine Science*, 6. <https://doi.org/10.3389/fmars.2019.00778>
- Bowering, K. L., Edwards, K. A., Prestegard, K., Zhu, X., & Ziegler, S. E. (2020). Dissolved organic carbon mobilized from organic horizons of mature and harvested black spruce plots in a mesic boreal region. *Biogeosciences*, 17(3), 581–595. <https://doi.org/10.5194/bg-17-581-2020>
- Canfield Jr., D. E., Linda, S. B., & Hodgson, L. M. (1984). Relations Between Color and Some Limnological Characteristics of Florida Lakes1. *JAWRA Journal of the American Water Resources Association*, 20(3), 323–329. <https://doi.org/10.1111/j.1752-1688.1984.tb04711.x>
- Christ, M. J., & David, M. B. (1996). Temperature and moisture effects on the production of dissolved organic carbon in a Spodosol. *Soil Biology and Biochemistry*, 28(9), 1191–1199. [https://doi.org/10.1016/0038-0717\(96\)00120-4](https://doi.org/10.1016/0038-0717(96)00120-4)

- Craig, H. (1961). Isotopic Variations in Meteoric Waters. *Science (American Association for the Advancement of Science)*, 133(3465), 1702–1703.
<https://doi.org/10.1126/science.133.3465.1702>
- de Wit, H. A., Mulder, J., Hindar, A., & Hole, L. (2007). Long-Term Increase in Dissolved Organic Carbon in Streamwaters in Norway Is Response to Reduced Acid Deposition. *Environmental Science & Technology*, 41(22), 7706–7713.
<https://doi.org/10.1021/es070557f>
- de Wit, H. A., Valinia, S., Weyhenmeyer, G. A., Futter, M. N., Kortelainen, P., Austnes, K., Hessen, D. O., Räike, A., Laudon, H., & Vuorenmaa, J. (2016). Current Browning of Surface Waters Will Be Further Promoted by Wetter Climate. *Environmental Science & Technology Letters*, 3(12), 430–435. <https://doi.org/10.1021/acs.estlett.6b00396>
- Dillon, P. J., & Molot, L. A. (2005). Long-term trends in catchment export and lake retention of dissolved organic carbon, dissolved organic nitrogen, total iron, and total phosphorus: The Dorset, Ontario, study, 1978–1998. *Journal of Geophysical Research: Biogeosciences*, 110(G1). <https://doi.org/10.1029/2004JG000003>
- Dupont, N., & Aksnes, D. L. (2013). Centennial changes in water clarity of the Baltic Sea and the North Sea. *Estuarine, Coastal and Shelf Science*, 131, 282–289.
<https://doi.org/10.1016/j.ecss.2013.08.010>
- Edmunds, W. M., & Smedley, P. L. (1996). Groundwater geochemistry and health: An overview. *Geological Society, London, Special Publications*, 113(1), 91–105.
<https://doi.org/10.1144/GSL.SP.1996.113.01.08>
- Einola, E., Rantakari, M., Kankaala, P., Kortelainen, P., Ojala, A., Pajunen, H., Mäkelä, S., & Arvola, L. (2011). Carbon pools and fluxes in a chain of five boreal lakes: A dry and

- wet year comparison. *Journal of Geophysical Research: Biogeosciences*, 116(G3).
<https://doi.org/10.1029/2010JG001636>
- Ekström, S. M., Kritzberg, E. S., Kleja, D. B., Larsson, N., Nilsson, P. A., Graneli, W., & Bergkvist, B. (2011). Effect of Acid Deposition on Quantity and Quality of Dissolved Organic Matter in Soil–Water. *Environmental Science & Technology*, 45(11), 4733–4739. <https://doi.org/10.1021/es104126f>
- Evanoff, D. D., & Chumanov, G. (2004). Size-Controlled Synthesis of Nanoparticles. 2. Measurement of Extinction, Scattering, and Absorption Cross Sections. *The Journal of Physical Chemistry B*, 108(37), 13957–13962. <https://doi.org/10.1021/jp0475640>
- Falkowski, P. G., Barber, R. T., & Smetacek, V. (1998). Biogeochemical Controls and Feedbacks on Ocean Primary Production. *Science*, 281(5374), 200–206.
<https://doi.org/10.1126/science.281.5374.200>
- Fenner, N., & Freeman, C. (2011). Drought-induced carbon loss in peatlands. *Nature Geoscience*, 4(12), Article 12. <https://doi.org/10.1038/ngeo1323>
- Finstad, A. G., Andersen, T., Larsen, S., Tominaga, K., Blumentrath, S., de Wit, H. A., Tømmervik, H., & Hessen, D. O. (2016). From greening to browning: Catchment vegetation development and reduced S-deposition promote organic carbon load on decadal time scales in Nordic lakes. *Scientific Reports*, 6(1), Article 1.
<https://doi.org/10.1038/srep31944>
- Frey, P. A., & Reed, G. H. (2012). The Ubiquity of Iron. *ACS Chemical Biology*, 7(9), 1477–1481. <https://doi.org/10.1021/cb300323q>
- Frigstad, H., Kaste, Ø., Deininger, A., Kvalsund, K., Christensen, G., Bellerby, R. G. J., Sørensen, K., Norli, M., & King, A. L. (2020). Influence of Riverine Input on Norwegian

Coastal Systems. *Frontiers in Marine Science*.

<https://doi.org/https://doi.org/10.3389/fmars.2020.00332>

Gat, J. R. (1996). Oxygen and hydrogen isotopes in the hydrologic cycle. *Annual Review of Earth and Planetary Sciences*, 24(1), 225–262.

<https://doi.org/10.1146/annurev.earth.24.1.225>.

Ghosh, S., Prasanna, V. L., Sowjanya, B., Srivani, P., Alagaraja, M., & Banji, D. (2013).

Inductively coupled plasma - Optical emission spectroscopy: A review. *Asian J. Pharm. Ana.*, 3, 24–33.

Gjessing, E. T., Egeberg, P. K., & Håkedal, J. (1999). Natural organic matter in drinking water—The “NOM-typing project”, background and basic characteristics of original water samples and NOM isolates. *Environment International*, 25(2), 145–159.

[https://doi.org/10.1016/S0160-4120\(98\)00119-6](https://doi.org/10.1016/S0160-4120(98)00119-6)

Grubisic, M., van Grunsven, R. H. A., Manfrin, A., Monaghan, M. T., & Hölker, F. (2018). A transition to white LED increases ecological impacts of nocturnal illumination on aquatic primary producers in a lowland agricultural drainage ditch. *Environmental Pollution*, 240, 630–638. <https://doi.org/10.1016/j.envpol.2018.04.146>

Harpole, W. S., Ngai, J. T., Cleland, E. E., Seabloom, E. W., Borer, E. T., Bracken, M. E. S., Elser, J. J., Gruner, D. S., Hillebrand, H., Shurin, J. B., & Smith, J. E. (2011). Nutrient co-limitation of primary producer communities. *Ecology Letters*, 14(9), 852–862.

<https://doi.org/10.1111/j.1461-0248.2011.01651.x>

Herzog, S. D., Persson, P., & Kritzberg, E. S. (2017). Salinity Effects on Iron Speciation in Boreal River Waters. *Environmental Science & Technology*, 51(17), 9747–9755.

<https://doi.org/10.1021/acs.est.7b02309>

- Herzog, S. D., Persson, P., Kvashnina, K., & Kritzberg, E. S. (2020). Organic iron complexes enhance iron transport capacity along estuarine salinity gradients of Baltic estuaries. *Biogeosciences*, *17*(2), 331–344. <https://doi.org/10.5194/bg-17-331-2020>
- Hessen, D. O. (1985). The relation between bacterial carbon and dissolved humic compounds in oligotrophic lakes. *FEMS Microbiology Ecology*, *1*(4), 215–223. <https://doi.org/10.1111/j.1574-6968.1985.tb01152.x>
- Hessen, D. O., Håll, J. P., Thrane, J.-E., & Andersen, T. (2017). Coupling dissolved organic carbon, CO₂ and productivity in boreal lakes. *Freshwater Biology*, *62*(5), 945–953. <https://doi.org/10.1111/fwb.12914>
- Hill, V. J., & Zimmerman, R. C. (2010). Estimates of primary production by remote sensing in the Arctic Ocean: Assessment of accuracy with passive and active sensors. *Deep Sea Research Part I: Oceanographic Research Papers*, *57*(10), 1243–1254. <https://doi.org/10.1016/j.dsr.2010.06.011>
- Hongve, D., Riise, G., & Kristiansen, J. F. (2004). Increased colour and organic acid concentrations in Norwegian forest lakes and drinking water ? A result of increased precipitation? *Aquatic Sciences - Research Across Boundaries*, *66*(2), 231–238. <https://doi.org/10.1007/s00027-004-0708-7>
- Hsieh, J. C. C., Chadwick, O. A., Kelly, E. F., & Savin, S. M. (1998). Oxygen isotopic composition of soil water: Quantifying evaporation and transpiration. *Geoderma*, *82*(1), 269–293. [https://doi.org/10.1016/S0016-7061\(97\)00105-5](https://doi.org/10.1016/S0016-7061(97)00105-5)
- Erickson III, D. J., Sulzberger, B., G. Zepp, R., & T. Austin, A. (2015). Effects of stratospheric ozone depletion, solar UV radiation, and climate change on biogeochemical cycling: Interactions and feedbacks. *Photochemical & Photobiological Sciences*, *14*(1), 127–148. <https://doi.org/10.1039/C4PP90036G>

- Jickells, T. D. (1998). Nutrient Biogeochemistry of the Coastal Zone. *Science*, 281(5374), 217–222. <https://doi.org/10.1126/science.281.5374.217>
- Kahle, D., & Wickham, H. (2013). ggmap: Spatial Visualization with ggplot2. *The R Journal*, 5(1), 144. <https://doi.org/10.32614/RJ-2013-014>
- Kritzberg, E. S. (2017). Centennial-long trends of lake browning show major effect of afforestation. *Limnology and Oceanography Letters*, 2(4), 105–112. <https://doi.org/10.1002/lol2.10041>
- Kritzberg, E. S., Bedmar Villanueva, A., Jung, M., & Reader, H. E. (2014). Importance of Boreal Rivers in Providing Iron to Marine Waters. *PLOS ONE*, 9(9), e107500. <https://doi.org/10.1371/journal.pone.0107500>
- Kritzberg, E. S., & Ekström, S. M. (2012). Increasing iron concentrations in surface waters – a factor behind brownification? *Biogeosciences*, 9(4), 1465–1478. <https://doi.org/10.5194/bg-9-1465-2012>
- Lampert, W. (1989). The Adaptive Significance of Diel Vertical Migration of Zooplankton. *Functional Ecology*, 3(1), 21–27. <https://doi.org/10.2307/2389671>
- Larsen, S., Andersen, T., & Hessen, D. (2011). Predicting organic carbon in lakes from climate drivers and catchment properties. *Global Biogeochemical Cycles - GLOBAL BIOGEOCHEM CYCLE*, 25. <https://doi.org/10.1029/2010GB003908>
- Lee, Z., Hu, C., Shang, S., Du, K., Lewis, M., Arnone, R., & Brewin, R. (2013). Penetration of UV-visible solar radiation in the global oceans: Insights from ocean color remote sensing. *Journal of Geophysical Research: Oceans*, 118(9), 4241–4255. <https://doi.org/10.1002/jgrc.20308>

- Lee, Z., Weidemann, A., Kindle, J., Arnone, R., Carder, K. L., & Davis, C. (2007). Euphotic zone depth: Its derivation and implication to ocean-color remote sensing. *Journal of Geophysical Research: Oceans*, *112*(C3). <https://doi.org/10.1029/2006JC003802>
- Li, X., Liu, L., Zhao, J., & Tan, J. (2015). Optical Properties of Sodium Chloride Solution within the Spectral Range from 300 to 2500 nm at Room Temperature. *Applied Spectroscopy*, *69*(5), 635–640. <https://doi.org/10.1366/14-07769R>
- Luther, G. W., Shellenbarger, P. A., & Brendel, P. J. (1996). Dissolved organic Fe(III) and Fe(II) complexes in salt marsh porewaters. *Geochimica et Cosmochimica Acta*, *60*(6), 951–960. [https://doi.org/10.1016/0016-7037\(95\)00444-0](https://doi.org/10.1016/0016-7037(95)00444-0)
- Maloney, K. O., Morris, D. P., Moses, C. O., & Osburn, C. L. (2005). The Role of Iron and Dissolved Organic Carbon in the Absorption of Ultraviolet Radiation in Humic Lake Water. *Biogeochemistry*, *75*(3), 393–407. <https://doi.org/10.1007/s10533-005-1675-3>
- Mascarenhas, V., & Keck, T. (2018). Introduction to Ocean Color, Fundamental Concepts, and Optical Tools, *Marine Optics and Ocean Color Remote Sensing*.
- Jungblut, Liebich, V., & Bode, M. (2018). YOU MARES 8 – Oceans Across Boundaries: Learning from each other : Proceedings of the 2017 conference for YOUng MARine REsearchers in Kiel, Germany. Springer International Publishing: Imprint: Springer. ISBN : 978-3-319-93283-5
- Matilainen, A., Vepsäläinen, M., & Sillanpää, M. (2010). Natural organic matter removal by coagulation during drinking water treatment: A review. *Advances in Colloid and Interface Science*, *159*(2), 189–197. <https://doi.org/10.1016/j.cis.2010.06.007>
- Moland, E., Synnes, A.-E., Naustvoll, L.-J., Freitas, C., Norderhaug, K. M., Thormar, J., Biuw, M., Erik, P., Knutsen, H., Dahle, G., Jelmert, A., Bosgraaf, S., Olsen, E. M., & Deininger,

- A. (2021). *Kunnskap for stedstilpasset gjenoppbygging av bestander, naturtyper og økosystem i Færder- og Ytre Hvaler nasjonalparker*. Havforskningsinstituttet.
<https://hdl.handle.net/11250/2725009>
- Monteith, D. T., Stoddard, J. L., Evans, C. D., de Wit, H. A., Forsius, M., Høgåsen, T., Wilander, A., Skjelkvåle, B. L., Jeffries, D. S., Vuorenmaa, J., Keller, B., Kopáček, J., & Vesely, J. (2007). Dissolved organic carbon trends resulting from changes in atmospheric deposition chemistry. *Nature*, *450*(7169), 537–540.
<https://doi.org/10.1038/nature06316>
- Neubauer, E., Köhler, S. J., von der Kammer, F., Laudon, H., & Hofmann, T. (2013). Effect of pH and Stream Order on Iron and Arsenic Speciation in Boreal Catchments. *Environmental Science & Technology*, *47*(13), 7120–7128.
<https://doi.org/10.1021/es401193j>
- Noji, T., Noji, C.-M., & Barthel, K.-G. (1993). Pelagic-benthic coupling during the onset of winter in a northern Norwegian fjord. Carbon flow and fate of suspended particulate matter. *Marine Ecology Progress Series*, *93*, 89–99.
<https://doi.org/10.3354/meps093089>
- Persson, I., & Jones, I. D. (2008). The effect of water colour on lake hydrodynamics: A modelling study. *Freshwater Biology*, *53*(12), 2345–2355.
<https://doi.org/10.1111/j.1365-2427.2008.02049.x>
- Rabalais, N. N. (2002). Nitrogen in Aquatic Ecosystems. *AMBIO: A Journal of the Human Environment*, *31*(2), 102–112. <https://doi.org/10.1579/0044-7447-31.2.102>
- Raymond, P., & Bauer, J. (2000). Bacterial consumption of DOC during transport through a temperate estuary. *Aquatic Microbial Ecology*, *22*, 1–12.
<https://doi.org/10.3354/ame022001>

- Rose, A. L., & Waite, T. D. (2003). Predicting iron speciation in coastal waters from the kinetics of sunlight-mediated iron redox cycling. *Aquatic Sciences - Research Across Boundaries*, 65(4), 375–383. <https://doi.org/10.1007/s00027-003-0676-3>
- Rothe, M., Kleeberg, A., & Hupfer, M. (2016). The occurrence, identification and environmental relevance of vivianite in waterlogged soils and aquatic sediments. *Earth-Science Reviews*, 158, 51–64. <https://doi.org/10.1016/j.earscirev.2016.04.008>
- Roulet, N., & Moore, T. R. (2006). Browning the waters. *Nature*, 444(7117), Article 7117. <https://doi.org/10.1038/444283a>
- Rue, E. L., & Bruland, K. W. (1995). Complexation of iron(III) by natural organic ligands in the Central North Pacific as determined by a new competitive ligand equilibration/adsorptive cathodic stripping voltammetric method. *Marine Chemistry*, 50(1), 117–138. [https://doi.org/10.1016/0304-4203\(95\)00031-L](https://doi.org/10.1016/0304-4203(95)00031-L)
- Schnitzer, M. (1983). Organic Matter Characterization. In *Methods of Soil Analysis* (pp. 581–594). John Wiley & Sons, Ltd. <https://doi.org/10.2134/agronmonogr9.2.2ed.c30>
- Schwertmann, U. (1991). *Solubility and dissolution of iron oxides*. *Plant and Soil*, 130(1), 1–25. <https://doi.org/10.1007/BF00011851>
- Shaked, Y., & Lis, H. (2012). Disassembling Iron Availability to Phytoplankton. *Frontiers in Microbiology*, 3, 123–123. <https://doi.org/10.3389/fmicb.2012.00123>
- Sholkovitz, E. R. (1976). Flocculation of dissolved organic and inorganic matter during the mixing of river water and seawater. *Geochimica et Cosmochimica Acta*, 40(7), 831–845. [https://doi.org/10.1016/0016-7037\(76\)90035-1](https://doi.org/10.1016/0016-7037(76)90035-1)
- Sholkovitz, E. R., Boyle, E. A., & Price, N. B. (1978). The removal of dissolved humic acids and iron during estuarine mixing. *Earth and Planetary Science Letters*, 40(1), 130–136. [https://doi.org/10.1016/0012-821X\(78\)90082-1](https://doi.org/10.1016/0012-821X(78)90082-1)

- Škerlep, M., Nehzati, S., Johansson, U., Kleja, D. B., Persson, P., & Kritzberg, E. S. (2022). Spruce forest afforestation leading to increased Fe mobilization from soils. *Biogeochemistry*, *157*(3), 273–290. <https://doi.org/10.1007/s10533-021-00874-9>
- Škerlep, M., Steiner, E., Axelsson, A.-L., & Kritzberg, E. S. (2020). Afforestation driving long-term surface water browning. *Global Change Biology*, *26*(3), 1390–1399. <https://doi.org/10.1111/gcb.14891>
- Stookey, L. L. (1970). Ferrozine—A new spectrophotometric reagent for iron. *Analytical Chemistry*, *42*(7), 779–781. <https://doi.org/10.1021/ac60289a016>
- Sundman, A., Karlsson, T., Sjöberg, S., & Persson, P. (2014). Complexation and precipitation reactions in the ternary As(V)–Fe(III)–OM (organic matter) system. *Geochimica et Cosmochimica Acta*, *145*, 297–314. <https://doi.org/10.1016/j.gca.2014.09.036>
- Suzuki, Y., Kuma, K., Kudo, I., Hasebe, K., & Matsunaga, K. (1992). Existence of stable Fe(II) complex in oxic river water and its determination. *Water Research*, *26*(11), 1421–1424. [https://doi.org/10.1016/0043-1354\(92\)90060-H](https://doi.org/10.1016/0043-1354(92)90060-H)
- Thrane, J.-E., Hessen, D. O., & Andersen, T. (2014). The Absorption of Light in Lakes: Negative Impact of Dissolved Organic Carbon on Primary Productivity. *Ecosystems*, *17*(6), 1040–1052. <https://doi.org/10.1007/s10021-014-9776-2>
- Tranvik, L. J. (1992). Allochthonous dissolved organic matter as an energy source for pelagic bacteria and the concept of the microbial loop. In K. Salonen, T. Kairesalo, & R. I. Jones (Eds.), *Dissolved Organic Matter in Lacustrine Ecosystems: Energy Source and System Regulator* (pp. 107–114). Springer Netherlands. https://doi.org/10.1007/978-94-011-2474-4_8

- Urtizberea, A., Dupont, N., Rosland, R., & Aksnes, D. L. (2013). Sensitivity of euphotic zone properties to CDOM variations in marine ecosystem models. *Ecological Modelling*, 256, 16–22. <https://doi.org/10.1016/j.ecolmodel.2013.02.010>
- Viollier, E., Inglett, P. W., Hunter, K., Roychoudhury, A. N., & Van Cappellen, P. (2000). The ferrozine method revisited: Fe(II)/Fe(III) determination in natural waters. *Applied Geochemistry*, 15(6), 785–790. [https://doi.org/10.1016/S0883-2927\(99\)00097-9](https://doi.org/10.1016/S0883-2927(99)00097-9)
- Weyhenmeyer, G. A., & Karlsson, J. (2009). Nonlinear response of dissolved organic carbon concentrations in boreal lakes to increasing temperatures. *Limnology and Oceanography*, 54 (6), 2513–2519. https://doi.org/10.4319/lo.2009.54.6_part_2.2513
- Weyhenmeyer, G. A., Prairie, Y. T., & Tranvik, L. J. (2014). Browning of Boreal Freshwaters Coupled to Carbon-Iron Interactions along the Aquatic Continuum. *PloS One*, 9(2), e88104. <https://doi.org/10.1371/journal.pone.0088104>
- Wickham, H. (2016). Data Analysis. In H. Wickham (Ed.), *Ggplot2: Elegant Graphics for Data Analysis* (pp. 189–201). *Springer International Publishing*. https://doi.org/10.1007/978-3-319-24277-4_9
- Zhu, J., Zhu, Z., Lin, J., Wu, H., & Zhang, J. (2016). Distribution of hypoxia and pycnocline off the Changjiang Estuary, China. *Journal of Marine Systems*, 154, 28–40. <https://doi.org/10.1016/j.jmarsys.2015.05.002>
- Zhuang, G., Yi, Z., & Wallace, G. T. (1995). Iron(II) in rainwater, snow, and surface seawater from a coastal environment. *Marine Chemistry*, 50(1–4), 41–50. [https://doi.org/10.1016/0304-4203\(95\)00025-M](https://doi.org/10.1016/0304-4203(95)00025-M)

Appendix

Hyperlinks (in order from the text)

Glomma catchment:

<https://temakart.nve.no/tema/nedborfelt>

Runoff area to the Oslofjord:

<https://temakart.nve.no/tema/nedborfelt>

Oslofjord transect:

<https://www.google.no/maps/@59.1601018,10.7280159,12z/data=!4m3!11m2!2sxGPjeNLXRFiBMdWe1r7MRg!3e3>

Stamen maps:

<http://maps.stamen.com/#watercolor/12/37.7706/-122.3782>

Glomma transect:

<https://www.google.no/maps/@/data=!3m1!4b1!4m3!11m2!2slrv-tZe3T9KE8wSJnU5tpA!3e3?shorturl=1>

Opentrons:

<https://opentrons.com/>

Ultimaker:

<https://ultimaker.com/>

CLIPT:

<https://www.mn.uio.no/ibv/english/research/infrastructure/facilities/life-science/bio-geochemical-analysis/isotope/>

Maps and coordinates

Table 1. Coordinates of the Oslofjord transect.

Site	Latitude	Longitude
OF2, Missingene	59.18	10.69
Ø1, Leira	59.13	10.83
I1, Ramsø	59.11	11.00
L5, Kjøkøy	59.14	10.96
L1, Glomma	59.21	10.96

Table 2. Coordinates and description of the Glomma transect

Site	Latitude	Longitude	Name	Description
G1	60.81	12.31	Kynna (tributary of the Flisa river, low water stream)	Forest
G2	60.77	12.31	Flisa river	Forest
G3	60.64	12.04	Kulpen (swimming area in the Flisa river)	Agriculture
G4	60.60	12.02	Glomma before the Flisa river enters	Agriculture / City
G5	60.59	12.02	Flisa river before it enters Glomma	Agriculture / City
G6	60.48	12.07	Grøset (rest area)	Agriculture
G7	60.32	11.00	Brandval (tributary under bridge)	Agriculture

G8	60.24	12.02	Glomma after Roverud	Agriculture/Forest
G9	60.19	11.00	Glomma Kongsvinger	City
G10	60.26	11.68	Glomma Skarnes	Agriculture / City
G11	60.16	11.41	Vorma (tributary)	Agriculture
G12	60.12	11.46	Glomma Årnes	Agriculture / City
G13	59.99	11.27	Glomma Sørumsand	Agriculture
G14	59.93	11.17	Glomma Fetsund (before lake Øyern)	Agriculture / City
G15	59.67	11.25	Øyern (lake, swimming area)	Agriculture
G16	59.60	11.10	Glomma Askim	Agriculture
G17	59.52	11.25	Tributary Glomma, Lekumfossen power plant	Agriculture
G18	59.49	11.24	Swimming area Glomma (wharf)	Agriculture
G19	59.44	11.23	Tributary Glomma, before Brekkefoss, at power plant	Agriculture
G20	59.27	11.09	Glomma Sarpsborg	City / Agriculture
G21	59.21	10.96	Glomma Fredrikstad (under the bridge)	City / Agriculture

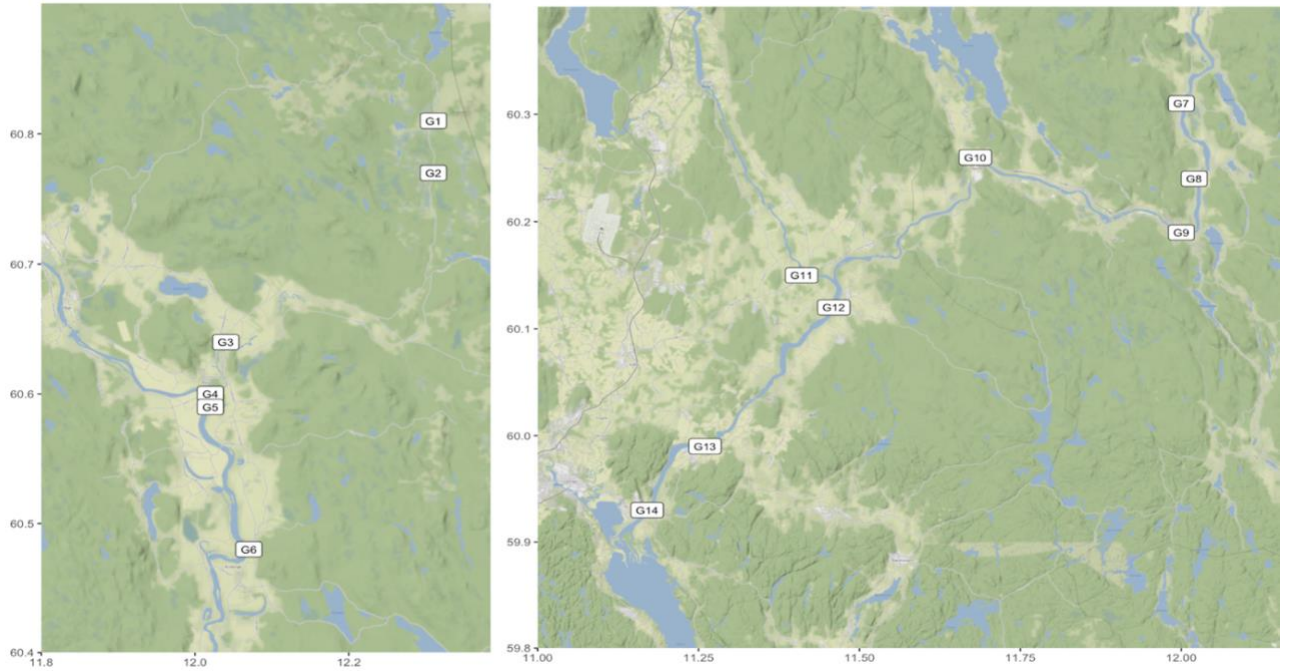


Figure 24. Sample sites 1-14, created from Stamen maps with ggmap.

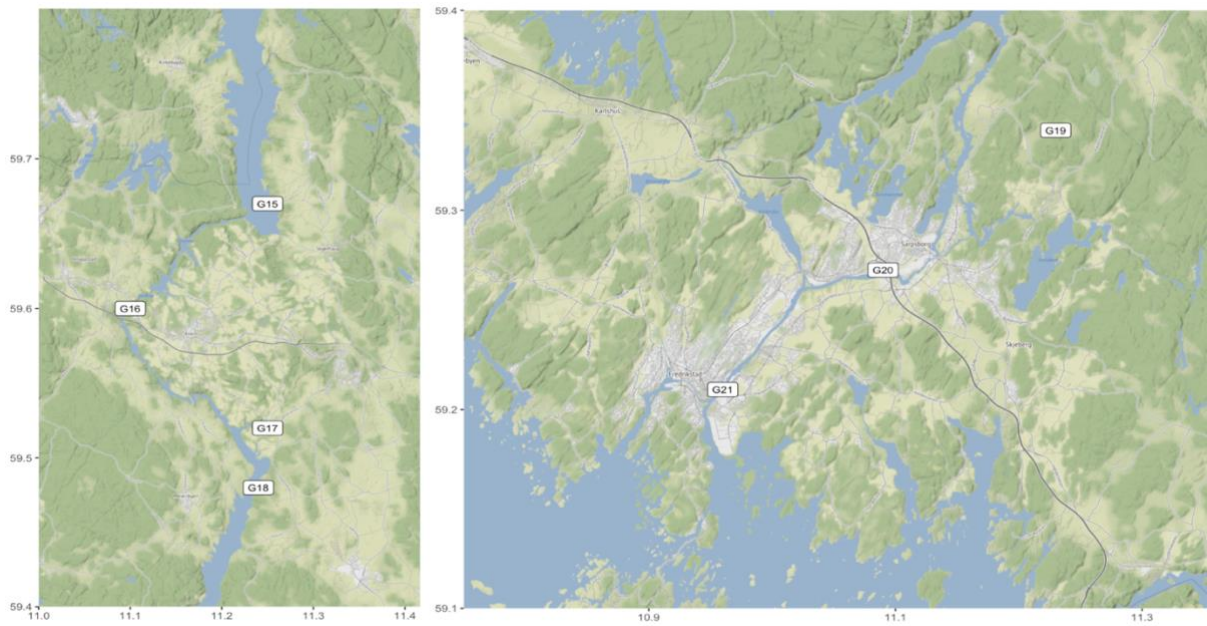


Figure 25. Sample sites 15-21, created from Stamen maps with ggmap.

Example of CTD data from cruise 3, station OF2.

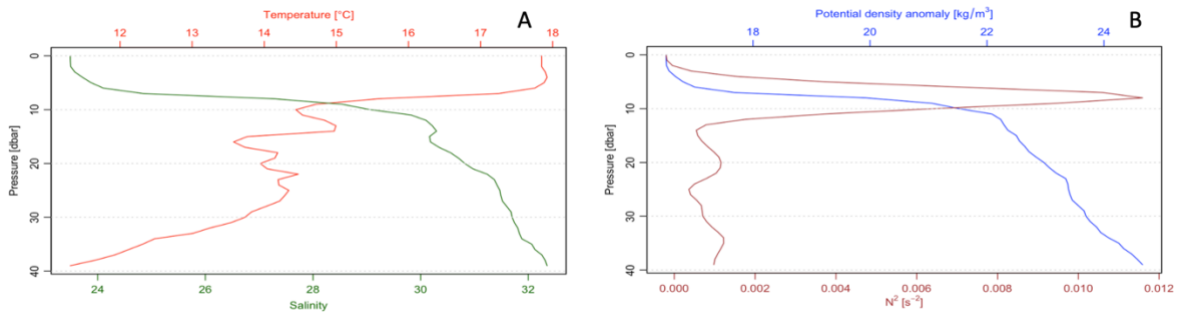


Figure 26. CTD data from cruise 3, station OF2. A) Plot illustrating temperature and salinity. B) Plot illustrating potential density anomaly, and thus the pycnocline.

The ferrozine method

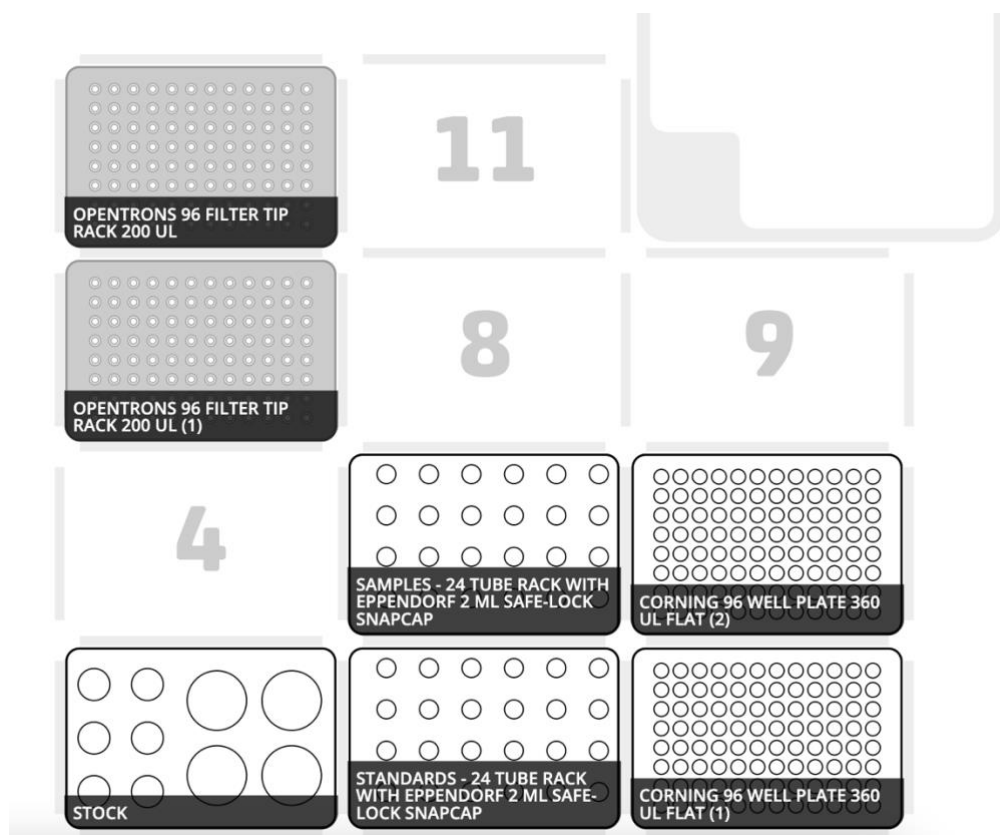


Figure 27. The Opentrons OT-2 lab robot layout for ferrozine method. Figure made in Opentrons Protocol Designer BETA.

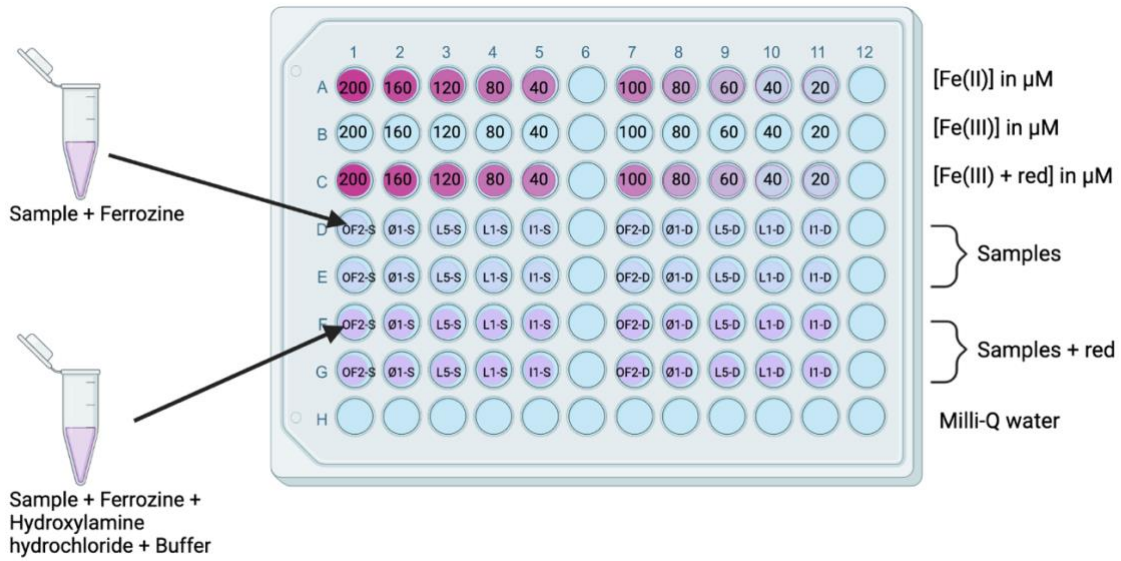


Figure 28. Schematic illustration of the plate layout for the samples from the Oslofjord transect. Illustration created with BioRender.com

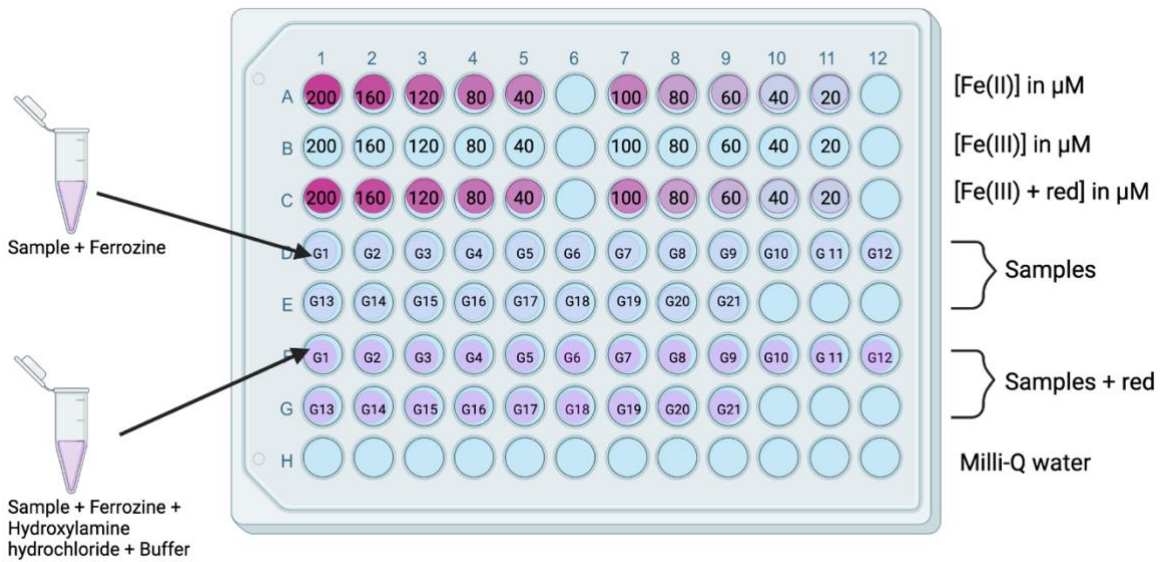


Figure 29. Schematic illustration of the plate layout for the samples from the Glomma transect. Illustration created with BioRender.com.

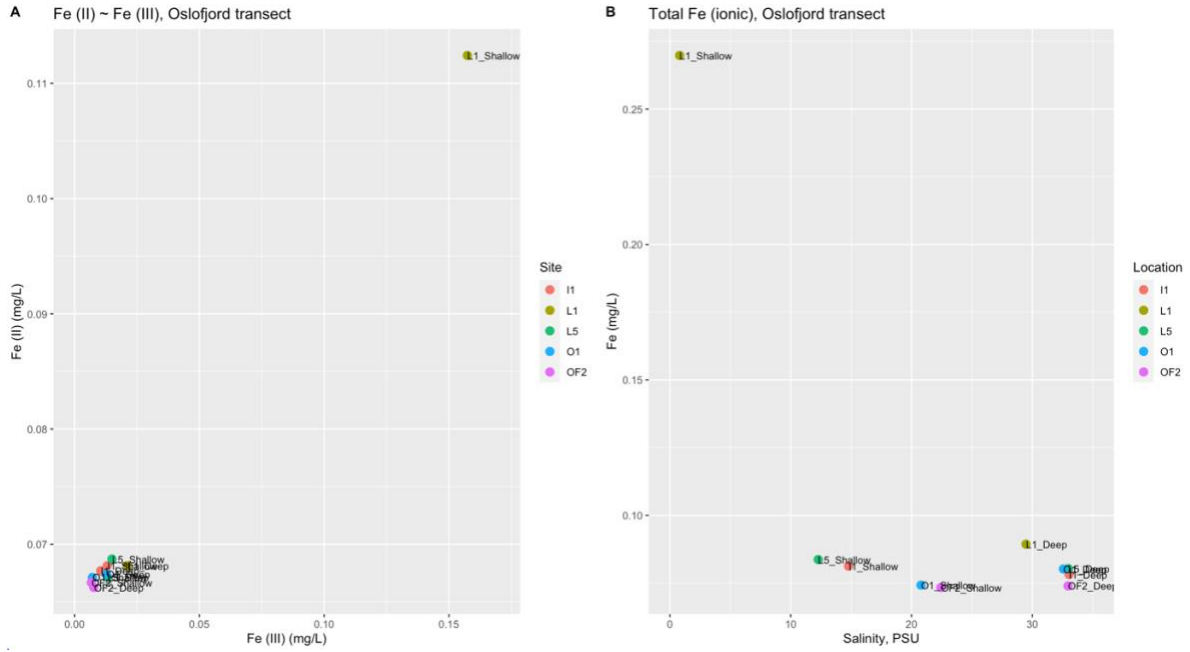


Figure 30. Iron in the Oslofjord transect determined by the ferrozine method: A) Determination of the concentrations of the iron species Fe(II) / Fe(III). B) Relationship between the concentration of total FR-Fe and salinity at each sampling site.

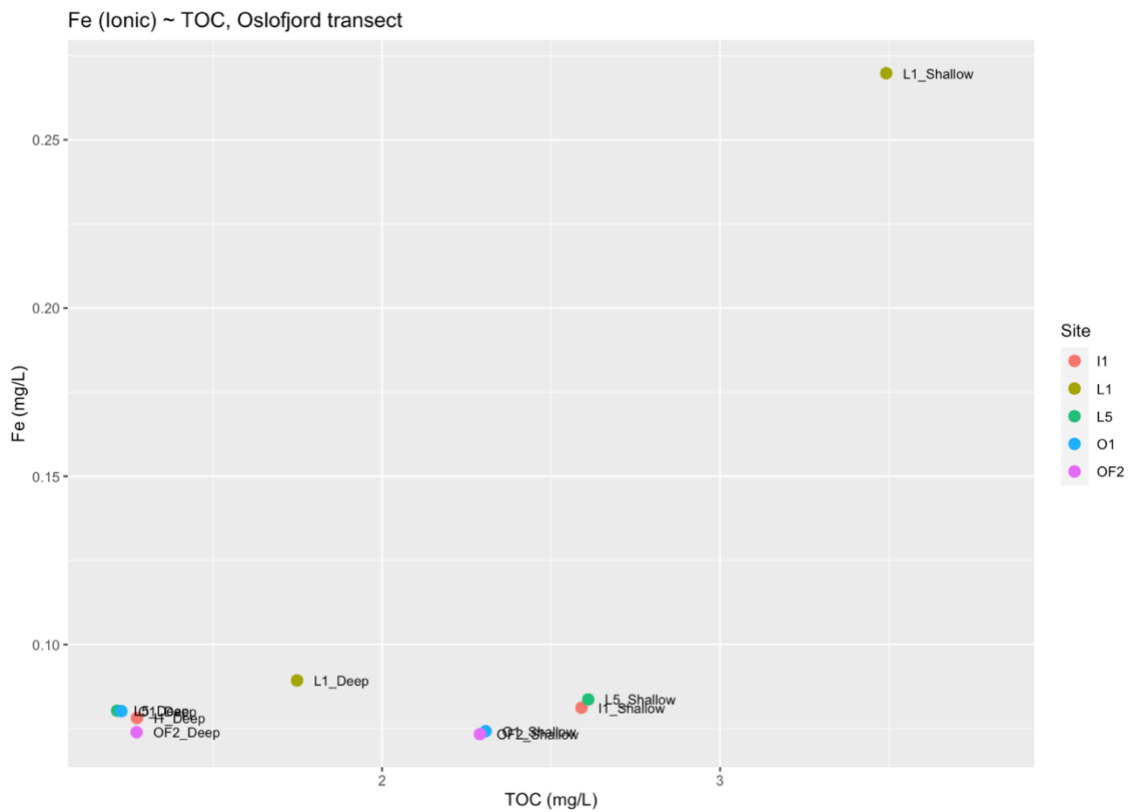


Figure 31. FR-Fe (mg/L) as a function of TOC (mg/L) Oslofjord transect all sampling sites.

ICP-OES

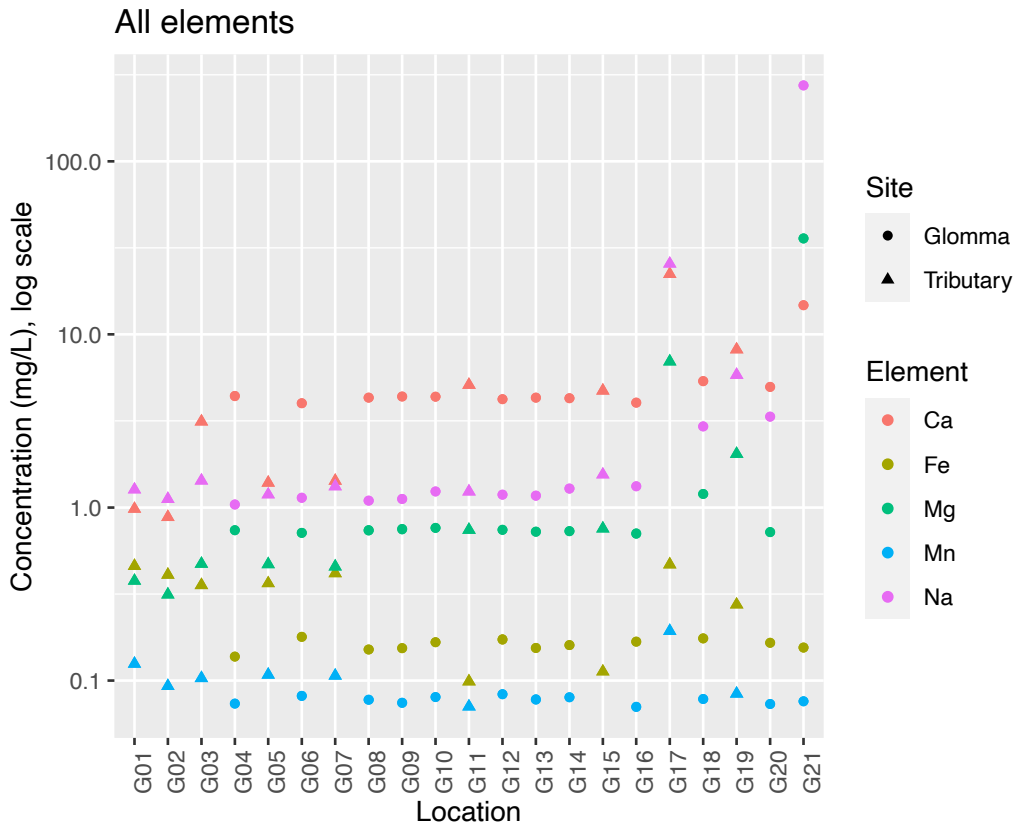


Figure 32. Concentration of all elements analysed determined by ICP-OES, y-axis log transformed.

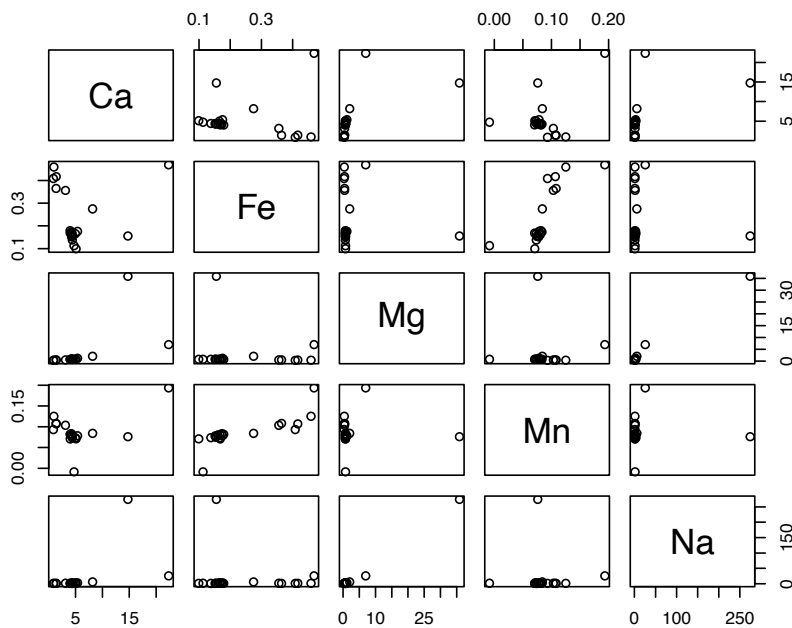


Figure 33. Scatter plot matrix of all the elements analysed by ICP-OES.

Organic matter

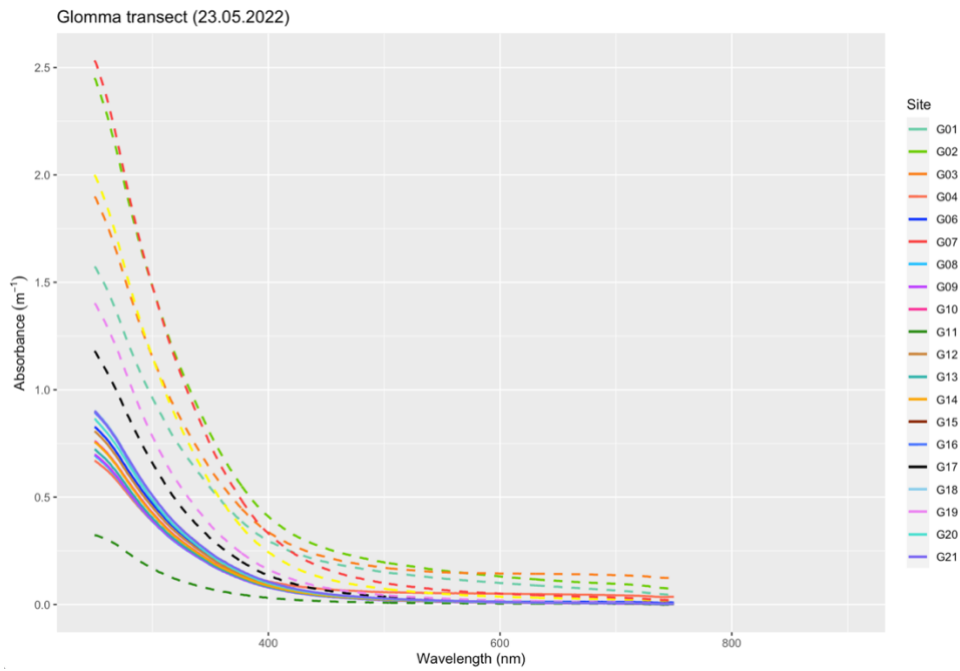


Figure 34. CDOM absorbance from Glomma transect. Glomma samples in solid lines and tributary samples in dashed lines.

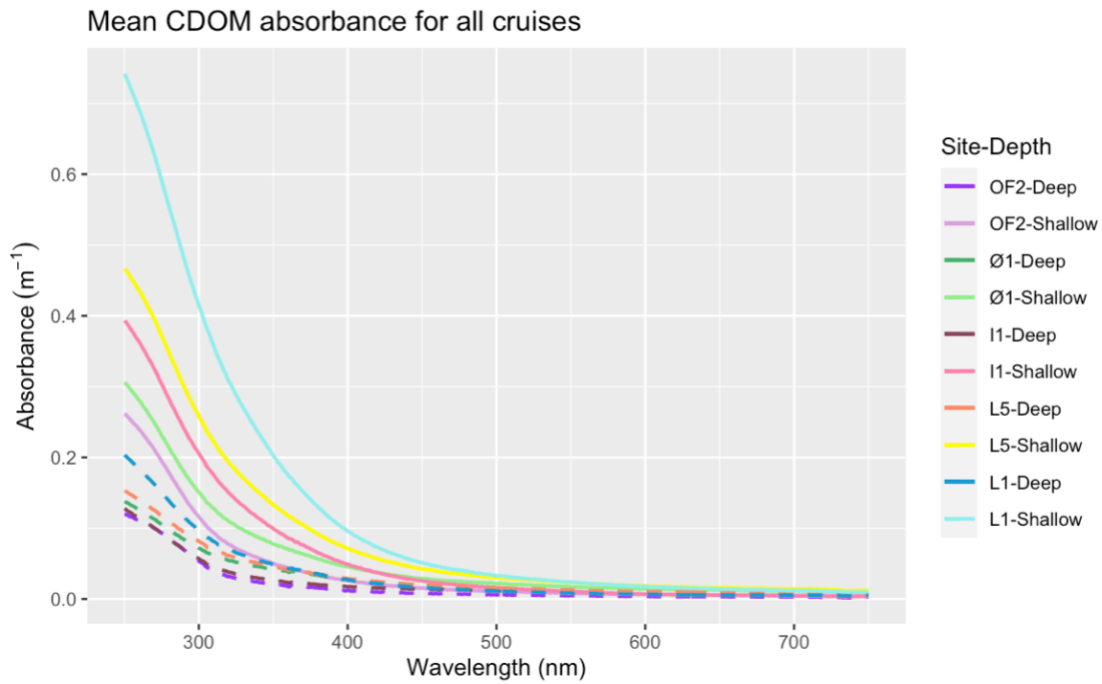


Figure 35. Mean CDOM absorbance from cruises 1-3. Surface water samples in solid lines and deep-water samples in dashed lines.

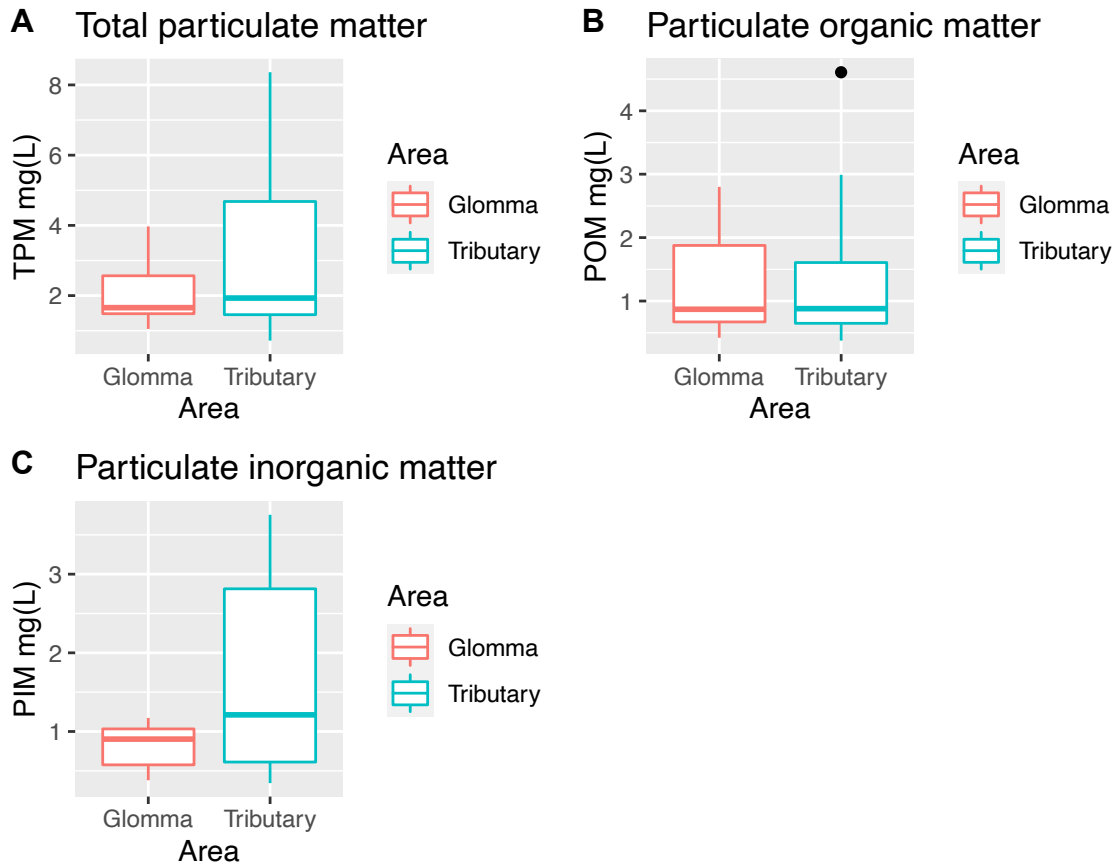


Figure 36. Distribution of TPM, POM and PIM from the Glomma transect.

Procedure with risk assessment: Preparing reagents for FE(II) / FE(III) analysis		Saks- og dokumentnr. i ePhorte:	
Written by : IBV; Nicolas Valiente Parra		Approved by: IBV; Cecilie Mathiesen	Version:
		Date:	30.10.2020
		Page:	67 of 89

Changes in this version:

- New SOP

1. INTRODUCTION/PURPOSE

This is a procedure including a detailed risk assessment for preparing reagents used in Fe(II) and Fe(III) spectrophotometric determination in waters.

2. NECESSARY SAFETY EQUIPMENT



Nitrile






Fume hood






3. CHEMICAL AND BIOLOGICAL HAZARDS

3.1 Chemicals

Chemical information	Health -, Precautions - and Emergency planning
<p>FerroZine™ Iron Reagent e.g. 160601 from Sigma CAS No: 63451-29-6</p> 	<p>H315: Irritating to skin H319: Causes serious eye irritation H335: Can cause respiratory irritation</p> <p>P261: Avoid inhalation of dust / fumes / gas / mist / vapors / aerosols</p> <p>P264: Wash skin thoroughly after use</p> <p>P271: Use only outdoors or in a well-ventilated area</p> <p>P280: Use protective gloves / goggles / face shield</p> <p>P302 + P352: IF ON SKIN: Wash with plenty of water</p> <p>P305 + P351 + P338: IF IN EYES: Rinse cautiously with water for several minutes. Remove any contact lenses if this is easy to do. Continue rinsing.</p>
<p>Ammonium acetate e.g. 73594 from Sigma CAS No: 631-61-8</p>	<p>Not a hazardous substance or mixture according to Regulation (EC) No 1272/2008.</p>

Chemical information	Health -, Precautions - and Emergency planning
<p>Hydroxylamine hydrochloride</p> <p>e.g. 159417 from Sigma</p> <p>CAS No: 5470-11-1</p> 	<p>H290: May be corrosive to metals.</p> <p>H302 + H312: Harmful if swallowed or in contact with skin.</p> <p>H315: Irritating to skin.</p> <p>H317: May cause an allergic skin reaction.</p> <p>H319: Causes serious eye irritation.</p> <p>H351: Suspected of causing cancer.</p> <p>H373: May cause damage to organs (spleen) with prolonged or repeated exposure if swallowed.</p> <p>H400: Very toxic to aquatic life.</p> <p>P201: Obtain special instructions before use.</p> <p>P273: Avoid release to the environment.</p> <p>P280: Wear protective gloves / protective clothing.</p> <p>P301 + P312 + P330: IF SWALLOWED: Contact a POISON CENTER / doctor if you feel unwell. Rinse mouth.</p> <p>P302 + P352 + P312: IF ON SKIN: Wash with plenty of water. Contact a POISON CENTER / physician if you feel unwell.</p> <p>P308 + P313: In case of exposure or suspected exposure: Get medical advice / attention.</p>
<p>Hydrochloric acid</p> <p>e.g. H1758 from Sigma</p> <p>CAS No: 7647-01-0</p> 	<p>H290: May be corrosive to metals.</p> <p>H314: Causes severe skin burns and eye damage.</p> <p>H335: May cause respiratory irritation.</p> <p>P260: Do not breathe dust or mist.</p> <p>P280: Wear protective gloves/ protective clothing/ eye protection/ face protection.</p> <p>P303 + P361 + P353: IF ON SKIN (or hair): Take off immediately all contaminated clothing. Rinse skin with water.</p> <p>P304 + P340 + P310: IF INHALED: Remove person to fresh air and keep comfortable for breathing. Immediately call a POISON CENTER/doctor.</p> <p>P305 + P351 + P338: IF IN EYES: Rinse cautiously with water for several minutes. Remove contact lenses, if present and easy to do. Continue rinsing.</p>

Chemical information	Health -, Precautions - and Emergency planning
<p>Ammonium hydroxide</p> <p>e.g. 221228 from Sigma</p> <p>CAS No: 1336-21-6</p> 	<p>H290: May be corrosive to metals. H302: Harmful if swallowed. H314: Causes severe skin burns and eye damage. H335: May cause respiratory irritation. H400: Very toxic to aquatic life.</p> <p>P261: Avoid breathing dust/fume/gas/mist/vapors/spray. P273: Avoid release to the environment.</p> <p>P280: Wear protective gloves / protective clothing.</p> <p>P301 + P312: IF SWALLOWED: Contact a POISON CENTER / doctor if you feel unwell.</p> <p>P303 + P361 + P353: IF ON SKIN (or hair): Take off immediately all contaminated clothing. Rinse skin with water.</p> <p>P305 + P351 + P338: IF IN EYES: Rinse cautiously with water for several minutes. Remove any contact lenses if this is easy to do. Continue rinsing.</p>
<p>Iron(III) chloride</p> <p>e.g. 157740 from Sigma</p> <p>CAS No: 7705-08-0</p> 	<p>H290: May be corrosive to metals. H302: Harmful if swallowed. H315: Irritating to skin. H318: Causes serious eye damage.</p> <p>P234: Keep only in original packaging.</p> <p>P264: Wash skin thoroughly after handling. P280: Wear protective gloves/ protective clothing/ eye protection/ face protection.</p> <p>P301 + P312: IF SWALLOWED: Contact a POISON CENTER / doctor if you feel unwell. P302 + P352: IF ON SKIN: Wash with plenty of water. P305 + P351 + P338: IF IN EYES: Rinse cautiously with water for several minutes. Remove contact lenses, if present and easy to do. Continue rinsing.</p>
<p>Iron(II) chloride tetrahydrate</p> <p>e.g. 44939 from Sigma</p> <p>CAS No: 13478-10-9</p> 	<p>H302: Harmful if swallowed. H318: Causes serious eye damage.</p> <p>P280: Wear protective gloves/ protective clothing/ eye protection/ face protection.</p> <p>P301 + P312 + P330: IF SWALLOWED: Call a POISON CENTER / doctor if you feel unwell. Rinse mouth. P302 + P352: IF ON SKIN: Wash with plenty of water. P305 + P351 + P338 + P310: IF IN EYES: Rinse cautiously with water for several minutes. Remove contact lenses, if present and easy to do. Continue rinsing. Immediately call a POISON CENTER/doctor.</p>

4. Special cautions necessary due to reproductive toxicity

Generally, it is not recommended to work with a chemical that has carcinogenic or reproductive effects if you are planning to be or are pregnant. If a chemical is proven to pass into breast milk it is not recommended to perform procedure if you are breast feeding.

Planning pregnancy (men and women): None

Pregnant: None

Breast feeding: None.

5. PROCEDURES and risk assessment

Necessary equipment

Scale

Magnetic stirrer

Magnet

Weighing boats

Spatulas

Glass equipment

Distilled water

5.1 Procedure

We always wear lab coat and gloves when working in the lab. The procedure should be carried out in the fume hood.

Preparing Ferrozine solution (0.01M)

Preparing Ammonium acetate solution (0.1 M):

1. Dissolve 385 mg ammonium acetate in 50 mL Milli-Q water in a beaker.
2. Transfer the dissolved ammonium acetate to a 50mL volumetric flask and fill up to 50 mL with Milli-Q water.

Part of procedure	Unwanted scenarios	Necessary precautions	S*K (Probability*Consequence)
1-2	Spillage or inhalation of hazardous chemical (ammonium acetate is non hazardous)	Wear gloves and lab coat	2*1

Dissolving ferrozine in ammonium acetate solution (0.1 M):

3. Weigh in 246.2 mg of ferrozine with a plastic spatula.
4. Add this to the 50mL 0.1M ammonium acetate solution (0.1 M).

3-4	Spillage or inhalation of hazardous chemical	Wear gloves and lab coat. Work in fume hood	2*2
-----	--	--	-----

Preparing Hydroxylamine hydrochloride solution (1.4 M)

Preparing 2M HCl:

5. Add about 30 mL Milli-Q water to a 50mL volumetric flask
6. Add 8.3 mL 37% HCl.
7. Fill up to 50mL with Milli-Q water.

5-7	Spillage or inhalation of hazardous chemical	Wear gloves and lab coat. Work in fume hood Add acid to water	2*2
-----	--	---	-----

Dissolving Hydroxylamine hydrochloride in 2M HCl

8. Weigh 4.86 g hydroxylamine hydrochloride.
9. Add this to the 50mL 2M HCl. Keep this reagent in the dark at 4 °C.

8-9	Spillage or inhalation of hazardous chemical	Wear gloves and lab coat. Work in fume hood	2*2
-----	--	--	-----

Preparing Buffer solution

Preparing ammonium hydroxide (NH₄OH) solution (30% w/v):

10. Dissolve 15 g ammonium hydroxide in 50 mL Milli-Q water in a beaker.
11. Transfer to a 50 mL volumetric flask and fill up to 50 mL with Milli-Q water.

10-11	Spillage or inhalation of hazardous chemical	Wear gloves and lab coat. Work in fume hood	2*2
-------	--	--	-----

Preparing Ammonium acetate solution (10 M):

12. Dissolve 19.3 g ammonium acetate in approximately 15 mL Milli-Q water in a beaker.
13. Measure the pH and adjust it to ≈ 9.5 adding progressively some drops of the NH₄OH solution.
14. When adjusted, transfer to a 25 mL volumetric flask and fill up to 25 mL with Milli-Q water.

12-14	Spillage or inhalation of hazardous chemical	Wear gloves and lab coat. Work in fume hood	2*2
-------	--	--	-----

Preparing 20 mM Fe(II) stock solution

Preparing 0.01M HCl:

15. Add about 83 μL of 37% HCl into a prefilled 100 mL volumetric flask with Milli-Q water up to $\frac{3}{4}$ of total volume.
16. Once added the acid, fill up to 100mL with Milli-Q water.

15-16	Spillage or inhalation of hazardous chemical	Wear gloves and lab coat. Work in fume hood Add acid to water	2*2
-------	--	---	-----

17. Dissolve 99.405 mg of Iron (II) chloride tetrahydrate (MW 198.81) in a beaker with approximately 25 mL 0.01M HCl.
18. Transfer to a 25 mL volumetric flask and fill up to 25 mL with 0.01M HCl. The solution can be stored at 4°C in the dark up to 3 months.

17-18	Spillage of hazardous chemical	Wear gloves and lab coat. Wear safety goggles	2*2
-------	--------------------------------	--	-----



Preparing 20 mM Fe(III) stock solution



19. Dissolve 81.1 mg of Iron (III) chloride (MW 162.20) in a beaker with approximately 25 mL 0.01M HCl.
20. Transfer to a 25 mL volumetric flask and fill up to 25 mL with 0.01M HCl. The solution can be stored at 4°C in the dark up to 3 months.
21. The unused HCl can be transferred into a 50 mL Falcon tube and stored for months at room temperature.



19-21	Spillage or inhalation of hazardous chemical	Wear gloves and lab coat. Work in fume hood	2*2
-------	--	--	-----

5.2 Labelling of new solutions

Chemical information	Health, Precaution, and Emergency planning
----------------------	--

<p>Ferrozine solution (0.01M)</p> 	<p>H315: Irritating to skin</p> <p>H319: Causes serious eye irritation</p> <p>H335: Can cause respiratory irritation</p> <p>P261: Avoid inhalation of dust / fumes / gas / mist / vapors / aerosols</p> <p>P264: Wash skin thoroughly after use</p> <p>P271: Use only outdoors or in a well-ventillated area</p> <p>P280: Use protective gloves / goggles / face shield</p> <p>P302 + P352: IF ON SKIN: Wash with plenty of water</p> <p>P305 + P351 + P338: IF IN EYES: Rinse cautiously with water for several minutes. Remove any contact lenses if this is easy to do. Continue rinsing.</p>
<p>Hydroxylamine hydrochloride solution (1.4 M)</p> 	<p>H290: May be corrosive to metals.</p> <p>H302 + H312: Harmful if swallowed or in contact with skin.</p> <p>H315: Irritating to skin.</p> <p>H317: May cause an allergic skin reaction.</p> <p>H319: Causes serious eye irritation.</p> <p>H351: Suspected of causing cancer.</p> <p>H373: May cause damage to organs (spleen) with prolonged or repeated exposure if swallowed.</p> <p>H400: Very toxic to aquatic life.</p> <p>P201: Obtain special instructions before use.</p> <p>P273: Avoid release to the environment.</p> <p>P280: Wear protective gloves / protective clothing.</p> <p>P301 + P312 + P330: IF SWALLOWED: Contact a POISON CENTER / doctor if you feel unwell. Rinse mouth.</p> <p>P302 + P352 + P312: IF ON SKIN: Wash with plenty of water. Contact a POISON CENTER / physician if you feel unwell.</p> <p>P308 + P313: In case of exposure or suspected exposure: Get medical advice / attention.</p>

<p>Ammonium hydroxide solution (30% w/v)</p> 	<p>H290: May be corrosive to metals.</p> <p>H302: Harmful if swallowed.</p> <p>H314: Causes severe skin burns and eye damage.</p> <p>H335: May cause respiratory irritation.</p> <p>H400: Very toxic to aquatic life.</p> <p>P261: Avoid breathing dust/fume/gas/mist/vapors/spray.</p> <p>P273: Avoid release to the environment.</p> <p>P280: Wear protective gloves / protective clothing.</p> <p>P301 + P312: IF SWALLOWED: Contact a POISON CENTER / doctor if you feel unwell.</p> <p>P303 + P361 + P353: IF ON SKIN (or hair): Take off immediately all contaminated clothing. Rinse skin with water.</p> <p>P305 + P351 + P338: IF IN EYES: Rinse cautiously with water for several minutes. Remove any contact lenses if this is easy to do. Continue rinsing.</p>
<p>Buffer solution</p>	<p>Not a hazardous substance or mixture according to Regulation (EC) No. 1272/2008.</p>
<p>20 mM Fe(II) stock solution</p> 	<p>H302: Harmful if swallowed.</p> <p>H318: Causes serious eye damage.</p> <p>P280: Wear protective gloves/ protective clothing/ eye protection/ face protection.</p> <p>P301 + P312 + P330: IF SWALLOWED: Call a POISON CENTER / doctor if you feel unwell. Rinse mouth.</p> <p>P302 + P352: IF ON SKIN: Wash with plenty of water.</p> <p>P305 + P351 + P338 + P310: IF IN EYES: Rinse cautiously with water for several minutes. Remove contact lenses, if present and easy to do. Continue rinsing. Immediately call a POISON CENTER/doctor.</p>

<p>20 mM Fe(III) stock solution</p> 	<p>H290: May be corrosive to metals. H302: Harmful if swallowed.</p> <p>H315: Irritating to skin. H318: Causes serious eye damage.</p> <p>P264: Wash skin thoroughly after handling. P280: Wear protective gloves/ protective clothing/ eye protection/ face protection.</p> <p>P301 + P312: IF SWALLOWED: Contact a POISON CENTER / doctor if you feel unwell. P302 + P352: IF ON SKIN: Wash with plenty of water. P305 + P351 + P338: IF IN EYES: Rinse cautiously with water for several minutes. Remove contact lenses, if present and easy to do. Continue rinsing.</p>
<p>Hydrochloric acid (0.01M)</p>  <p>Based on sds of 2104 from Sigma</p>	<p>H290: May be corrosive to metals.</p>

6. WASTE management

Waste	Volume	Disposal method	Environmental risk
1 Used disposables	-	Dispose of in hazardous waste box	None, since this is according to procedure and handled by trained staff and collected by professionals
2 Chemical spillage	-	Wipe up using absorbent material and dispose of in hazardous waste box	None, since this is according to procedure and handled by trained staff and collected by professionals

Procedure with risk assessment (SOP): FE(II)/FE(III) DETERMINATION IN FRESHWATER		Saks- og dokumentnr. i ePhorte:	
Written by: IBV; Nicolas Valiente Parra		Version	[Category]
Approved by: IBV; Cecilie Mathiesen		Date	30.10.2020
		Page	76 av 89

Changes in this version:

- New SOP

1. INTRODUCTION/PURPOSE

Standard procedure for iron (Fe) spectrophotometric determination in water based on the ferrozine method. This method consists on two steps, based on the reaction of ferrozine (monosodium salt hydrate of 3-(2-pyridyl)-5,6-diphenyl-1,2,4-triazine-p,p'-disulfonic acid) with Fe(II). First, Fe(II) reacts with ferrozine to form a stable magenta complex. The absorbance of the complex is measured at 562 nm between pH 4 and 9. Then, hydroxylamine hydrochloride is used to reduce Fe(III) to Fe(II), which is subsequently measured at 562 nm. The application range of this method is 5 to 200 µM for Fe.

2. NECESSARY SAFETY EQUIPMENT



Nitrile






Fume hood






3. Chemical and biological hazards

3.1 Chemicals

Chemical information	Health, Precaution, and Emergency planning
<p>Ferrozine solution (0.01M)</p> <p><u>IBV made; see S-SOP-171</u></p> 	<p>H315: Irritating to skin</p> <p>H319: Causes serious eye irritation</p> <p>H335: Can cause respiratory irritation</p> <p>P261: Avoid inhalation of dust / fumes / gas / mist / vapors / aerosols</p> <p>P264: Wash skin thoroughly after use</p> <p>P271: Use only outdoors or in a well-ventillated area</p> <p>P280: Use protective gloves / goggles / face shield</p> <p>P302 + P352: IF ON SKIN: Wash with plenty of water</p> <p>P305 + P351 + P338: IF IN EYES: Rinse cautiously with water for several minutes. Remove any contact lenses if this is easy to do. Continue rinsing.</p>

<p>Hydroxylamine hydrochloride solution (1.4 M)</p> <p><u>IBV made; see S-SOP-171</u></p> 	<p>H290: May be corrosive to metals.</p> <p>H302 + H312: Harmful if swallowed or in contact with skin.</p> <p>H315: Irritating to skin.</p> <p>H317: May cause an allergic skin reaction.</p> <p>H319: Causes serious eye irritation.</p> <p>H351: Suspected of causing cancer.</p> <p>H373: May cause damage to organs (spleen) with prolonged or repeated exposure if swallowed.</p> <p>H400: Very toxic to aquatic life.</p> <p>P201: Obtain special instructions before use.</p> <p>P273: Avoid release to the environment.</p> <p>P280: Wear protective gloves / protective clothing.</p> <p>P301 + P312 + P330: IF SWALLOWED: Contact a POISON CENTER / doctor if you feel unwell. Rinse mouth.</p> <p>P302 + P352 + P312: IF ON SKIN: Wash with plenty of water. Contact a POISON CENTER / physician if you feel unwell.</p> <p>P308 + P313: In case of exposure or suspected exposure: Get medical advice / attention.</p>
<p>Ammonium hydroxide solution (30% w/v)</p> <p><u>IBV made; see S-SOP-171</u></p> 	<p>H290: May be corrosive to metals.</p> <p>H302: Harmful if swallowed.</p> <p>H314: Causes severe skin burns and eye damage.</p> <p>H335: May cause respiratory irritation.</p> <p>H400: Very toxic to aquatic life.</p> <p>P261: Avoid breathing dust/fume/gas/mist/vapors/spray.</p> <p>P273: Avoid release to the environment.</p> <p>P280: Wear protective gloves / protective clothing.</p> <p>P301 + P312: IF SWALLOWED: Contact a POISON CENTER / doctor if you feel unwell.</p> <p>P303 + P361 + P353: IF ON SKIN (or hair): Take off immediately all contaminated clothing. Rinse skin with water.</p> <p>P305 + P351 + P338: IF IN EYES: Rinse cautiously with water for several minutes. Remove any contact lenses if this is easy to do. Continue rinsing.</p>

<p>Buffer solution</p> <p><u>IBV made; see S-SOP-171</u></p>	<p>Not a hazardous substance or mixture according to Regulation (EC) No. 1272/2008.</p>
<p>20 mM Fe(II) stock solution</p> <p><u>IBV made, see S-SOP-171</u></p> 	<p>H302: Harmful if swallowed.</p> <p>H318: Causes serious eye damage.</p> <p>P280: Wear protective gloves/ protective clothing/ eye protection/ face protection.</p> <p>P301 + P312 + P330: IF SWALLOWED: Call a POISON CENTER / doctor if you feel unwell. Rinse mouth.</p> <p>P302 + P352: IF ON SKIN: Wash with plenty of water.</p> <p>P305 + P351 + P338 + P310: IF IN EYES: Rinse cautiously with water for several minutes. Remove contact lenses, if present and easy to do. Continue rinsing. Immediately call a POISON CENTER/doctor.</p>
<p>20 mM Fe(III) stock solution</p> <p><u>IBV made; see S-SOP-171</u></p> 	<p>H290: May be corrosive to metals.</p> <p>H302: Harmful if swallowed.</p> <p>H315: Irritating to skin.</p> <p>H318: Causes serious eye damage.</p> <p>P264: Wash skin thoroughly after handling.</p> <p>P280: Wear protective gloves/ protective clothing/ eye protection/ face protection.</p> <p>P301 + P312: IF SWALLOWED: Contact a POISON CENTER / doctor if you feel unwell.</p> <p>P302 + P352: IF ON SKIN: Wash with plenty of water.</p> <p>P305 + P351 + P338: IF IN EYES: Rinse cautiously with water for several minutes. Remove contact lenses, if present and easy to do. Continue rinsing.</p>
<p>Hydrochloric acid (0.01M)</p> <p><u>IBV made; see S-SOP-171</u></p> 	<p>H290: May be corrosive to metals.</p>

4. Special cautions necessary due to reproductive toxicity:

Generally, it is not recommended to work with a chemical that has carcinogenic or reproductive effects if you are planning to be or are pregnant. If a chemical is proven to pass into breast milk it is not recommended to perform procedure if you are breast feeding.

Planning pregnancy (men and women): None

Pregnant: None

Breast feeding: None.

5. PROCEDURE and risk assessment

Equipment

Multifunctional microplate reader (we plan to use this instead of the “normal” spectrophotometer)

Balance

Pipette: volume 100 – 1000 μL and 20 – 200 μL

Pipette tips, assorted sizes

Fume hood

Rack for snap-cap tubes

5.1 Solution preparation as follows (S-SOP-XXX):

- A. Ferrozine in an ammonium acetate solution. Prepare fresh.
- B. Reducing agent – hydroxylamine hydrochloride. Prepare fresh.
- C. Buffer – Ammonium acetate. Prepare fresh.
- D. Fe(II) and Fe(III) stock solutions, if they are not in stock (preserved for 3 months).
- E. Fe(II) and Fe(III) working solutions, if they were not prepared within the last week.
See table below.

Solution	Preparation
Fe(II) work solution	Fe(II) work solution ($200 \mu\text{M} = 11.2 \text{ mg/L Fe}^{2+}$): Dissolve 0.25 mL of the Fe(II) stock solution in 25 mL Milli-Q water. The solution can be stored at 4 °C in the dark up to one week. Prepare immediately before analysis.
Fe(III) work solution	Fe(III) work solution ($200 \mu\text{M} = 11.2 \text{ mg/L Fe}^{2+}$): Dissolve 0.25 mL of the Fe(III) stock solution in 25 mL Milli-Q water. The solution can be stored at 4 °C in the dark up to one week. Prepare immediately before analysis.

5.2 Standards:

1. For Fe(II) standards, prepare two sets of six 2 mL snap-cap reaction tubes. First set will range from 0 to 200 μM . For that, first tube will contain 1 mL of Fe(II) working solution, second one 0.8 mL, third one 0.6 mL, fourth one 0.4 mL, fifth one 0.2 mL and nothing to the last vial, as it will contain only water/extractant (sample blank).
2. To each vial, add the remaining volume to reach 1 mL of water/extractant (0 to the first, 0.2 mL to the second, and so on). Standards have to be diluted into the correct matrix due to the matrix effect, which affects to the colour sensitivity. For freshwaters Milli-Q water is suitable. For soil/sediment extracts or marine water, a saline matrix must be necessary.
3. The second set of six 2 mL snap-cap reaction tubes will range from 0 to 100 μM . So, first tube will contain 0.5 mL of Fe(II) working solution, second one 0.4 mL, third one 0.3 mL, fourth one 0.2 mL, fifth one 0.1 mL and nothing to the last vial, as it will contain only water/extractant (sample blank).
4. To each vial of these second set, add the remaining volume to reach 1 mL of water/extractant: 0.5 mL to the first, 0.6 to the second, and so on.

- Close the 12 vials and mix thoroughly.
- Repeat the procedure for Fe(III) standards using the Fe(III) work solution (another 12 vials, ranging to 200 and 100 μM respectively).

Part of procedure	Unwanted scenarios	Necessary precautions	S*K (Probability*Consequence)
1-6	Spillage or inhalation of hazardous chemicals	Wear gloves and lab coat. Work in fume hood	2*1

5.2 Fe(II) determination.

- Add 1 mL of sample to individual snap-cap tubes (one tube per sample).
- Add 0.1 mL of Ferrozine solution to each tube (both standards and samples). Close the vials and mix thoroughly.
- Pipet 200 μL of each sample to a 96-well plate. Standards for Fe(II) will be in the first row, standards for Fe(III) in the second one, and the samples from the third row on.
- Measure the absorbance at 562 nm (or the closest if the multiplate reader uses filters). Don't touch the microtiterplate at the bottom since fingerprints or any contamination at the bottom will affect the absorbance.

7-10	Spillage or inhalation of hazardous chemicals	Wear gloves and lab coat. Work in fume hood	2*1
------	---	--	-----

5.3 Reduction and Fe(III) determination.

- From here, tubes with Fe(II) standards won't be used. Add 150 μL of hydroxylamine hydrochloride solution to each snap-cap tube. Close the vials and mix thoroughly.
- Keep the tubes at room temperature ($\approx 25\text{ }^\circ\text{C}$) for 10 min.
- Add 50 μL of Buffer solution to each tube (both standards and samples). Close the vials and mix thoroughly.
- Transfer 200 μL of each Fe(III) standards and samples to a 96-well plate, and measure the absorbance at 562 nm.

11-14	Spillage or inhalation of hazardous chemicals	Wear gloves and lab coat. Work in fume hood	2*2
-------	---	--	-----

6. Waste management

Waste type	Approx volume	Disposal method	Environmental risk
1 Tips and gloves contaminated with hazardous chemicals	-	Dispose in risk waste box. Big yellow box.	None, since this is according to procedure and handled by trained staff and collected by professionals.
2 96-well plates	-	Microplates covered with lids are put into plastic bags which are then sealed with tape and put in risk waste.	None, since this is according to procedure and handled by trained staff and collected by professionals.
3 Snap-cap tubes	-	Close the tubes properly and dispose in a risk waste box.	None, since this is according to procedure and handled by trained staff and collected by professionals.
4 Hazardous chemical leftovers	-	Risk waste box	None, since this is according to procedure and handled by trained staff and collected by professionals.
5 Non-hazardous chemical leftovers	-	Risk waste box	None, since this is according to procedure and handled by trained staff and collected by professionals

7. REFERENCES

Viollier, E., Inglett, P. W., Hunter, K., Roychoudhury, A. N., & Van Cappellen, P. (2000). The ferrozine method revisited: Fe(II)/Fe(III) determination in natural waters. *Applied geochemistry*, 15(6), 785-790.

